

Paper and pulp mill waste valorisation via the production of phosphate ceramic composites

by

Eddie Gustav Barnard

Thesis presented in partial fulfilment
of the requirements for the Degree

of

MASTER OF ENGINEERING
(CHEMICAL ENGINEERING)

in the Faculty of Engineering
at Stellenbosch University



Supervisor

Prof JF Görgens

Co-Supervisor

Dr L Tyhoda

March 2021

DECLARATION

By submitting this thesis electronically, I declare that the entirety of the work contained therein is my own, original work, that I am the sole author thereof (save to the extent explicitly otherwise stated), that reproduction and publication thereof by Stellenbosch University will not infringe any third party rights and that I have not previously in its entirety or in part submitted it for obtaining any qualification.

Date: March 2021

PLAGIARISM DECLARATION

1. Plagiarism is the use of ideas, material and other intellectual property of another's work and to present is as my own.
2. I agree that plagiarism is a punishable offence because it constitutes theft.
3. I also understand that direct translations are plagiarism.
4. Accordingly, all quotations and contributions from any source whatsoever (including the internet) have been cited fully. I understand that the reproduction of text without quotation marks (even when the source is cited) is plagiarism.
5. I declare that the work contained in this assignment, except where otherwise stated, is my original work and that I have not previously (in its entirety or in part) submitted it for grading in this module/assignment or another module/assignment.

Initials and surname: EG Barnard

Date: December 2020

ABSTRACT

Paper and pulp mills in South Africa annually generate approximately 500 000 tonnes of wet paper and pulp sludge that is sent to landfill sites. Additionally, lignin is one of the most abundant biomaterials, second only to cellulose, yet due to its recalcitrance, it is mainly utilised as a low-value energy source. New legislation, that prohibits landfill disposal of solid waste that contains more than 40 wt% moisture, and an ever-increasing focus on green, sustainable production drives the paper and pulp industry towards enhanced waste valorisation. To this end, a possible solution is the production of eco-friendly bio composites that utilise paper sludge and lignin as feedstock materials. To achieve this goal, magnesium phosphate ceramic is used as binder, since it has 20 % lower carbon emissions compared to other binding agents (such as Portland cement) some of which have adverse effects on human health. The phosphate requires reinforcing fibres to ensure inexpensive production for economic viability. The paper sludge contains sufficiently sized fibres, while lignin is a bonding and “stiffening” agent in wood materials with an inherent affinity towards cellulose and hemicellulose. Previous studies have shown that these characteristics enable the utilisation of the paper sludge and lignin in the phosphate ceramic composites. However, at present there is little information on lignin/ceramic and lignin/paper sludge composites and consequently the bonding mechanisms that explain their interfacial interactions.

Paper sludge and technical lignin samples from three pulping mills across South Africa were used in this study. The mills were chosen based on waste emission and pulping process. Results showed that lignin from kraft pulping black liquor must be precipitated with sulfuric acid to unlock the properties that ensure optimal bonding and mechanical performance. The precipitated kraft lignin composites performed well with moduli of rupture and elasticity respectively at 7.2 MPa and 2 793 MPa. Furthermore, the addition of pine veneer improved mechanical performance such that the moduli of rupture and elasticity becomes 22.1 MPa and 3 616 MPa, satisfying several industrial standards for composites that may be used in the construction of furniture and non-loadbearing partitioning walls. These standards, as given by the European Standards Organisation and International Organisation for Standardisation, are 9 – 18 MPa and 1 600 – 4 000 MPa respectively for moduli of rupture and elasticity. Conversely, lignosulfonates from the sulfite pulping process could only form composites with moduli of rupture and elasticity of 6.4 MPa and 1 602 MPa after lamination.

The effects of lignin addition to the paper sludge reinforced phosphate composites were determined by investigating the chemical and morphological characteristics as well as the reactions to thermal changes exhibited by the individual components. The precipitated kraft lignin yielded better performing composites compared to composites that contained the kraft black liquor and lignosulfonate. Chemical and elemental analyses showed that the sulfuric acid precipitation caused alteration of lignin hydroxyl groups to form carbonyl groups (-C=O) – improving chemical bonding between the paper sludge fibres and lignin particles, while also reducing the overall hydrophilicity of the composites as well as improving the compatibility between the organic and inorganic phases. Additionally, the precipitated kraft lignin softens upon heating to mould around the fibres, resulting in improved fibre dispersion and encapsulation. These effects aid with stress transfer through the composite across phases, and ultimately increases the load bearing ability and stiffness of the composite, while reducing moisture-imposed deformation.

The precipitated kraft lignin composites showcased technical viability; however valorisation also requires economic viability. Thus, a production process that include lignin precipitation, composite production, and veneering stages was developed. Mass balances were completed using paper sludge emission rates from industry as well as the experimentally determined composite ratios. All major equipment was sized and costed accordingly before total capital and annual operating expenses were predicted to determine economic viability parameters. Using a desired internal rate of return of 20 %, the minimum required selling price of R 171/m² was calculated for kraft mills with sludge emissions of at least 13 500 dry ton/year (and a composite production rate of 800 000 panels per annum). The required selling price is competitive in the market for inexpensive construction materials, sold at wholesale prices for between R 158/m² and R 295/m², depending on product finishing.

In conclusion, the precipitated kraft lignin composites yielded better mechanical and physical properties compared to composites that contained no additional lignin, kraft black liquor, or lignosulfonate. These precipitated lignin composites also display economic potential with competitive minimum required selling prices and strong return on investment. The properties of the precipitated kraft lignin enable the production of a bio composite that sufficiently valorises paper and pulp mill waste towards a lower carbon economy.

Key words: *Kraft lignin precipitation, lignin composite, paper sludge composite, phosphate ceramic, interfacial adhesion mechanisms*

OPSOMMING

Die Suid-Afrikaanse papier en pulp industrie genereer jaarliks ongeveer 500 000 ton papier en pulp slyk wat na stortingsterreine geneem word. So ook is lignien, naas sellulose, die volopste biomateriaal, maar word slegs as 'n goedkoop brandstof gebruik. Nuwe wetgewing en die toenemende fokus op groen, volhoubare produksie dryf die papier en pulp industrie om hul afval te omskep in waardevolle produkte. Een so 'n oplossing is die produksie van 'n saamgestelde materiaal deur die papier slyk, lignien, en magnesium fosfaat keramiek as roumateriaal te gebruik. Die fosfaat veroorsaak 20 % laer koolstof vrystelling as ander binders, waarvan sommige binders nuwe effekte op menslike gesondheid het. Die fosfaat keramiek moet vir ekonomiese vatbaarheid deur vesels aangevul word en die papier slyk bestaan grootliks uit vesels wat voldoen aan grootte vereistes, terwyl lignien in sy natuurlike vorm as binder en verstywingsmiddel optree en inherent 'n affiniteit het tot die sellulose. Huidiglik bestaan beperkte inligting omtrent die lignien/keramiek mengsels asook die bindingsmeganismes wat die koppelvlak interaksies verduidelik.

Hierdie studie maak gebruik van papier slyk en tegniese lignien monsters van drie pulp meule regoor Suid-Afrika, gebaseer op totale afval vrystelling en tipe pulp proses. Eksperimentele werk het bewys dat kraft lignien gepresiteer moet word ten einde die gesogte eienskappe te ontsluit wat die samestellings se meganiese vermoë verhoog. Die gepresiteerde kraft lignien samestellings kon onderskeidelik modulusse vir skeuring en elasticiteit van 7.2 MPa en 2 793 MPa behaal, wat dit moontlik maak om die materiale te gebruik vir die produksie van meubels en nie-lasdraende strukture. Hierdie standaarde, soos uiteengesit deur die Europese Standaard Organisasie en die Internasionale Organisasie for Standardisering, is respektiewelik 9 – 18 MPa en 1 600 – 4 000 MPa vir die modulusse van skeuring en elasticiteit. In teenstelling het die lignosulfonaat samestellings swakker gevaar met modulusse vir skeuring en elasticiteit van 6.4 MPa en 1 602 MPa na laminasie.

Die utwerking wat lignien op die papier slyk samestellings het is bepaal deur die chemiese en morfologiese eienskappe, asook termiese invloede op die komponente te ondersoek. Die gevolgtrekking is dat die gepresiteerde lignien samestellings die beste resultate toon omdat die lignien presipitasie plaasvind deur die hidroksiel groepe te verander in vry suurstof radikale wat gelyktydig die chemiese bindings tussen die lignien en papier slyk verhoog, die algehele hidrofilisiteit van die samestelling verlaag, en die versoenbaarheid tussen die organiese en anorganiese fases verbeter. Verder versag die gewysigde lignien met 'n toename in temperatuur

om sodoende om die papier slyk vesels te vorm, wat lei tot verbeterde vesel verspreiding en omhulling. Hierdie meganismes bevorder stres oordrag tussen fases om sodoende die lasdraende vermoë van die samestelling te verhoog terwyl vog veroorsaakte vervorming verlaag.

Die gewysigde lignien samestellings het uitstekende tegniese vermoë getoon, maar om 'n produk met toegevoegde waarde te produseer, is ekonomiese lewensvatbaarheid belangrik. Dus, 'n produksie proses wat die lignien wysiging, samestelling vervaardiging, en finerings fases insluit is ontwerp. Massa balanse, gebaseer op industriële papier slyk vrystellingstempo's en eksperimenteel bepaalde komponent verhoudings, is voltooi ten einde die grootte en koste van die hoof toerusting te bepaal. Verder is totale kapitaal- en jaarlikse vervaardigingskoste bereken voordat die ekonomiese vatbaarheidsparameters voorspel is. Deur 'n begeerde interne verdieningskoers op belegging van 20 % aan te neem, is 'n minimum verkoopsprys van R 171/m² bereken vir kraft meule wat ten minste 13 500 ton slyk per jaar vrystel – gelykstaande aan 800 000 standaard panele per jaar. Hierdie verkoopsprys is kompetender in 'n mark vir goedkoop boumateriaal wat verkoop word teen groothandel pryse tussen R 158/m² en R 295/m², afhangend van produk afwerking.

Ter samevatting, die gewysigde lignien samestellings het die beste meganiese en fisiese eienskappe in vergelyking met samestellings wat geen addisionele lignien bevat, samestellings met ongewysigde kraft lignien, en samestellings met lignosulfonaat. Die samestellings blyk ook ekonomies vatbaar te wees met kompeterende verkoopspryse en 'n stewige koers op belegging. Dit is die uiteindelijke eienskappe van die gewysigde kraft lignien wat die produksie van die biomateriaal moontlik maak om sodoende waarde te heg aan die papier en pulp afval in die strewe na 'n laer koolstof ekonomie.

ACKNOWLEDGEMENTS

Nothing is truly possible without the assistance of people that are capable and willing to impart their knowledge and experience. Subsequently, this project would have been impossible without the support of the following people:

Parents and close family: Family is the support we don't have to pay for. They are always willing to lend a helping hand. Thank you for being there during the late nights and making my journey as smooth as possible.

Mondi Group and PAMSA: For believing and investing in the project.

Prof. JF Görgens: For his perceptive ideas, instilling a better understanding of project management and pushing me to a deeper grasp of research.

Dr. L Tyhoda: For his good advice, irreplaceable inputs that helped form this project, and overall supervision.

Mr. HJ Solomon (Oom Sollie): For all the laboratory training and patience.

Mr. W Hendrikse: For all the administration that ensured smooth operation of the laboratory equipment.

Me. C du Toit and Mr. N Bezuidenhout: For her assistance with lignin preparation, overall guidance regarding administration, and his laboratory assistance.

Dr. SO Amiandamhen and Mr. A Chiphango: For their immaculate research on phosphate ceramics and paper sludge that formed the basis of this project.

CONTENT

DECLARATION	i
PLAGIARISM DECLARATION.....	ii
ABSTRACT.....	iii
ACKNOWLEDGEMENTS.....	vii
CONTENT	viii
LIST OF FIGURES	xiii
LIST OF TABLES.....	xvi
ACRONYMS AND ABBREVIATIONS.....	xviii
GLOSSARY	xix
THESIS OUTLINE.....	xx
CHAPTER 1: BACKGROUND.....	1
1.1. Introduction.....	1
1.2. Research question.....	2
CHAPTER 2: LITERATURE REVIEW.....	3
2.1. Introduction.....	3
2.2. Paper and pulp industry.....	3
2.2.1. Raw materials used in the South African pulping industry.....	4
2.2.2. Paper and pulp mill operations in South Africa.....	4
2.3. Paper and pulp mill sludge.....	5
2.4. Phosphate binder	7
2.5. Additives and fillers.....	10
2.5.1. Effects of fillers on phosphate ceramic properties.....	11
2.6. Lignin	12
2.6.1. Technical lignin produced by various pulping processes.....	13
2.6.2. Current uses for technical lignin.....	14

2.6.3.	Lignin chemistry	14
2.6.4.	Modification of lignin structures	17
2.7.	Wood Composites	18
2.7.1.	Interfacial adhesion mechanisms	19
2.7.2.	Phosphate ceramic composite products	21
2.7.3.	Lignin composites	22
2.8.	Veneer/lamination	23
2.9.	Industry standards	24
2.9.1.	Composite classification	24
2.9.2.	Standards	26
2.10.	Gap in literature	28
2.11.	Research questions and objectives	29
2.11.1.	Primary research questions	29
2.11.2.	Research objectives	30
2.11.3.	General objective/aim	30
CHAPTER 3: RESEARCH DESIGN AND METHODOLOGY		31
3.1.	Experimental approach	31
3.2.	Materials	32
3.2.1.	Paper sludge	32
3.2.2.	Lignin	33
3.2.3.	Binder	33
3.2.4.	Filler	33
3.3.	Experimental methods	33
3.3.1.	Lignin precipitation	33
3.3.2.	Feedstock characterisation	34
3.3.3.	Composite formation	36
3.3.4.	Veneer application	38

3.3.5.	Composite property testing.....	38
3.3.6.	Chemical and physical analyses of lignins and composites.....	39
3.3.7.	Data analysis	40
CHAPTER 4: EXPERIMENTAL RESULTS AND DISCUSSION		41
4.1.	Sludge feedstock characterisation	41
4.1.1.	Sludge chemical composition	41
4.1.2.	Sludge fibre water holding capacity	42
4.1.3.	Functional group identification.....	42
4.1.4.	Particle diameter	43
4.1.5.	Bulk density	44
4.1.6.	Thermal stability	44
4.2.	Lignin feedstock characterisation.....	45
4.2.1.	Chemical characteristics of technical lignin	45
4.2.2.	Thermal characteristics	49
4.3.	Composite performance	53
4.3.1.	Constituent interactions	54
4.3.2.	Composite properties	61
4.3.3.	Binder reduction.....	74
4.4.	Composite performance enhancements to reach industrial standards.....	74
4.4.1.	Performance enhancements via the addition of pine veneer.....	75
4.4.2.	Composite classification	78
CHAPTER 5: TECHNO-ECONOMIC ANALYSIS.....		81
5.1.	Introduction	81
5.2.	Process flow diagrams.....	81
5.2.1.	Lignin preparation plant.....	81
5.2.2.	Composite production plant.....	82
5.2.3.	Lamination plant	82

5.3.	Plant capacity	87
5.3.1.	Mass balance	87
5.3.2.	Equipment sizing and cost calculation.....	89
5.4.	Capital and operating expense.....	92
5.4.1.	Capital expense	93
5.4.2.	Operating expense.....	96
5.4.3.	Cash flow calculations	99
5.5.	Profitability indicators.....	100
5.5.1.	Market research.....	100
5.5.2.	Minimum required selling price.....	101
5.5.3.	Payback period.....	102
5.5.4.	Net present value.....	102
5.5.5.	Internal rate of return (discounted cash flow percentage)	103
5.6.	Sensitivity analysis.....	104
5.6.1.	Deviation in product selling price.....	104
5.6.2.	Deviation in CAPEX and OPEX	104
5.6.3.	Deviation in individual operating expenses	105
5.6.4.	Deviation in sludge emission from paper and pulp mills	106
5.6.5.	Reduced production capacity.....	106
5.6.6.	Various lignin contents utilised in composite production.....	107
5.6.7.	Various fractions of veneered product.....	108
5.7.	General discussion.....	108
CHAPTER 6: CONCLUSIONS AND RECOMMENDATIONS.....		110
6.1.	Conclusions	110
6.2.	Recommendations	113
REFERENCES		114
APPENDIX A: Statistical model verification and process optimisation.....		A

A.1. Mechanical performance results for FFD, steepest ascent, and CCD experimental designs.....	A
A.2. Response surface model parameters	C
A.3. Analysis of variance (ANOVA) of process variables.....	D
A.4. Confirmation of statistical models via experimental results	D
APPENDIX B: Economic analysis.....	E
B.1. Mass balance equations.....	E
B.2. Equipment sizing.....	F
B.3. Total capital investment	J
B.4. Total annual operating expense.....	K
B.5. Discounted cash flow	L

LIST OF FIGURES

Figure 1: The experimental approach used to complete this study.....	32
Figure 2: General design of experiments, showing the progression where an FFD was used initially based on literature. The FFD failed to contain the maximum of the response variable, thus a path of steepest ascent was determined, whereafter a CCD was set up around the range that would most likely yield optimum performance as determined by the stepwise setup.....	38
Figure 3: Composite products without and with pine veneer.	38
Figure 4: Chemical composition of the sludge from different mills.....	42
Figure 5: FTIR spectra of various sludge types.	43
Figure 6: TGA curves for MK, SK, and MS paper sludge, The first derivative of the mass left is depicted by the dotted curves.....	45
Figure 7: FTIR spectra of various lignin types.	48
Figure 8: TGA curves for MK lignin contained within black liquor (MBL) and that underwent acid precipitation (MKL). The first derivative of the mass left is depicted by the dotted curves.	50
Figure 9: TGA curves for SK lignin contained within black liquor (SBL) and that underwent acid precipitation (SKL). The first derivative of the mass left is depicted by the dotted curves.	51
Figure 10: TGA curves for MS lignosulfonate (MLS). The first derivative of the mass left is depicted by the dotted curves.....	51
Figure 11: DSC curves for MK and SK acid precipitated lignin. The TGA responses are denoted by the dotted curves, while the softening onset temperature at 130 °C is highlighted by a dashed line.....	53
Figure 12: FTIR spectra for A) MK, B) SK, and C) MS composites.	56
Figure 13: TGA curves for composites containing: (A) MK; (B) SK kraft black liquor (MBC and SBC) and precipitated kraft lignin (MKC and SKC); and (C) MS lignosulfonate (MSC). The first derivative of the mass left is depicted by the dotted curves.....	58
Figure 14: Micrographs of composites that contain no additional lignin (A and B); 20 wt% kraft black liquor (C and D); 20 wt% lignosulfonate (E and F); and 40 wt% precipitated kraft lignin (G and H). The micrographs on the left were taken at a larger zoom factor than on the right.	60
Figure 15: Fitted response of modulus of rupture as a function of lignin content and process temperature for A) MK composites, B) SK composites, and C) MS composites.	64

Figure 16: MOR for various lignin types and contents, split between different paper and pulp mills.....	65
Figure 17: Fitted response of modulus of elasticity as a function of lignin content and process temperature for A) MK composites, B) SK composites, and C) MS composites.	66
Figure 18: MOE for various lignin types and contents, split between different paper and pulp mills.....	67
Figure 19: Density at different lignin contents for the composites from the different mills. .	70
Figure 20: Visible loss in structural integrity of MS composites that contain 40 wt% lignosulfonate.....	71
Figure 21: Water absorption at different filler contents for the composites from the different mills.....	72
Figure 22: Effects of sludge WHC on composite water absorption.	72
Figure 23: Thickness swelling at different filler contents for the composites from the different mills.....	73
Figure 24: The maximum force before rupture used to calculate MOR is compared to t^2 from Equation 16.	77
Figure 25: The force per deflection parameter used to calculate MOE compared to t^3 from Equation 15.	77
Figure 26: Kraft lignin precipitation plant. This plant prepares the lignin for use during composite production.....	83
Figure 27: Lignosulfonate preparation plant. This plant prepares the lignosulfonate for use during composite production.	84
Figure 28: Composite production plant.	85
Figure 29: Lamination plant. This plant adds veneer onto the composites produced. It is assumed that veneer and resin is bought instead of produced on-site.	86
Figure 30: Comparing capital and operating expenses of different paper and pulp mills.	92
Figure 31: Equipment cost for a) major unit operations divided between lignin preparation, composite production, and lamination for each of the paper and pulp mills, and b) additional equipment, material, installation labour, and other unit operations.....	94
Figure 32: Economics of production scale is investigated by plotting A) CAPEX and B) MRSP against various plant capacities. A zero per cent change implies current sludge production as observed by Boshoff (2015).....	95
Figure 33: Cost of feedstock for different paper and pulp mills.....	96
Figure 34: Utility expenses for different paper and pulp mills.....	98

Figure 35: The minimum required selling price is compared to a minimum market price of R509 and a high market price of R850.	102
Figure 36: Payback period when a selling price of R636 is assumed.....	102
Figure 37: NPV at intermediate market price (R636/panel).	103
Figure 38: Discounted cash flow percentage obtained by the paper and pulp mills if market price of R636 is assumed.	103
Figure 39: The IRR for various product selling prices (green) and the minimum required selling price (orange).	104
Figure 40: The effects of a 25 % deviation in capital expenses, overall annual operating expenses, and working capital on the IRR.....	105
Figure 41: The effects of feedstock cost, salaries, and utilities on IRR.....	105
Figure 42: Effects of deviation in dry sludge emission from the paper and pulp mills on IRR.	106
Figure 43: The effect of reduced production rate on DCF%.	107
Figure 44: The effect of lignin content used to produce the composites on IRR.	107
Figure 45: The effect of the fraction of product to be veneered on IRR.....	108

LIST OF TABLES

Table 1: Wood fibre sources used in the South African pulping industry (Donkor, 2019).	4
Table 2: Fibre sources and mill operations of the mills that were considered.	4
Table 3: Properties of the three sludge samples used in this study are compared (Boshoff, 2015).	7
Table 4: Composition of various lignin types as measured by Schorr et al. (2014).	15
Table 5: The elemental composition of different types of technical lignin.	16
Table 6: Standards for density of different kinds of composite.	26
Table 7: Standards for modulus of rupture and modulus of elasticity of different kinds of composite.	27
Table 8: Standards for water absorption, thickness swelling, and volume swelling of different kinds of composite.	27
Table 9: Levels for the process variables tested via a full factorial design.	37
Table 10: Sludge fibre water holding capacity.....	42
Table 11: Sauter mean diameter for sludge particles.	44
Table 12: Bulk density of sludge from different paper mills.	44
Table 13: Estimated empirical formula for lignin from elemental analysis.	46
Table 14: Relative peak intensities compared to aromatic ring structures in kraft lignin.....	47
Table 15: Verify optimum phosphate to paper sludge ratio obtained by Chimphango (2020).	61
Table 16: Summary of the three experimental setups completed for each of the paper mills.	62
Table 17: Process conditions for optimum composite properties.	68
Table 18: Percentage change in dry mass before and after water absorption test.....	71
Table 19: Binder and filler reduction due to the addition of lignin.....	74
Table 20: Experimental design to showcase the effects of veneer on composite performance.	75
Table 21: Physical and mechanical properties of optimum lignin and lignin-free composites, as well as optimum lignin content composites with pine veneer.	76
Table 22: Standards for various composites compared to the properties of the new veneered and unveneered composites.	80
Table 23: Annual sludge formation (Boshoff, 2015).	87
Table 24: Summary of optimised process conditions for composite production from the three pulp mills.	87

Table 25: Assumptions made to fully specify the mass balance of the process.....	88
Table 26: Flow rates over the entire process.....	89
Table 27: Parameters used in Equation 17 (Sinnott, 2005).....	90
Table 28: Composite formation equipment design specifications and sizing factors.....	91
Table 29: Comparing CAPEX and OPEX per unit annual waste feed rate.....	93
Table 30: Break down of total fixed capital investment (Westney, 1997).	95
Table 31: Cost per unit mass of feedstock.....	96
Table 32: Salary expense to operate the suggested process, adapted from Chimphango (2020).	97
Table 33: Annual depreciation.....	98
Table 34: Cost per unit for operating utilities required.....	98
Table 35: Annual operating expenses (Westney, 1997).....	99
Table 36: Assumptions regarding the annual cash flow of the proposed project, adapted from Chimphango (2020).	100
Table 37: Market price from different sources.....	101

ACRONYMS AND ABBREVIATIONS

Acronym/abbreviation Description

Used in the technical investigation

ANOVA	Analysis of variance
AP-KL	Acid precipitated kraft lignin
CBPC	Chemically bonded phosphate ceramic
DSC	Differential scanning calorimetry
FTIR	Fourier transform infrared spectroscopy
HPLC	High performance liquid chromatography
KL	Kraft lignin (in the form of spent pulping liquor)
LS	Lignosulfonate (spent pulping liquor)
MOE	Modulus of elasticity
MOR	Modulus of rupture
MK	Mondi Richards Bay Kraft pulping
MS	Mpact Piet Retief Sulfite pulping
NREL	National Renewable Energy Laboratory
NSSC	Neutral sulfite semi chemical
PAMSA	Paper Makers Association of South Africa
SEM	Scanning electron microscope
SK	Sappi Ngodwana Kraft pulping
TGA	Thermal gravimetric analysis
TS	Thickness swelling
WA	Water absorption
WHC	Water holding capacity

Used in the economic evaluation

IRR	Internal rate of return
MRSP	Minimum required selling price
NPV	Net present value
DCF	Discounted cash flow

GLOSSARY

Additive. Constituent added to composite mixtures to perform critical functions as well as to improve performance/cost ratio.

Binder. A substance that is used to keep material together through mechanical and/or chemical mechanisms to form a new cohesively whole material

Binder ratio. The ratio of components that is mixed to react and form the binder. In this study, more specifically, the ratio between monopotassium phosphate and magnesium oxide.

Composite plywood. A composite where laminate material sandwiches a core layer of particles and binder.

Fibre-binder ratio. A ratio between the mass of fibre and binder added to a composite.

Filler. A cost-effective material used to partially replace more expensive binders without reducing performance of the composite.

Kraft pulping. Pulping process of lignocellulosic materials using sodium hydroxide and sodium sulfide as the main digesting chemicals.

Laminate. A thin covering layer of plastic or other protective material.

Lignin content. A fraction of the total composite mass that must be attributed by lignin.

Modulus of elasticity. The ratio of the applied stress to the strain of a material within its elastic limit.

Modulus of rupture. Or bend strength, is the stress a material experiences just before it yields in a flexure/bending test.

Sulfite pulping. Acidic or neutral pulping process using sulfur dioxide that react and remove lignin from cellulosic materials in the form of water-soluble sulfonated lignin.

Veneer. A thin covering of wood applied to another material for decorative and/or performance purposes.

THESIS OUTLINE

CHAPTER 1: BACKGROUND. This chapter gives context to this research study.

CHAPTER 2: LITERATURE REVIEW. This chapter presents literature on bio-composites, phosphate ceramics, paper sludge, and lignin from pulping industries. Current uses for paper sludge and lignin is reviewed, as well as lignin properties, and possible modification techniques, that should aid in composite formation.

CHAPTER 3: RESEARCH DESIGN AND METHODOLOGY. The experimental and analytical methods applied in this study are outlined in this chapter.

CHAPTER 4: EXPERIMENTAL RESULTS AND DISCUSSION. This chapter exhibits the findings of this study and discusses the physical and chemical mechanisms studied and analysed in line with the research objectives.

CHAPTER 5: TECHNO-ECONOMIC ANALYSIS. The possible economic viability of lignin composites containing paper sludge in a competitive market of inexpensive biomaterials is shown in this chapter.

CHAPTER 6: CONCLUSIONS AND RECOMMENDATIONS. This chapter concludes the research based on findings of this study and gives recommendations for future research.

CHAPTER 1: BACKGROUND

1.1. Introduction

This study addresses the viability of paper sludge reinforced phosphate ceramics via addition of lignin as a binder replacement. Lignin is one of the most abundant biomaterials, second only to cellulose, yet due to the recalcitrance of lignin molecules, it is currently mainly utilised as a low-value fuel. Paper and pulp mills in South Africa annually generate approximately 500 000 tonnes of wet sludge (Boshoff, 2015) that could be used in bio-composite production.

Previous studies have established that magnesium potassium phosphate ceramic is a viable binder for composite production, while paper and pulp mill sludge could be used as a fibre reinforcement (Amiandamhen, 2017; Chimphango, 2020; Mngomezulu, 2019). These researchers investigated the effects of sludge fibre type and content, filler type and content, and binder ratios on the physical and mechanical performances of the phosphate bonded composites. However, the ceramic binder is an expensive alternative to other cement-based binders, while the paper sludge fibres result in reduced performance compared to virgin fibres from pine or black wattle due to the reduced lignin content, average fibre size, and increased inert materials from the pulping process. Lignin, as a binder, could be used to reduce the amount of phosphate required, while also having a positive impact on the composite properties.

Previous studies have investigated the use of lignin as a binder replacement in formaldehyde and epoxy bonded bio-composites (Cetin and Özmen, 2002; Salanti et al., 2018; Toriz et al., 2002; Younesi-Kordkheili et al., 2016). Furthermore, phosphate ceramics have been investigated extensively Amiandamhen et al. (2019), Singh et al. (1996), Wagh A.S (2004) and Wagh (2013 and 2016), but to the knowledge of this researcher this study is the first to investigate the combination of lignin and phosphate binders, as well as the combination of lignin and paper sludge in inorganically bound composites. Hence, there are no reports in literature on the effects that lignin has on phosphate ceramics, and no research has been found on the ideal lignin properties to ensure chemical compatibility with the inorganic binder. Based on the current knowledge of lignin, the lignin, depending on source, pulping process, and modification, could increase the mechanical performance of the composites due to its natural affinity to wood-based biopolymers, and its natural rigid molecular structure (Wool and Sun, 2011), but must be investigated, since hygroscopic properties of certain types of lignin could also reduce composite performance. The lignin could also affect the apparent properties of the paper waste sludge due to chemical binding or encasement that will change the polarity,

hydrophilicity, surface roughness, and stiffness of the paper sludge. Furthermore, technical lignin has a dark colour and could negatively impact composite appearance and reduce market demand.

This study investigated optimisation of composite performance of the paper sludge reinforced lignin phosphate composites by quantifying the effects of varying lignin types and content on known adhesion mechanisms. The composite properties were further improved via lamination with pine veneer. Finally, a techno-economic viability study was performed.

1.2. Research question

Does the natural affinity of lignin to cellulose and hemicellulose increase the overall interfacial adhesion between constituents to improve mechanical strength, stiffness and dimensional stability of the composites? Should spent pulping liquor (kraft and sulfite pulping), or precipitated lignin be used for enhanced composite performance by improving compatibility with the inorganic phosphate binder, as well as increasing chemical activity? Do these composites achieve industrial standards, or should additional performance be added via veneer? Permitting the technical viability of the composites, does this project show economic viability for adequate paper and pulp mill waste valorization?

CHAPTER 2: LITERATURE REVIEW

2.1. Introduction

Currently paper sludge (PS), a waste product from the paper pulping process, is mostly sent to landfill as a disposal mechanism, since the pulp and paper industry has no existing alternative eco-friendly solution (Donkor, 2019). Previous researchers have shown the possibility of PS utilization in bio-composites, but major downfalls of these composites were that the phosphate binder, at roughly R 14 000 per ton, is expensive compared to other inorganic binders, as well as the incompatibility of the PS to be used in the composite, since the PS are inherently hygroscopic with large water holding capacities, are smaller than virgin wood fibres, and have a higher ash content that can inhibit intimate surface bonding – resulting in inferior performances compared to industrially available composites and international load-bearing composite standards set out by the European Standards Organisation (EN) and International Organisation for Standardisation (ISO) (Chimphango, 2020). Fillers and additives, including calcium carbonate, silica fume, fly ash, and other metal oxides, were investigated to reduce the cost of production while also aiming to improve certain composite properties. However, while these fillers improved the performance of the composites, the advances were not sufficient to achieve the mentioned industry standards, and did not significantly reduce production cost (Chimphango, 2020). Lignin contained in spent pulping liquor, is mainly used as a low-value fuel in an energy recovery process (Han et al., 2018; Lora, 2008), but could be a versatile chemical in the composite material industry due to its “stiff” structure and natural affinity to hydrocarbons (Zeng et al., 2017) and this study aimed to investigate the influence of lignin on the PS reinforced phosphate composites formed via mould pressing at elevated temperatures, including reduction in processing cost and improvements in performance. While this study contributes new knowledge regarding lignin phosphate ceramic interactions, it also improves the performance of phosphate bonded composites, as found by previous research studies.

2.2. Paper and pulp industry

According to PAMSA (2019) the pulp and paper industry directly contributed R 6.63 billion to the balance of trade of South Africa in 2019. Furthermore, the total paper consumption is about 2.16 million tonnes per annum (PAMSA, 2019). During the paper making processes, the different operations result in ash, residual wood material, spent pulping liquor (containing lignin, water, and chemicals used in pulping) and sludge (Monte et al., 2009). The different types of waste are treated accordingly, where ash is sent to landfill, residual wood and spent

liquor is burnt for energy recovery, and sludge is treated via wastewater treatment, where sedimentation (or clarification) and anaerobic digestion remove the solids known as sludge (Thompson et al., 2001). The sludge is commonly sent to landfill, but landfill capacity is reaching a critical limit and as a result it is an increasingly costly method of waste disposal (Bajpai, 2011). Also, the South African *National Norms and Standards for the Disposal of Waste to Landfill* prohibits waste with a moisture content higher than 40 % to be sent to landfill.

2.2.1. Raw materials used in the South African pulping industry

There are two main fibrous sources of pulpwood used in the South African paper and pulping industry: Eucalyptus, as the main hardwood source, is utilized in high strength corrugated paper production; while pine, as the main softwood source, is used in newsprint, packaging, and printing (Donkor, 2019). These fibre sources are usually supplemented by recovered and recycled paper and forestry residues. **Table 1** shows the utilization of the fibre sources as percentages of the total fibre requirement in the South African pulping industry.

Table 1: Wood fibre sources used in the South African pulping industry (Donkor, 2019).

Raw material	% of material utilized in industry
Softwood	39
Hardwood	50
Other	13

2.2.2. Paper and pulp mill operations in South Africa

The PS and lignin samples used in this study was sourced from the paper and pulp mills shown in **Table 2**. An extensive investigation of pulp mill operations was done by Boshoff (2015) and is briefly discussed in this section.

Table 2: Fibre sources and mill operations of the mills that were considered.

Company: mill	Fibre source	Mill processes	Sludge production (dry ton/year)
Mondi: Richards Bay	Recycled fibre; virgin wood; Eucalyptus.	Re-pulping; kraft	12 500
Mpact: Piet Retief	Recycled fibre; virgin pulp; bagasse pulp.	Re-pulping; sulfite	500
Sappi: Ngodwana	Virgin wood; Eucalyptus; Pine	Mechanical; kraft	15 000

Paper and pulp mills are spread across South Africa, although mainly focused in the east, where weather and terrain favour large forests and mills. The mills utilize a variety of fibre sources, including recycled fibre, newsprint, virgin pulp, and virgin wood (mainly pine and eucalyptus) in de-inking, re-pulping processes, as well as mechanical, kraft, soda and sulfite pulping to produce a range of products that include tissue paper, office paper, newsprint paper, packaging materials, and linerboard (Boshoff, 2015).

2.3. Paper and pulp mill sludge

As already mentioned, large quantities of wet paper sludge is annually sent to landfill in South Africa (Boshoff, 2015), and alternative applications for paper mill sludge are also being developed to fully utilise sludge to its total value. Research for these alternative functions include incineration, gasification, pyrolysis, conversion to bioethanol, and bio-composites, and showed good prospects for sludge valorisation (Amiandamhen, 2017; Boshoff, 2015; Chimphango, 2020; Monte et al., 2009). Among the numerous alternative uses for sludge, researchers have studied the possibility of it being utilized to produce cement composites (Amiandamhen et al., 2016; Soucy et al., 2014; Chimphango, 2020). More specifically Amiandamhen *et al.* (2016) and Mngomezulu (2019) used wood-based industrial residues to produce phosphate ceramic composites to effectively convert the large amounts of waste into valorised products.

Different mills utilize a variety of pulping processes and feedstocks, depending on the targeted product of the mill. Two main pulping processes are mechanical and chemical pulping, where the former has the objective of separating raw material into individual fibres, where lignin is maintained for strength purposes (Bajpai, 2011), and chemical pulping methods are efficient treatments where the wood source is cooked in chemicals to dissolve lignin and hemicellulose, thus liberating individual cellulose fibres (Börjesson and Ahlgren, 2015). These different processes, which include sulfite pulping, Kraft (using sodium sulfide and sodium hydroxide), soda (sodium hydroxide with or without anthraquinone), and Organosolv (range of organic solvents) pulping all achieve the liberation of cellulose using different methods (Börjesson and Ahlgren, 2015; Grāvītis et al., 2010). After pulping, the fibrous pulp is separated into useable fibres and inferior fibres, the latter being sent to waste treatment to ultimately become paper sludge.

The paper waste sludge properties depend heavily on the pulping process, wood source, and effluent treatment used (Monte et al., 2009), and have a vast range of properties available to

use in the production of bio-composites. The variations include mixtures of organic and inorganic constituents, where the organic materials are matrices of cellulose, hemicellulose, and lignin, and inorganic materials are ash, kaolinite, calcium carbonate, grass, plastics, and bacteria (Boshoff, 2015; Kuokkanen et al., 2008), which are grouped as the total ash content. Furthermore, the cellulose contains numerous hydroxyl groups that can bond with oxygen atoms on adjacent atoms, which increases the structural strength of bio-composites (Konduo, 1997). It is thus preferable to construct composites with sludges that contain more cellulose and less ash, since ash may inhibit the bonding of fibres. The variability in sludge composition and properties, such as fibre length, cellulose content, and degree of polymerisation, can influence the characteristics of the composite materials (Mngomezulu, 2019). However, it is possible to treat the sludge to decrease the variability in properties, and conceivably improve adhesion that will result in stronger composite materials (Amiandamhen et al., 2017; Bledzki and Gassan, 1999).

Paper sludge may contain more than twice its dry mass in moisture (Davis, Shaler & Goodell, 2003), and in South Africa the sludge is dewatered to about 50 – 80 % moisture content at the mill to save in transport costs (Boshoff, 2015). However, it is recommended that sludge should only contain six to eight percent moisture for the proper manufacturing of composite materials (Davis *et al.*, 2003). Mechanical pressing cannot dry the sludge to these low moisture contents due to the substantial water holding capacity of sludge, therefore thermal energy is required during drying. The high water holding capacity of the PS will increase the composite water absorption - previous research showed that the water absorbed by sludge-phosphate composites range between 22 % and 60 % of the dry material (Chimphango, 2020), which is unacceptable, since EN standards for cement bonded particleboards and ISO standards for general particleboards respectively allow maximum water absorbances of 35 % and 19 % .

Paper sludge fibre length distribution influences the composite stiffness and strength, and must therefore have a minimum length of 0.3 mm (de Alda, 2008). This is to increase the available bonding surface areas of the fibres, thus resulting in better adhesion and proper dispersion of shear stresses in the composite. To investigate and understand the mentioned properties, three paper sludge samples were chosen for this study based on the type of mill, and the composition of the sludge obtained from the mill. Some of the sludge properties, as observed by Boshoff (2015), are given in **Table 3**.

Table 3: Properties of the three sludge samples used in this study are compared (Boshoff, 2015).

	Mondi: Richards bay	Sappi: Ngodwana	Mpact: Piet Retief
Mill abbreviation in this text	MK	SK	MS
Pulping process	Repulping and Kraft	Kraft and mechanical	Lignosulfonates
Sludge production (dry ton/year)	12 500	15 000	500
Moisture content (%)	64	80	70
Composition			
Cellulose (%)	25	50	35
Hemicellulose (%)	11	19	18
Lignin (%)	19	13	25
Extractives (%)	5	8	8
Ash (%)	40	10	14

2.4. Phosphate binder

This section discusses the arguments for using phosphate ceramic binders to produce the PS fibre and lignin composites. Binders, or adhesives, join surfaces via surface attachment, which contributes to the performance of a composite (Saheb and Jog, 1999). Generally, the binder is chosen by considering its suitability for the end composite product in terms of moisture content, mechanical properties, materials that require bonding, and durability (Youngquist, 1999). Different types of adhesives should be tested for sustainable and compatible use when composites are manufactured (Dhakal et al., 2007), since the opportunity for cheap products are created from fibres of wood waste (Mngomezulu, 2019). Some of the different adhesives that could be used include thermoplastics, thermosetting resins, renewable adhesives, and inorganic cement adhesives (Mngomezulu, 2019) and is discussed below.

Thermoplastics can be heated recurrently but will harden when cooled again. It has several unique characteristics, such as fire resistance, toughness, and flexibility (Sorrentino et al., 2015), but is quite expensive and therefore only constitutes 30 % of the market (Mngomezulu, 2019). Thermosets are solids materials that cure (set) irreversibly during heating and subsequent cooling, to form an infusible network (Mngomezulu, 2019). Popular thermosets are phenol-, urea-, and melamine formaldehyde as well as isocyanate that are mainly used for external, indoor, decorative, and wood composite products (Amiandamhen et al., 2018; Younesi-Kordkheili et al., 2016). Renewable adhesives contain several advantages such as

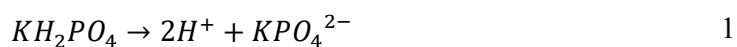
availability, and eco-friendliness (Mngomezulu, 2019), but also hold numerous challenges such as high cost, low water resistance, and low strength (Norström et al., 2018).

Inorganic cement adhesives are binder substances that have widespread uses, since mixing them with water results in hardening to bind materials (Mngomezulu, 2019). Lignocellulosic fibres have been bonded with many inorganic binders throughout the years, which include Portland cement, geopolymer cement, gypsum, and phosphate cement (Irle et al., 2013; Wagh, 2013; Youngquist, 1999). The inorganic cements have a great advantage, since they have the ability to bind several bio-based waste materials (Mngomezulu, 2019). However, Portland cement is unable to bind hardwood fibres. Research has further shown that these inorganic cements could have negative impacts on the environment. Portland cement production has a high energy requirement (Liao et al., 2017) and contributes about 7 % of global carbon dioxide emissions (Akbari et al., 2015). Researchers have proposed using fly ash as a filler to reduce the amount of Portland cement used, but limitations on availability due to environmental concerns linked to the burning of coal could inhibit the use of fly ash (Bentz et al., 2017).

An alternative should be considered for sustainable, utilisation of pulp and paper mill sludges, hence phosphate bonded composite production has been applied in the present study and is therefore of interest in terms of optimisation of formulations, product properties, and economics. Phosphate ceramic bonding is a relatively new field of study (Amiandamhen et al., 2016), but initial research has shown that lignocellulosic material could be used as a fibre source in phosphate composites (Laufenberg and Aro, 2004). Phosphate binders compare in strength with Portland cement (Mngomezulu, 2019) and could possibly reduce the environmental impact, since the ceramic formation has a lower carbon dioxide emission compared to Portland cement (Liao et al., 2017). Furthermore, research has shown that by using phosphate binders instead of conventional Portland cement, composite production becomes a less energy-intensive operation (Ding et al., 2014; Laufenberg and Aro, 2004; Wagh, 2004). According to Amiandamhen *et al.* (2016) phosphates are ores that occur naturally and are mined for phosphorous that is required for industrial application. In an effort to contain nuclear waste, research was done to develop the phosphate binder, which has very low permeability (Jeong and Wagh, 2002). Today, the phosphate is produced from an acid-base reaction and can be used in wood composites (Amiandamhen et al., 2016; Mngomezulu, 2019). The formulation of the phosphate is inexpensive in large quantities (Amiandamhen et al., 2017; Wagh, 2013), since it sets rapidly at room temperature (Wagh and Jeong, 2003) but the cost should be decreased by adding aggregates for economic viability (Amiandamhen et al., 2016).

To use the phosphate in composite production, the acid-base reaction must be studied to determine the required processing steps including acid-base mixing ratios, amount of water required, and processing and setting period. It has been shown that the phosphate binders should be formulated by reacting either a carbonate or an oxide of divalent metals with a salt of phosphoric acid (Amiandamhen et al., 2016; Wagh, 2004; Wagh and Jeong, 2003). When in solution the acid releases anions (phosphate ions) that causes a drop in pH. The drop in pH in turn causes an increase in the solubility of the alkaline metal oxide, which releases cations upon dissolving (Wagh, 2004). Ultimately the anions and cations react to form CBPCs, which are crystalline salt precipitates (Wagh, 2013). Different metal oxides could be used in this reaction and magnesium and calcium were tested (Amiandamhen et al., 2016, 2017; Wagh, 2004, 2013). Due to the extreme exothermic reactions caused by calcium oxide to form a wide range of salts that cannot be identified or measured without some effort, calcium phosphates are deemed to be impossible to produce on a large scale (Wagh, 2013, 2016). A more detailed description of this mineral can be found elsewhere (Mosselmans et al., 2007; Wagh, 2013, 2016; Wagh et al., 2003).

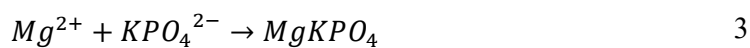
Magnesium oxide, on the other hand, has a moderate level of solubility that results in its widespread use (Wagh and Jeong, 2003). The magnesium oxide is reacted with potassium dihydrogen phosphate to form the magnesium potassium phosphate adhesive used in composite production. The reactions in Equation 1 through Equation 4 are given by Wagh (2013) to describe the mechanisms by which the overall reaction, as shown by Equation 5, occurs. Firstly, the acid phosphate releases hydrogen protons via dissolution and is shown by



The drop in pH induced by the released hydrogen ions causes the magnesium oxide to dissociate according to



The resulting ions then react to neutralise the mixture, and is shown by



Then, the total reaction is obtained and given as



The magnesium potassium phosphate hexahydrate product is known as a chemically bonded phosphate ceramic (CBPC), of which the viscosity is time dependent. It cures into a rigid structure with a certain degree of crystallinity (Amiandamhen et al., 2016). One of the advantages of this CBPC is its fast setting ability that prohibits extractives from dissolving into the slurry, which enhances bonding (Frybort et al., 2008) and increases the range of applications, since the phosphate binder is not affected by the composition of the lignocellulosic fibres, nor any sugars that may be present (Amiandamhen, 2017; Mngomezulu, 2019). This is crucial since the mechanical properties of lignocellulosic composites depend on the interfacial bonding and proper dispersion to prevent agglomeration and increase well-bonded interfaces (Tserki et al., 2005). The natural fibre phosphate composite could hold advantages compared to wood composites currently produced (Amiandamhen et al., 2016).

One concern expressed by Dolan (2013) is the diminishing source of phosphates required to produce the CBPCs. The author states that the price of binder would steadily increase until a point of economical processing of low-grade phosphate rocks are reached. For this reason, it is required to use additives in the new composite material, as it would decrease the cost of production and increase the longevity of the phosphate sources. Another area of concern is the compatibility between the phosphate binder and natural fibres. Lignocellulosic fibres are a natural choice for the production of composite materials. However, the natural fibres are hydrophilic while the phosphates are hydrophobic, and this incompatibility may weaken the adhesive strength of the composite (Hajiha et al., 2014).

2.5. Additives and fillers

Additives are used to increase the performance of composite materials but involve additional material and processing costs (Tserki et al., 2005). They are also known as compatibilisers and several are usually used to improve the bonding as well as composite performance (Amiandamhen et al., 2016; Bhaskar et al., 2012) such as improved impact and flammability resistance, as well as degradation stabilisation (Youngquist, 1999). Additives can also improve processability of the composite materials since the wood fibres do not necessarily need to be soaked before mixing with the binders (Amiandamhen and Izeke, 2013; Youngquist, 1999). Another argument for using additives is the relative ease with which they can be applied to the wood matrix, since proper dispersion between the fibres is possible (Rowell and Rowell, 1996).

Fillers, on the other hand, are particles that are added to the composite to lower the consumption of expensive binders (Wypych, 2016) as well as lower processing cost due to less abrasion during processing, and less strain on process equipment (Tserki et al., 2005). Additionally, the carbon footprint of bio-industries is lowered by employing industrial waste as fillers in the composites that ultimately will increase the environmental benefits from composite materials' production and use (Amiandamhen et al., 2016). Fillers have relatively good strength properties, are light weight and important for economic production of composites (Bledzki and Gassan, 1999). In the case of phosphate based lignocellulosic fibre composites, fillers could possibly reduce the number of free hydroxyl groups to increase moisture absorption resistance and other mechanical properties such as the moduli of elasticity and rupture (Tajvidi and Ebrahimi, 2002; Xiao et al., 2018). Wypych (2016) discusses numerous fillers used in industry, some being kaolin, fly ash, calcium carbonate, silica fume, carbon black, clay and even metal flakes, all of which could reduce the cost of the phosphate cement with limited effects on the composite properties. By increasing the fly ash and bark content it is possible to surround and encapsulate the biomass fibres to reduce the apparent hydrophilicity of the lignocellulosic fibres (Amiandamhen et al., 2018). The effects of fly ash, silica fume, and calcium carbonate is discussed in the following section. Lignin from paper and pulp mills could also be used as filler/additive and is discussed in detail section 2.6.

2.5.1. Effects of fillers on phosphate ceramic properties

Fly ash is obtained as a waste product when coal is burned (Mngomezulu, 2019) and is used as a partial replacement of certain composite binders (Amiandamhen et al., 2017). Recent studies found that up to 20 % of the phosphate binder mass could be replaced by fly ash without significant alterations of the composite properties (Amiandamhen et al., 2016), and it has even been found that the ash improves bonding and composite strength (Wagh, 2016). Although fly ash causes a decrease in material and production costs (Wagh, 2013), some researchers are concerned that the use of fly ash may not be a sustainable, long term solution, since the burning of coal is not only scrutinised, but the fossil fuel is also a limited source (Coyne, 2018).

Silica fume is obtained as a by-product from the silicon melting process. Silica fume is commonly used to improve the performance of Portland cement, since research is clear on the physical and mechanical improvements caused by adding the silica fume to the cement mixtures (Mngomezulu, 2019). However, it was found that if silica fume replaces more than 5 % of the cement, the structural stability is negatively impacted (Jiang et al., 2017).

Calcium carbonate is extremely abundant and is usually found in sedimentary rocks (Osman et al., 2004). It is used in composite production since it is an inexpensive method of increasing cement composite material performance. Although the extraction of calcium carbonate adds to the production of carbon dioxide and consumption of energy of the phosphate composite production process, it is still far less compared to Portland cement production (Cai and Panteki, 2016). Calcium carbonate is an economically important filler for large-scale cement production and is used as a micro fibrous filler since the particle diameters range from 0.5 μm to 2 μm (Qian et al., 2009). Comparisons done by Mngomezulu (2019) showed that calcium carbonate fillers resulted in superior composites when compared to fly ash or silica fume.

Furthermore, an investigation to compare fly ash, silica fume, and calcium carbonate as fillers in PS fibre reinforced phosphate ceramics were done by Chimphango (2020). They found that due to CaCO_3 that participate in the acid-base reaction that form the CBPC crystalline structure, the resulting mechanical and physical properties of the composite materials were superior to those containing fly ash and silica fume as fillers. Further investigation of the composite crystal structures indicated that minimal strain defects are caused when CaCO_3 is used, since the calcium carbonate reacts like magnesium oxide (a component used in the formation of the phosphate ceramic) to improve the crystal structure. This finding is supported by similar results obtained and discussed in more detail by Singh and Wagh (1998), and Wagh (2013).

2.6. Lignin

There is an increasing awareness of the necessity to fully utilise biomaterials to reach a sustainable circular economy where products are recycled, and waste streams are valorised (Bruijninx et al., 2016; Kadla et al., 2002). Thus, bio-refineries, such as paper and pulp mills, are increasingly targeting zero-waste processes. This includes improved valorisation of lignin waste streams, instead of only using it as a low-value fuel. However, due to the varying morphological and chemical properties of lignin, it is not widely utilized, but application of lignin has become an increasingly popular research topic (Salanti et al., 2018). It is important to understand the chemical and physical properties of lignin to comprehend the wide range of possibilities that exist regarding the utilisation of lignin. In this section, the production, different types, properties, modifications, and applications of lignin are discussed to better identify if and why lignin could be used in composite production.

2.6.1. Technical lignin produced by various pulping processes

Natural lignin occurs as the main adhesive in wood cells to increase cell wall stiffness and constitutes about 25 – 30 % of the mass of the large quantities of wood processed by paper and pulp mills. This means that around 300 million tonnes of lignin are produced annually as technical lignin that differ in chemical and physical properties from natural lignin (Bruijninx et al., 2016; Frigerio et al., 2014). The commonly used processes to produce technical lignin are neutral, acidic, and alkaline sulfite, alkaline Kraft, and alkaline soda pulping. Steam explosion, hydrolysis and Organosolv pulping are also used but to a far lesser extent (de Alda, 2008; Constant et al., 2016; Frigerio et al., 2014). It must be noted that different lignin isolation processes may not necessarily produce lignin with the properties (chemical composition, solubility, molecular structure, and hydrophilicity) desired for certain final products (Lora, 2008; Sipponen, 2016). It is thus required to look at the lignin valorisation chain as a whole to prevent the use of unmanageable lignin types even if the processes are cost-effective (Bruijninx et al., 2016). The main pulping processes are discussed below.

Acid sulfite pulping produces lignosulfonates via chemical cooking with a mixture of sulfur dioxide and a metal bisulfite of sodium, calcium, or magnesium (Lora, 2008). The process is operated at around a pH of one and in a temperature range of 125 to 145 °C. Lignosulfonates are formed when sulfonate functional groups (SO_3^-) attach onto the α -position of the propyl chain of the phenylpropanoid alcohols after the carbon-oxygen bonds are cleaved (Lora, 2008). Although some sulfite pulping mills burn the lignosulfonates, most do not need to burn it for energy recovery (Sipponen, 2016). Due to high functional group density, lignosulfonates are utilised as stabilisers, surfactants, and polymer adhesives (Bruijninx et al., 2016; Lora, 2008).

The kraft pulping process utilises sodium sulfide and sodium hydroxide to separate cellulose fibres and lignin at a temperature of about 170 °C. Kraft lignin mainly contains organically bound sulfide groups (S^{2-}) from the sodium sulfide pulping chemical (Han et al., 2018), but subsequent sulfonation modification processes after pulping can cause sulfonate groups to covalently attach to the aromatic rings of the monolignol monomers of kraft lignin (Bruijninx et al., 2016). Furthermore, kraft lignin has lower relative ash content and contains a high hydroxyl group content, which increases the hydrophilicity of the lignin. (Bruijninx et al., 2016). Up to six percent of the black liquor (waste stream consisting mainly of lignin) from the kraft pulping process could be utilised in other valorisation processes without negatively impacting the energy recovery process required to make the kraft pulping processes economically viable (Bruijninx et al., 2016). For both the Kraft and soda processes, the lignin

is dissolved into the spent pulping liquor in the form of lignin phenolates (Bruijninx et al., 2016).

The soda pulping process only utilises sodium hydroxide at a maximum temperature of 160 °C resulting in a sulfur free lignin, and is mainly used to treat non-wood fibres such as bagasse, flax, and straw (Bruijninx et al., 2016; Lora, 2008). The harsh pulping conditions cause considerable degradation of the natural lignin present in biomass materials, producing technical lignin that resist further chemical interactions (Bruijninx et al., 2016).

2.6.2. Current uses for technical lignin

There is a wide range of technical lignin types that are produced on a large scale. However, lignin is usually burnt for energy recovery due to its calorific value of about 26.5MJ.kg⁻¹ dry lignin (Berlin and Balakshin, 2014; Bruijninx et al., 2016). Furthermore, there are markets for the application of lignin in the manufacturing of industrial products. It is used: to produce heat stable asphalt emulsions; to increase the stiffness properties of corrugated board; as viscosity reducing and plasticiser additives in cement products; as a form of dust control; a binding agent in pesticides and animal feed; and in a wide range of dispersants (Berlin and Balakshin, 2014; Bruijninx et al., 2016; Sipponen, 2016; Wool and Sun, 2011).

Alternative applications of lignin were investigated (Berlin and Balakshin, 2014; Bruijninx et al., 2016; Sahoo et al., 2011). The researchers found that lignin could be used in the production of activated carbon, to reinforce plastics, and as partial replacement of adhesive in particleboard production (Bruijninx et al., 2016; Sahoo et al., 2011). Grāvītis *et al.* (2010) studied the possibility of steam exploded lignin replacing phenol-formaldehyde, a common composite adhesive that is known to have health risks and was classified in 2004 as a carcinogen by the International Agency for Research on Cancer (Grāvītis et al., 2010; Jakab et al., 2005; Marsh, 1982). Velásquez, Ferrando & Salvadó (2003) tested the possibility of lignin as natural adhesive in a binder-free fibreboard. The authors found that by utilising steam explosion, the lignin is plasticised and could be used in the production of the binderless fibreboards.

2.6.3. Lignin chemistry

Natural lignin is a polymeric substance produced via an enzyme initiated dehydrogenative polymerisation reaction that utilize three main monomers: trans-sinapyl, trans-coniferyl, and trans-p-coumaryl (Wool and Sun, 2011). The natural lignin cross-links with cellulose and hemicellulose in wood materials to act as a natural stiffener and to protect the cellulose against microbial destruction and chemical treatment (Zeng et al., 2017). Pulping processes, as already

discussed, aim to remove or relocalise the lignin from its native association with the hemicellulose and cellulose to expose the fibres to chemical treatment (Zeng et al., 2017). These pulping processes remove and alter lignin in various ways, producing numerous types of technical lignin. This means that there is no single uniquely defined molecule with constant properties (Bruijninx et al., 2016). This section aims to inform the reader about the elemental content and subsequent functional groups that form part of the technical lignin structures to give insight into the chemical properties of lignin that will affect possible adhesion in the phosphate ceramic composites.

Table 4 summarises the composition of precipitated kraft (from black liquor), soda, and pyrolytic lignin. It is clear that the sugars content (mainly from cellulose and hemicellulose) is insignificant compared to the more than 90 % insoluble and soluble lignin present in the technical lignin streams (Schorr et al., 2014). Ash content varies depending on the method and extent of washing of the lignin streams (Naron et al., 2017; Schorr et al., 2014).

Table 4: Composition of various lignin types as measured by Schorr et al. (2014).

Component	Precipitated Kraft lignin	Wheat straw Soda lignin	Pyrolytic lignin
Insoluble lignin	91.5 ± 2.0	79.0 ± 1.0	85.0 ± 1.0
Soluble lignin	4.7 ± 0.5	9.0 ± 1.0	9.0 ± 1.0
Total sugars	1.1 ± 0.2	1.3 ± 0.1	0.4 ± 0.1
Glucose	15.5	3.0	90.0
Xylose	5.5	11.0	5.0
Mannose	72.0	73.0	5.0
Ash	3.6 ± 0.7	0.7 ± 0.1	1.6 ± 0.1

Table 5 summarises the elemental composition of lignin obtained from various sources and pulping processes. Lignin structures and functional groups are usually presented as per phenylpropane units (PPU) to simplify discussions by excluding molecular weight effects (Wool and Sun, 2011). When the elemental compositions in **Table 5** are converted to these PPU formulae, it becomes clear that per C₉ unit, kraft lignin contains on average between nine and eleven hydrogen, between three and four oxygen, and 0.1 sulfur atoms, while lignosulfonate contain between twelve and thirteen hydrogen, more than six oxygen, and more than 0.5 sulfur atoms. The higher oxygen and sulfur content of lignosulfonates is due to the sulfonation (addition of SO₃⁻) as a result of the pulping conditions (Lora, 2008). The sulfonate anion contributes to the

water solubility of lignosulfonates (Gao et al., 2019), which could be of concern when the composites are produced, and modifications may possibly be needed.

Table 5: The elemental composition of different types of technical lignin.

Lignin source	Elemental content						Reference
	%C	%H	%O	%S	%N	%OMe	
Wood	59.0	6.0	31.0	-	-	13.0	(Froass et al., 1996)
Kraft*	60.9	5.6	32.4	1.1	-	12.0	(Froass et al., 1996)
Kraft**	61.8	6.4	31.8	-	-	18.0	(Chandra, 1997)
Kraft	65.0	5.4	28.2	1.3	0.1	-	(El Mansouri and Salvadó, 2007)
Soda	65.0	6.1	28.6	0.0	0.2	-	
Lignosulfonate	44.9	5.2	44.1	5.9	0.0	-	
Sulfonated kraft***	46.8	3.4	39.3	8.3	0.0		(Inwood et al., 2018)

* Averaged value of Kraft lignin from different mills

** Averaged value of Kraft lignin from coniferous and deciduous wood

*** Kraft lignin modified for utilization as a lignosulfonate replacement in dispersion applications

Ultimately, the overall properties of the composite materials that utilize lignin are influenced by the molecular weight of the lignin, where the molecular weight is dependent on functional group content and cross-linking (Grāvītis et al., 2010). Some of the most common functional groups present on lignin structures include phenolic and aliphatic hydroxyl, methoxyl, aldehyde, and carbonyl groups (Brodin, 2009). The hydroxyl groups occur in amounts that widely range from 10 to 150 groups per 100 PPU's (Chandra, 1997; Froass et al., 1996; El Mansouri and Salvadó, 2007). The molecular weight, together with the wood source and pulping process used, also affect the thermal stability of the lignin, where lignin is mostly very stable up to 220 °C, but due to the various chemical bonds that exhibit different bonding strengths, lignin degradation occurs over a relatively wide temperature range, losing only about 40 % of its mass before 700 °C (Culbertson Jr., 2017). Furthermore, the glass transition temperature can be as low as 69 °C to 86 °C for softwood lignin, but can range between 154 °C and 200 °C for hardwood lignin, depending on the pulping process (Culbertson Jr., 2017), while kraft lignin has also shown glass transition temperatures between 119 °C and 148 °C (Brodin, 2009).

Ultimately, the cleavage of aryl-ether links in the lignin structure due to elevated processing temperatures results in reactive free radicals that are resonance stabilised by the mentioned functional groups and existing double bonds (Kaewtatip et al., 2010), and may possibly react with other hydrocarbons to form thermally stable products (Brebū and Vasile, 2010). It was

further comprehensively shown that lignin bind to polysaccharides via oxygen radicals to form ether, ester, acetal, and glycoside links – all R-O-R' containing groups (Brodin, 2009; Zeng et al., 2017). However, it is almost always the case that natural fibres show poor interfacial compatibility, due to the relatively high hydroxyl group content that inherently forms intermolecular hydrogen bonds with water to ultimately impede close interfacial contact required for any adhesion mechanism to occur (Wang et al., 2019). Impurities due to natural minerals from wood and chemicals from the pulp digestion stages will also affect how lignin interacts with other constituents in composite materials (Frigerio et al., 2014). It is for these reasons that lignin modification is considered in the next section.

2.6.4. Modification of lignin structures

Lignin is naturally recalcitrant to utilization as a specialty chemical due to its chemical and physical properties after pulping, and it is thus necessary to alter lignin structures to increase the compatibility between lignin and other constituents in bio-composites or polymer blends by introducing reactive sites (Culbertson Jr., 2017; Wool and Sun, 2011). Furthermore, the hydroxyl groups inhibit adequate interfacial adhesion, and modification should aim to remove these groups, which will not only improve adhesion, but will also reduce the hydrophilicity of the constituents used to form the composite material (Wang et al., 2019).

Previous research showed that modification or reduction of the hydroxyl groups on lignin is an effective behavioral alteration method and is the preferred route of free radical formation (Wool and Sun, 2011). Some of the modifications include: phenolation of kraft lignin and lignosulfonates (Cetin and Özmen, 2002; Podschun et al., 2016; Younesi-Kordkheili et al., 2016); epoxidation of lignin to use as a cross-linking substitution of toxic bisphenol A in epoxy resin (Salanti et al., 2018); esterification of kraft lignin by reacting acetic anhydride, dioxane, and pyridine with the lignin to ultimately reduce hydroxyl content and increase ester functional groups (Kaewtatip et al., 2010); and oxidation of lignin to deposit the lignin on aminosilicas, where oxidation was achieved by acids, sodium periodate, and metal oxides, respectively (Budnyak et al., 2019). The oxidised lignin exhibited increased carbonyl and carboxyl functional groups compared to unmodified kraft lignin. Other alteration techniques include acetylation, amination, cross-linking of lignin structures, halogenation, methylation, nitration, and sulfonation (Jeong et al., 2012; Kamoun et al., 2003; Sipponen, 2016; Wool and Sun, 2011). Hydrocracking and phenylation are also used to remove the hydroxyl functional groups from lignin to decrease its hydrophilicity (Kadla et al., 2002; Sun et al., 2016).

Lignin modification is mostly extensive, complicated, and expensive due to the addition of chemicals, the large number of processing steps, and extreme process conditions required. Sulfuric acid treatment is one of the least complex and most inexpensive alteration techniques applied to lignin (Aro and Fatehi, 2017). Sulfonation is a replacement reaction, where aliphatic hydroxyl groups on the lignin structure is altered to increase the free oxygen radical content (Kamoun et al., 2003). However, sulfuric acid sulfonation will not work for lignosulfonates, since there are sulfonate groups present that also result in the hydrophilic properties of lignosulfonate (Aro and Fatehi, 2017; Naron et al., 2017). Isolation of lignosulfonates include expensive ultrafiltration, amine extraction, ion-exchange, and calcium oxide induced precipitation at pH higher than 12 (Aro and Fatehi, 2017). On the other hand, kraft lignin sulfonation via sulfuric acid and via sodium sulfite were tested (Inwood et al., 2018). **Table 5** shows that sulfonation causes a reduction in hydrogen content, while oxygen and sulfur content increased, to result in a lignin with low solubility due to reduced hydroscopic properties (Inwood et al., 2018). As far as this researcher knows, no previous work has explicitly used these C-O[•] radicals in binding mechanisms to bind lignin to any organic or inorganic material, but rather this alteration is usually utilized as a pretreatment before another modification, such as methylation, sulfomethylation, or epoxidation (Aro and Fatehi, 2017).

2.7. Wood Composites

Wood composites are defined as wood-based particles glued together (Rowell and Rowell, 1996), where multiple materials (particles, adhesive, fillers) with different properties are mixed to form composites with altered characteristics (Youngquist, 1999). The purpose of any composite material is to improve the performance compared to the individual constituents, while also targeting reduced production costs (Rowell and Rowell, 1996). Heated pressing processes account for most of the particleboards produced, while extruded boards, where parallel dyes are used to force the particle-resin mixture into a board, are rarely produced (Carll, 1986). During the heated pressing process, the fibres are sized via mechanical processes, and the adhesives are added to form a mat that is then treated by applying heat and pressure to produce composite panels (Youngquist, 1999).

Different types of composite boards can be produced, depending on the materials used. These include natural fibres, which are normally wood based, and inorganic fibres such as extruded polymers and glass fibres. Natural fibres are used as building materials and in engineering, since it has strength properties comparable to cement composites, yet it is lightweight (Mngomezulu, 2019). Careful consideration is required, however, since there exists improper

interfacial bonding in some natural composites that causes variation in quality (Tserki et al., 2005). In South Africa most of the bio-based composites are wood-based and range from fibreboards to laminated products (Youngquist, 1999), where the composite industry utilizes mill residues such as chips, shavings and, more recently, paper sludge (Amiandamhen et al., 2016). Inorganic composites exist as discontinuous phases of natural fibres and inorganic adhesives (Bledzki and Gassan, 1999), where the amount of binder can range from 30 – 90 % (Youngquist, 1999). Adhesives must be chosen to increase the bonding and reduce the natural hydrophilicity of the lignocellulosic fibres that contain hydroxyl groups (Dhakal et al., 2007).

Particleboards, a subset of composites, are generally used to manufacture flooring panels and furniture, whereas medium to high density particleboards such as fibre-cement boards could be used as wall partitions, false ceilings, structural beams, and load bearing walls, (Amiandamhen *et al.*, 2016; Youngquist, 1999). These applications are made possible due to the composite properties such as resistance to decay and good dimensional stability, as well as increased fracture toughness when fibres are added to the cement matrices (Amiandamhen et al., 2016). There are drawbacks when the cement-fibre composites are used. Firstly, the cement forms an alkaline environment that causes the degradation of natural fibres. Secondly, the hydrophilicity of the fibres and the hydrophobicity of the cement matrix cause a bonding incompatibility (Raftery et al., 2009) via agglomeration of unhydrated cement particles by the formation of impermeable hydrates (Frybort et al., 2008). Hence, interfacial adhesion significantly influences the final performance of any composite and must be analysed during the formation of a new composite.

2.7.1. Interfacial adhesion mechanisms

It is widely accepted that interfacial interactions have a major part in regulating global composite behaviour, since it influences the stress transfer between binding matrices and fibre reinforcements (Zhou et al., 2016), that alters the mechanical characteristics, and the resulting applications of the composite, via the effect of varying type and locality of the adhesion. Mechanical interlocking, Van der Waal's forces, chemical bonding, and electrostatic bonds are widely accepted as the main mechanisms of interfacial adhesion (Matthews and Rawlings, 1999; Zhang et al., 2016), although electrostatic bonds only have a significant influence in bonding of metallic interfaces (Amiandamhen et al., 2016).

Mechanical interlocking, or engagement, is a universal adhesion mechanism used in the composite industry, and can be classified as locking, one-way sliding, or two-way sliding

(Zhang et al., 2016). If composite fracture occurred due to either fibre destruction or matrix failure, instead of at the fibre-matrix interface, then mechanical interlocking is the dominant adhesion mechanism (Zhou et al., 2016). Adhesive penetration is a significant factor in wood adhesion in composite materials, since wood is porous and improved mechanical interlocking could be obtained since greater penetration into fibres yields better mechanical interlocking (Emblem and Hardwidge, 2012; Giles et al., 2005; Younesi-Kordkheili et al., 2016). Furthermore, the irregular shapes of lignin after plasticisation could aid in mechanical interlocking at the fibre-matrix interface (Thielemans et al., 2002) and processing temperature could play a significant role in the final composite properties.

Van der Waal's forces are very weak electrostatic attraction forces between all molecules, as a result of respective positive and negative charges, where larger molecules usually exhibit stronger forces due to increased contact surfaces (Emblem and Hardwidge, 2012). Van der Waal's forces are weak forces compared to chemical bonding, and ultimately impart weaker properties on composites than chemical binding, so much so that Wagh (2016) claims that these forces show insignificant influences on phosphate ceramics.

Chemical bonds are found at interfaces where the fibres and binders can react to form new chemical bonds and can only occur when the constituents are compatible – with similar polarity or functional groups that tend to react and bind (Amiandamhen et al., 2016; Giles et al., 2005). If constituent surfaces are smooth and impenetrable, it is more likely that chemical bonding dominates mechanical interlocking, pending chemical compatibility (Emblem and Hardwidge, 2012). FTIR spectroscopy can be used to identify distinctive chemical bonds that could possibly form at the constituent interfaces and is extensively used in composite material analysis (Zhou et al., 2016).

It is rarely the case that only one of the three main adhesion mechanisms can fully account for the total adhesion force between the composite constituents, since van der Waal's forces, however weak, exist between compounds in close proximity, while mechanical interlocking requires rough surfaces and improves with fibre penetrability, and chemical bonding depends on interfacial surfaces and compound chemical compatibility (Emblem and Hardwidge, 2012; Zhou et al., 2016). However, it is usually a case where one of the adhesion mechanisms dominate (Zhou et al., 2016). Various factors, such as chemical incompatibility and interfacial micro voids that inhibit chemical bonding and reduce van der Waal's forces, can cause inadequate adhesion where fibres can easily be separated from the binding matrix under applied

stress (de Lemos et al., 2017). Weak force dispersion will result in poor strength properties (Kabir et al., 2011), since the composites will be unable to function at larger strain limits (Amiandamhen et al., 2016).

2.7.2. Phosphate ceramic composite products

The chemically bonded phosphate ceramic can be used as binder in bio-composites, but is more expensive than the traditionally used Portland cement, and due to the exothermic nature of the formation reaction, could cause difficulty in up-scaling (Amiandamhen, 2017; Wagh, 2013). However, the addition of fibres, fillers, and additives will result in less heat generation, and lower production cost (Wagh, 2013). Paper, pulp, and saw mills, as well as agricultural businesses produce wood-based residues, such as lignocellulosic fibres, that could be used to manufacture these inorganically bonded composites (Frybort et al., 2008) with advantages such as high stiffness and tensile strengths, impact resistance, low cost production, biodegradability, flexibility, and renewability (Mngomezulu, 2019; Mohr et al., 2004; Sgriccia et al., 2008). This valorisation of wood-based waste will cause a reduction in energy costs and its resulting influences on human health (McDougall and Hruska, 2000). Additionally, the drive towards waste utilization will increase the development of technology and sustainable use of forestry materials (Mngomezulu, 2019).

The use of the phosphate ceramic to produce composites using fibres from bagasse, grass, trees, and even paper and pulp mill sludge was investigated by various researchers (Amiandamhen et al., 2017; Chimphango, 2020; Mngomezulu, 2019; Wagh, 2013). The reaction mechanisms for the acid-base formation of the phosphate ceramic is discussed in detail by Wagh (2013), including required temperatures, alkali solubility and crystal structure variation due to different ceramic formation tempos. This led to various optimum process conditions found by these researchers, namely the fibre to inorganic binder ratio (fibre:binder), binder ratio ($\text{KH}_2\text{PO}_4:\text{MgO}$), and amount of filler (% of binder), of 1.94, 5.05 – 5.07, and 15 – 22.5 %, respectively, while also showing that a maximum of 66 % sludge loading can be achieved for satisfactory composite performance (Amiandamhen et al., 2017; Chimphango, 2020; Mngomezulu, 2019).

Composite panels created with the phosphate binder could be engineered to adjust the strength, moisture resistance and stiffness, depending on the requirement of the final product, where, for example, roof tiles must have a high moisture resistance, and walls require high strength properties (Wagh, 2016). The reasons for the changes in properties when process parameters

are altered are discussed at length by Amiandamhen *et al.* (2016, 2017a); Mngomezulu (2019); and Mohr *et al.* (2004). The authors found that by increasing the amount of fibres the applied stresses are dispersed more evenly through the composite, thus increasing the modulus of elasticity (MOE), but moisture absorption also increases because of the hydrophilic nature of the lignocellulosic fibres. The authors further stated that by adding fly ash the board density is increased through filling the voids in the matrix, resulting in increased adhesion and stronger boards, but more ash decreases the amount of binder that can enclose the hydrophilic fibres, causing an increase in moisture absorption. The final product could have higher performance properties than the natural materials used in production when the processing variables are properly chosen (Rowell and Rowell, 1996).

However, even if the PS fibres are conditioned and mixed comprehensively with the binder to ensure even distribution and full encapsulation of the fibres for adequate support and proper strength properties, Amiandamhen *et al.* (2019) still found clean pullout of the fibres from the binder matrix to be the main failure mechanism of composite fracture at elevated stress loading. This suggests that the Van der Waal's forces predicted by Wagh (2013) do not yield satisfactory interfacial adhesion between the wood fibres and inorganic phosphate binder, and that no chemical bonding occurs between the ceramic and natural fibres (Mansur *et al.*, 2005). PS fibres that are bound with the magnesium potassium phosphate binder also exhibit comparably high water uptake due to large surface areas caused by fibrillation during the pulping process, and a high PS fibre content reduces the likelihood of the fibres being fully encased to further increase water absorption of the composites (Chimphango, 2020; Donahue and Aro, 2010). Numerous techniques can be used to improve the interfacial adhesion mechanisms such as increasing chemical compatibility and constituent contact. A reduction in inter-constituent void volume will ultimately improve strength properties due to enhanced stress transfer between the binder matrix and fibres (Mngomezulu, 2019). Fillers, especially calcium carbonate, reduce composite void volume to improve particle packing, due their fine size (Chimphango, 2020), while also possibly reacting with the phosphate binder to improve matrix crystallinity (Wagh, 2013). Increased processing temperature will result in accelerated solidification of the phosphate ceramic to finally improve bonding of wood particles to increase composite properties (Mngomezulu, 2019).

2.7.3. Lignin composites

Due to the chemical and physical properties exhibited by technical lignin, it is possible that lignin could improve the ceramic properties, and this section summarises studies that

researched the effect of lignin on different composites. Lignin is a naturally “stiff” molecule due to its high cross-linking rate and hydrogen bonds and could enhance the mechanical strength of bio-composites (Thielemans et al., 2002; Toriz et al., 2002).

The easiest utilization of lignin in composites is as a filler in thermosets as well as thermoplastics, resulting in composites with limited alteration in mechanical performance (Wool and Sun, 2011). Most composites, polymers, and polymer blends exhibit deteriorated performance at lignin contents more than 40 wt%, but recently, due to modification of lignin prior to inclusion in composites, thermoplastic composites contained 85 wt% kraft lignin, while still maintaining the required properties (Wool and Sun, 2011). Podschun et al. (2016) produced phenol-formaldehyde particleboards using phenolated lignin, where the active sites on the lignin was suggested to reduce water uptake, as well as increasing bonding strength. These composites contained between 20 and 40 wt% phenolated lignin. Cetin and Özmen (2002) used phenolated lignosulfonate to substitute 50 wt% of an expensive phenol-formaldehyde resin used to produce particleboards without reduced mechanical performance – achieving MOR of 10 to 16 MPa and MOE between 1 800 and 2 400 MPa. However, they found that increased lignin content improves MOE, but reduced MOR. Toriz et al. (2002) stated that if MOR decreases with lignin increase, then poor adhesion exists between components, since there are increased chances of failure due to improper stress transferal, while on the other hand, since lignin is a stiff particle it is expected to increase MOE. Toriz et al. (2002) came to this conclusion after producing polypropylene resin mixtures where 30 wt% replacement by lignin showed a threshold where MOE did not further improve, while MOR of the resin was maintained at the performance levels of the pure polypropylene resins up to 40 wt% replacement by lignin. Kraft lignin was also added to an epoxy adhesive, consisting of a polyamine and a diglycidyl ether of bisphenol A, to produce composites with maximum mechanical strength at 20 wt% lignin (Wool and Sun, 2011).

2.8. Veneer/lamination

Veneer is the fine wood that is applied to the composite material, whereas laminates are usually made of plastic to produce materials with improved strength and water-resistant properties. Both veneer and laminates are also used to improve product appearance (Mngomezulu, 2019), and could be necessary, since the addition of spent pulping liquor into the composite material could result in particleboards that are aesthetically unpleasing due to the dark colours introduced via the liquor. Research done by Mngomezulu (2019) has also shown that the performance of the PS fibre phosphate composites could be increased significantly by as much

as four-fold via laminates or veneer. The researcher used polyurethane glue to attach pine veneer, rotary cut to 3 mm, to phosphate ceramic composites and showed that mechanical strength and elasticity are improved to well beyond industry standards for particleboard.

The downside to adding extra material, adhesives, and processing steps to the composite material is the increased cost. If the same adhesive is used to bind the particles in a particleboard as well as for the laminating process, the process would be more economic, making it more competitive to use sludge in composite production (Raftery et al., 2009). Adhesive bonding is chosen over mechanical bonding, since it is a more effective method for binding wood composites with laminating materials due to the uniform transferral of shear stresses (Raftery et al., 2009). These adhesive bonded boards are used in numerous applications from furniture to construction (Grāvītis et al., 2010). Another property that must be considered when veneer is added to bio-composites is the difference in hygroscopic affected deformation between the veneer and the composite that could be detrimental to the wood-laminate bonds, and it is necessary that an adequate adhesive be selected (Raftery et al., 2009).

2.9. Industry standards

Composite materials technology aims to reduce material and production costs while also creating composite materials that combine the constructive aspects of the different materials used (Rowell and Rowell, 1996). Many combinations of particles (fibres, fibre bundles, flakes, chips, strands, and cellulose) and adhesives could be mixed to form composites with a wide range of structural and physical characteristics. Properties that largely influence the performance of composites are strength, stiffness, and dimensional stability (Rowell and Rowell, 1996). Depending on the final application of a composite, the desired properties will differ, and standards are required to ensure that the product meets a minimum specified quality.

2.9.1. Composite classification

To find the standards that should be considered when a new composite is tested, it is important to classify the various composite types as given by standards organisations. At present, “composite” is an umbrella term that describes any material where wood is adhesively bonded, and is divided into four main groups: composite material, edge-glued material, laminates, and veneer-based composites (Youngquist, 1999). Composite materials include fibreboard (insulation board, medium density fibreboard, and hardboard), particleboard, waferboard, wood-inorganic board, and wood-plastic board, while veneer-based and laminate materials are made from layering of thin sheets of material – where veneer is wood-based and laminate can

be made from any protective material such as plastic or rubber (Stark et al., 2010; Youngquist, 1999). Veneer overlays is also used to improve the appearance and mechanical properties of the composite (Stark et al., 2010). The classification can be done based on the size of the wood particle, properties of the wood particle, processing used to attain the particle, or the type of adhesive used (Cai and Ross, 2010; Stark et al., 2010).

Fibreboard is roughly categorised into insulating board ($160 - 500 \text{ kg.m}^{-3}$), medium density fibreboard ($500 - 800 \text{ kg.m}^{-3}$), and hardboard ($800 - 1450 \text{ kg.m}^{-3}$), where a homogeneous material is produced from lignocellulosic fibres that have been joined under heat and varying degrees of pressure – hardboard being formed under the largest pressures. Uses for fibreboard include sound deadening insulation, sheathing, furniture, door cores, trimming, construction, and furniture such as cabinets (Youngquist, 1999). Fibreboards can be produced using either a wet or a dry process, depending on the required properties and adhesive used, which is usually phenol- or urea formaldehyde or epoxy-based adhesives.

The prominent difference between fibreboard and particleboard ($600 - 800 \text{ kg.m}^{-3}$) is the manner in which the wood elements are configured, since particleboard utilises wood particles that are mechanically obtained, such as cut flakes, planar shavings, or sawdust, while fibres or fibre bundles can be formed via abrasive mechanical processes that are usually supplemented by chemical treatments (Cai and Ross, 2010). Particleboard is mainly used in interior applications such as furniture, cabinets, and for other decorative purposes. The production process is considered to be a dry process, since the fibres should contain around 7 % moisture when the panels are formed (Amiandamhen et al., 2016; Rowell and Rowell, 1996).

Another set of composites are wood-nonwood composites that is further divided into inorganic-bonded composites (gypsum-, cement-, and ceramic-bonded) and wood-thermoplastic composites (Stark et al., 2010). These wood-nonwood composites typically contain less than 60 wt% wood elements that are suspended in the nonwood binding matrix, resulting in higher density materials. Inorganic-bonded composites are formed by mixing the wood and inorganic materials with water and left to cure – with or without heat – and only yield acceptable performance properties when the wood is completely encased by a continuous inorganic matrix which is achieved by conversely mixing 10 wt% to 60 wt% wood with 90 wt% to 30 wt% binder (Stark et al., 2010). Furthermore, the phosphate ceramic binder that is focused on in this study can either be utilised as an adhesive – “spot-welding” the fibres together with an adhesive content between 15 and 20 wt% – or as a cement – encapsulating the fibres completely with a

cement content more than 30 wt%. Wood-thermoplastic material, another wood-nonwood composite, is defined as a composite where the binding agent softens with added heat. Thermoplastics that are deemed suitable for this type of composite must have a softening/melting temperature well below the degradation temperature of wood, around 200 °C (Stark et al., 2010).

2.9.2. Standards

The standards organisations used to determine the performance criteria of the new composites are: American Society for Testing and Materials (ASTM), American National Standards Institute (ANSI), which is a branch of the International Standards Organisation (ISO), and the British Standard European Norm (BS-EN) (Stark et al., 2010; Youngquist, 1999). The critical property standards are summarised in Table 6 to Table 8.

Firstly, density is an important property that is considered since it usually has a large influence on other properties of the material (Amiandamhen et al., 2017). **Table 6** summarises the density ranges of the different types of particleboard.

Table 6: Standards for density of different kinds of composite.

Type of board	Density range (kg.m ⁻³)	Standard
Medium density particleboard	640 – 800	ANSI A208 (1999)
High density particleboard	> 800	ANSI A208 (1999); EN 634-2 (2007)
Medium density fibreboard	500 – 850	(ANSI A208.2 (1994)
Hardboard	500 – 1 450	ANSI/AHA A194.1 (1985)
Inorganic cement resin boards	1 000	BS EN 634-2 (2007)
Inorganic cement resin boards	290 – 1 250	ASTM (2013)
Fibre reinforced cement boards	1 260 – 1 500	(AAAMSA Group, 2004)

Secondly, the strength and elastic properties of the composites are measured by testing the modulus of rupture (MOR), also known as the bending strength, the modulus of elasticity, or tensile elasticity (MOE), and the internal bonding (IB). The standards for these properties are summarised in **Table 7**. The internal bonding should range between 0.5 MPa (BS EN 634-2, 2007) and 0.7 MPa (EN 634 - 2, 2007). Chimphango (2020) found that the phosphate cement boards only achieved performance levels of low-density particleboards, and further investigation is required to increase the performance.

Table 7: Standards for modulus of rupture and modulus of elasticity of different kinds of composite.

Type of board	MOR (MPa)	MOE (MPa)	Standard
Insulating fibreboard	-	965	ANSI A208.2 (1994)
Low density fibreboard ($< 640 \text{ kg.m}^{-3}$)	14	1 400	ANSI A208.2 (1994)
Medium density fibreboard ($640 - 800 \text{ kg.m}^{-3}$)	24	2 400	ANSI A208.2 (1994)
High density fibreboard ($> 800 \text{ kg.m}^{-3}$)	34.5	3 450	ANSI A208.2 (1994)
Hardboard	31	-	ANSI/AHA A135.4 (1995)
Density of 800 kg.m^{-3}	4	3 000	EN 634-2 (2007)
Density of 1000 kg.m^{-3}	9	14 500	EN 634-2 (2007)
Particleboard	10 – 18	-	ISO16893 (2006)
Particleboard	16.5 – 23.5	2 400	ANSI A208.1 (1993)
Flooring underlayment	11	1 725	ANSI A208.1 (1993)
Low density cement board	0.7 – 5.5	621 – 1 241	Ref: (Cai and Ross, 2010)
Inorganic cement resin boards	9	4 000	BS EN 634-2 (2007)
Fibre reinforce cement board	7.5 – 14.4	3 974 – 7 747	(AAAMSA Group, 2004)
Wood plastics	25.4 – 52.3	1 530 – 4 230	Ref: (Cai and Ross, 2010)

Structural integrity is another important property that should adhere to standards developed for product quality. It is tested via water absorption (WA) and thickness swelling (TS) and is summarised in **Table 8**.

Table 8: Standards for water absorption, thickness swelling, and volume swelling of different kinds of composite.

Type of board	WA (%)	TS (%)	Standard
Fibreboard	10	-	ASTM C208-94 (1994)
Particleboard	50	-	ISO16893 (2006)
Portland cement boards	25	15	BS EN 634-2 (2007)
Particleboard	30	20	EN 634-2 (2007)

2.10. Gap in literature

As far as the knowledge of this researcher, there is at present, no research done on lignin/ceramic and lignin/paper sludge composites in literature. Numerous studies have investigated the modification of lignin to utilise as a replacement of epoxy- or formaldehyde resins, but none was found that utilise lignin treatment to improve the compatibility between lignin and ceramic materials. There is thus a lack in information on the formulation of lignin/paper sludge composites that meet the relevant industrial standards. Bonding mechanisms that explain interfacial interactions between lignin and ceramic binders, as well as between technical lignin and paper sludge fibres in composite materials should be explored, together with possible lignin precipitation from spent pulping liquor to achieve the desired paper sludge ceramic composite performance. Additionally, numerous economic studies of lignin modification and composite production have been found, but none on the economic viability of a lignin/paper sludge mixed composite project that can be developed by an existing paper and pulp mill.

2.11. Research questions and objectives

Key questions and research objectives central to this study were formed after a thorough literature review. The research questions arise from gaps found in literature regarding lignin phosphate composites. This section summarises these questions and objectives, while the next section outlines the experimental approach utilised to investigate these questions.

2.11.1. Primary research questions

1) Can lignin be used as a constituent (filler, additive, or binder replacement) in phosphate ceramic composites?

There is a gap in literature regarding the use of lignin as a solid adhesive replacement in phosphate ceramic composites. This study will determine if lignin can be used in these composites and in what amounts the expensive binder will be reduced if filler content is kept constant. Results from these tests will ultimately be used to identify the lignin as filler, additive, or a binder replacement, as well as for the classification of the new composite. Objective I aims to answer this research question.

2) Can spent pulping liquor be used or is lignin precipitation required to enhance the compatibility between lignin and other constituents in the paper sludge phosphate composite to ultimately achieve desired performance while maximising replacement of the said expensive components?

It is unknown if spent pulping liquor (that contain lignin) will be compatible with the inorganic binder. This study will investigate the altering effects of acid precipitation on lignin properties, as well as the compatibility between lignin (as acid precipitated lignin, as well as within kraft black liquor and spent sulfite liquor) and the phosphate binder to maximise lignin content while meeting industrial standards. Objectives I, II, and III work in tangent to answer this research question.

3) What interfacial adhesion mechanisms are influenced by the addition of lignin, and how are these mechanisms affected?

There are several interfacial adhesion mechanisms that govern composite properties. The effect of technical lignin on these mechanisms that occur among constituents in paper sludge fibre reinforced phosphate composites are unknown, and it will be investigated in this study. Objective IV focuses on this question.

4) How does the addition of lignin affect the techno-economic viability of the phosphate composite in a competitive market of inexpensive materials?

The effect of lignin addition to the composites will ultimately affect the production cost of the material, since possible alteration and quantity of lignin will influence processing equipment and the amount of binder used. Objective V aims to determine the economic viability.

2.11.2. Research objectives

- I. Determine the characteristics of different types of technical lignin that could be useful in phosphate ceramic composites.
- II. Determine if precipitated lignin will yield significant improvements compared to spent pulping liquors.
- III. Determine the technical viability of the lignin composites by evaluating the performance against previous research and industry standards.
- IV. Determine the effects of lignin on the interfacial adhesion mechanisms that control composite properties
- V. Determine the economic competitiveness of the new lignin composite in a competitive market of inexpensive construction materials.

2.11.3. General objective/aim

Valorise primary clarifier paper sludge and technical lignin emitted by paper and pulp mills by producing an industrially accepted and economically viable green composite material.

CHAPTER 3: RESEARCH DESIGN AND METHODOLOGY

This chapter aims to provide a detailed description of the experimental approach followed, the materials used, how these materials were prepared, and the methods utilised in forming and analysing the composite materials.

3.1. Experimental approach

The research done in this study follows the experimental approach as set out in **Figure 1**. Firstly, paper waste sludge and technical lignin were collected from three paper and pulp mills across South Africa. Kraft lignin samples were precipitated with sulfuric acid, whereafter the paper sludge, lignin in kraft black liquor, precipitated kraft lignin, and lignosulfonate, were chemically and physically characterised. This included moisture content, particle diameter, bulk density, water holding capacity, elemental analysis, and chemical composition, and was ultimately used to understand composite properties.

Composite production, testing, and statistical analyses of significant influence of process parameters were done iteratively to finally achieve maximum composite performance. This iterative process was used to find and refine the ranges of significant influencers, and finally determine the exact magnitude of lignin type, lignin content, and processing temperature that yield the best composite properties.

A selected number of composite products were then analysed via Fourier transform infrared spectroscopy, scanning electron microscopy, thermo-gravimetric analysis, and differential scanning calorimetry. The results of these analyses were used in conjunction with constituent characteristics to ultimately gain insight into the various interactions between lignin, sludge, and the phosphate that affect adhesion and consequently composite performance. The dark blocks in **Figure 1** indicate contributions to the novelty of this study, where it is the first time, as far as the knowledge of this researcher, that technical lignin (lignosulfonate, kraft black liquor, and precipitated kraft lignin) is used as a binder replacement in phosphate ceramics reinforced with paper sludge.

Finally, veneer was added for increased aesthetic appearance, as well as physical and mechanical performance that is required to achieve industry standards if this composite is to be a competitor in the market for inexpensive building materials. Preferred options based on technical performances were then assessed in terms of economic viability for local production.

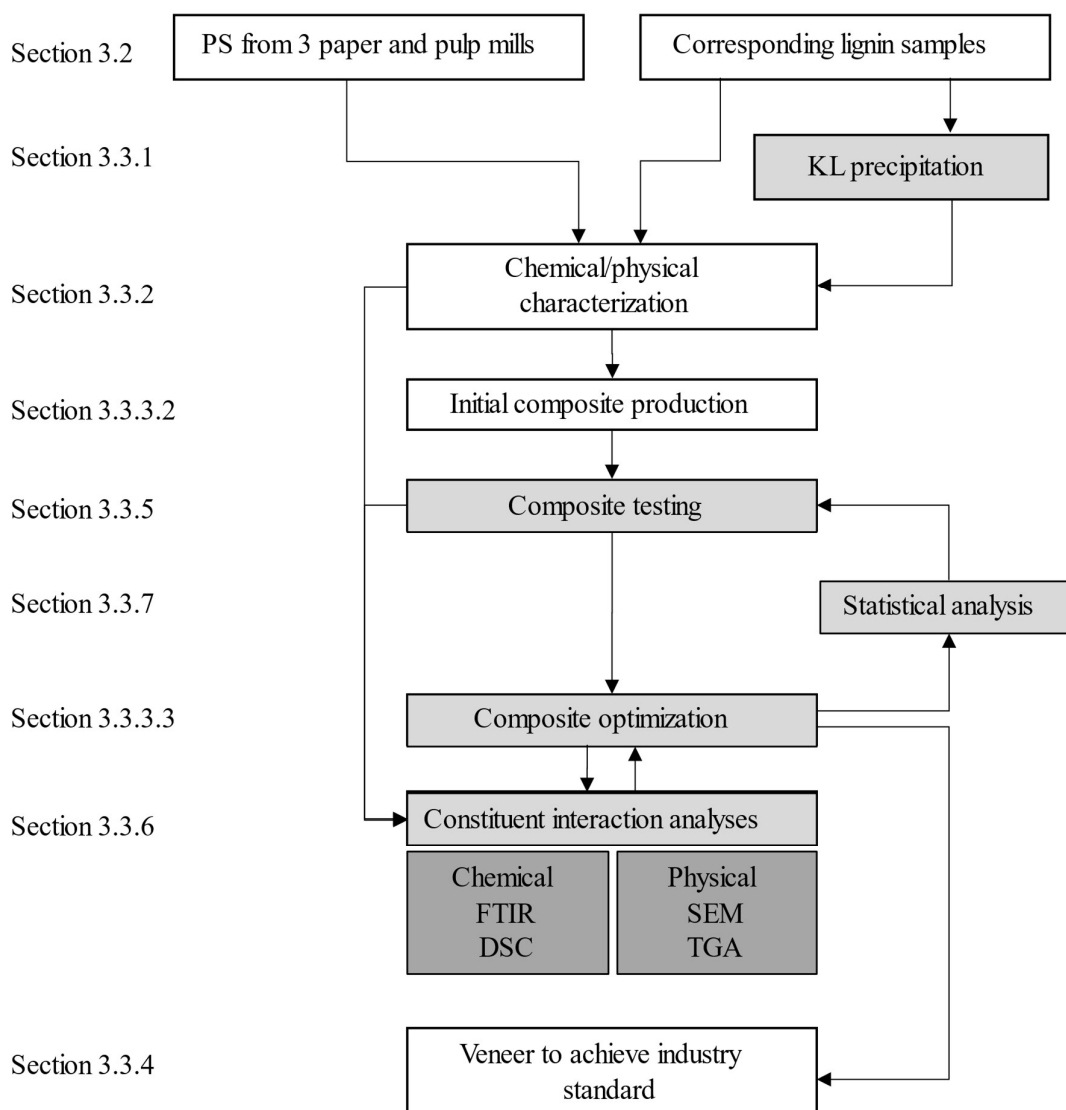


Figure 1: The experimental approach used to complete this study.

3.2. Materials

3.2.1. Paper sludge

Paper sludge (PS) was gathered from three paper and pulp mills across South Africa, namely Sappi Ngodwana, Mondi Richards Bay, and Mpact Piet Retief. These mills were chosen to represent the majority of technical lignin liberation processes in South Africa and across the globe – kraft and sulfite pulping. As set out by Donkor (2019), large impurities such as leaves and plastics were removed before the PS was dried at 40 to 45 °C. Thereafter the use of a quarter-coning subsampling method ensured homogenous PS mixtures per paper and pulp mill. A DrotskyS1 hammer mill with a 2 mm screen was used to mill the PS before it was stored in sealed plastic bags at room temperature.

3.2.2. Lignin

Technical lignins were collected in correspondence with the PS from Sappi Ngodwana, Mondi Richards Bay, and Mpact Piet Retief. These technical lignins represent the most dominant lignin types, i.e. kraft lignin (KL) and lignosulfonates (LS). Since LS is not suitable for acid precipitation (Naron et al., 2017) it was stored in sealed plastic containers as a liquor to use in subsequent analyses and composite production. Some of the KL was precipitated via sulfuric acid, while, for comparison, strong black liquor as received from kraft pulping mills was used and was thus also stored in sealed plastic containers.

3.2.3. Binder

The phosphate binder was produced by mixing magnesium oxide and monopotassium phosphate in an optimal ratio of 5.07:1 as found by Chimphango (2020). Heavy magnesium oxide (batch no. 303163576 K13/0619) from Kimix Chemical and Lab Supplies Co, South Africa was also used. The monopotassium phosphate (batch no. 3037581 K27/03/18) was also supplied by Kimix Chemical and Lab Supplies Co, South Africa and has the following chemical composition: assay 100.1 %; arsenic < 0.0003 %, and lead < 0.0005 %.

3.2.4. Filler

Calcium carbonate was used as a filler in the composite production. This filler with chemical composition of assay > 99.5 %, heavy metal < 0.0005 %, chloride < 0.001 %, and sulfate < 0.005 % was supplied by Kimix Chemical and Lab Co, South Africa.

3.3. Experimental methods

3.3.1. Lignin precipitation

One of the least complex lignin alteration techniques is sulfuric acid precipitation of the lignin, where the acidification of black liquor results in the precipitation of KL due to the conversion of ionic phenolic hydroxyl groups present on the KL molecule into its free form (Aro and Fatehi, 2017). The sulfuric acid precipitation method was adapted from Naron et al. (2017). 99 % sulfuric acid was used to reduce the pH of the KL to about 2, and after 24 h the KL was recovered via centrifugation at 8 000 rpm for 15 min. The KL was air dried for 48 h before it was milled with a DrotskyS1 hammer mill to a particle size range of 172 – 378 μm , and finally stored in sealed plastic bags. AP-KL and BL will be used to distinguish between the acid precipitated lignin and black liquor. To ultimately minimise processing costs, it was decided that, unlike Naron et al. (2017), the precipitated lignin should not be washed to remove impurities.

3.3.2. Feedstock characterisation

3.3.2.1. Moisture content

The moisture content of the dried PS and AP-KL was determined using the standard for wood preparation for chemical analysis (TAPPI T264 cm-07 in Donkor, 2019). Approximately 1.5 g of each of the samples were placed on a weighing glass and oven-dried for 24 h at 105 (±3) °C. The samples were cooled in a desiccator, weighed, and placed back into the oven for 1 h. This process was done iteratively until a constant mass was measured. Equation 6 shows how the moisture content was calculated.

$$MC (\%) = \frac{mass_{wet\ sample} (g) - mass_{dry\ sample} (g)}{mass_{wet\ sample} (g)} \times 100 \quad 6$$

3.3.2.2. Chemical composition

The lignocellulosic chemical compositions of paper waste sludge samples were determined in line with the NREL laboratory analytical procedure discussed by Sluiter et al. (2008, 2012) and is reviewed below.

Ash content

Ash content of the PS samples were determined according to the NREL/TP-510-42622 method (Sluiter et al., 2005). A crucible dish was placed into a muffle furnace at 575 ±25 °C for four hours, left to cool in a desiccator and weighed. Then, a carefully weighed oven-dried sample (0.5 – 1.5 g) is placed into the crucible that is then placed back into the muffle furnace at 575 ±25 °C for 24 h after which it was cooled in a desiccator for two hours before it was weighed. Thereafter the process is repeated with four-hour cycles until a constant mass is achieved. Equation 7 was used to calculate the ash content.

$$\%Ash = \frac{m_{ash\ and\ crucible} - m_{crucible}}{m_{oven-dried\ sample}} \times 100 \quad 7$$

Lignin and structural carbohydrates

Lignin, cellulose, and hemicellulose contents were determined using the NREL/TP-510-52618 method (Sluiter et al., 2012) and was adapted from Donkor (2019). The biomass sample was weighed and 0.5 ±0.1 g was hydrolysed with 72 wt% sulfuric acid at 30 ± 3 °C for 1 h. The solution was diluted to a 4 wt% acid concentration and autoclaved at 121 °C for 1 h, before it was filtered. The filtrate was analysed via UV-spectrophotometry (205 nm) to determine the acid soluble lignin (ASL) using equation 9, while HPLC measured the sugar content of the

filtrate that is used to predict the cellulose and hemicellulose content. The filter cake was dried at 105 °C and placed into the muffled furnace to ultimately determine the acid insoluble lignin (AIL) using equation 10. The total lignin content was taken to be the sum of the ASL and AIL.

$$dilution = \frac{volume_{filtrate\ sample} + volume_{dilutant}}{volume_{filtrate\ sample}} \quad 8$$

$$\%ASL = \frac{UV_{absorbance} \times Volume_{hydrolysis\ liquor} \times dilution}{absorptivity(\epsilon) \times m_{oven-dried\ sample} \times pathlength} \times 100 \quad 9$$

$$\%AIL = \left(\frac{m_{residue\ and\ crucible} - m_{crucible}}{m_{oven-dried\ sample}} - \frac{m_{ash\ and\ crucible} - m_{crucible}}{m_{oven-dried\ sample}} \right) \times 100 \quad 10$$

3.3.2.3. Elemental analysis

ASTM D4239 and ASTM D5373 standard methods for elemental composition was used to perform an ultimate analysis on the PS and lignin samples. The samples were combusted in a tungsten trioxide and oxygen enriched column at 1 050 °C to liberate water, carbon dioxide, sulfur dioxide, sulfur trioxide, and NO_x, which is used to determine the amounts of different elements using a Vario El Cube Elemental Analyser.

3.3.2.4. Bulk density

The bulk density of the PS was determined by filling a 200 mL measuring cylinder and recording the sample mass. Triplicate determination was completed to obtain a consistent bulk density measurement as calculated by equation 11.

$$\rho_B = \frac{mass_{sludge\ in\ cylinder} (g)}{volume_{cylinder} (mL)} \quad 11$$

3.3.2.5. Particle size distribution

The paper sludge particle size distributions were determined using a method of mass distribution as discussed by Bayvel and Jones (1981). The samples are sieved into groups with diameters < 250, < 425, < 600, < 800, and < 2 000 µm, after which the mass of each category is measured to finally calculate a weighted average diameter of the homogenous mixture using the Sauter mean diameter calculation as shown in equation 12. The mean diameter, sieve tray diameter, and sieve tray sample mass, as a fraction of the total sample mass, are denoted by d_{sm} , $d_{p,i}$, and x_i .

$$d_{sm} = \frac{1}{\sum_{i=1}^n \left(x_i / d_{p,i} \right)} \quad 12$$

3.3.2.6. Sludge water holding capacity

The water holding capacity (WHC) of the PS samples were determined according to procedures given by Boshoff (2015). The PS was oven-dried for 24 h at 105 (± 3) °C. Roughly 1.5 g of the sample was measured and placed into a weighed container, after which 30 mL reverse osmosis water was added. Adequate mixing of the sludge/water mixture was ensured before it was left to saturate for 24 h at ambient temperature. The sludge mixture was centrifuged at 5 000 rpm for 15 min and the supernatant decanted. Equation 13 shows how the WHC was calculated.

$$WHC \left(\frac{g \text{ water}}{g \text{ sludge}} \right) = \frac{m_{wet \text{ PS}}(g) - m_{dry \text{ PS}}(g)}{m_{dry \text{ PS}}(g)} \quad 13$$

3.3.3. Composite formation

3.3.3.1. Feedstock preparation

According to BS EN 634-2 (2007) the previously dried and milled materials were conditioned for 24 h at 25 °C and 65 % relative humidity before utilization in composite production. The equilibrium moisture content of the sludge after conditioning was measured at 7.1 %.

3.3.3.2. Board production

The method discussed in this section is based on previous research by Amiandamhen (2017), Chimphango (2020), and Mngomezulu (2019). The previously conditioned PS fibres were mixed with magnesium oxide, monopotassium phosphate, and calcium carbonate so that the fibre to binder ratio was 1.94:1, the MgO to KH₂PO₄ ratio was 5.07:1, and the CaCO₃ contributed 10 % of the total mass of the composite panel, as these were found to produce the best performing panels in the aforementioned reports. As per experimental design, varying contents of acid precipitated lignin, kraft black liquor, or lignosulfonate were mixed into the composite. Water was added based on equation 14, while also considering the water in the pulping liquors.

$$W = B + (FSP - MC)F \quad 14$$

The water required (mL), the inorganic components (g), fibre saturation point (%), fibre moisture content (%), and fibre content (g) are denoted by W , B , FSP , MC , and F , respectively. The B term includes the MgO, KH₂PO₄, CaCO₃, and the precipitated kraft lignin where applicable.

The slurry was mixed thoroughly to ensure homogeneity before it was placed in a mould that will ultimately produce panels with dimensions of 218x77x13 mm³. The moulds were pressed under 20 MPa of pressure to remove excess water and compact the material. The pressure was maintained for 15 min at a temperature specified by the experimental design, before the panels were demoulded and conditioned at 25 °C and 65 % relative humidity for seven days. All panels were fabricated in triplicate. The pressing force and period were based on results obtained by Amiandamhen (2017), Chimphango (2020), and Mngomezulu (2019).

3.3.3.3. Experimental design

The experiments were designed according to the initial ranges for the process variables shown in **Table 9** and is comparable to literature (Amiandamhen, 2017; Cetin and Özmen, 2002; Toriz et al., 2002; Younesi-Kordkheili et al., 2016). The process variables are lignin type (acid precipitated kraft lignin, black liquor, and lignosulfonates), lignin content, and processing temperature. Other process parameters, such as the paper sludge fibre to phosphate ratio, inorganic filler type and content, and the phosphate acid/base reactants ratio were previously optimized by Amiandamhen (2017), Chimphango (2020), and Mngomezulu (2019). The full factorial design (FFD), green squares in **Figure 2**, was initially used to determine the effects of the process variables on the physical and mechanical properties of the composites.

Table 9: Levels for the process variables tested via a full factorial design.

Process variables	Base				Levels			
Lignin type	None	AP-KL	BL	LS				
Parameter magnitude		Low	Medium	High				
Lignin content (wt%)	0	5	13	20				
Process temperature (°C)	100	25	63	100				

Analysis of the effects, together with fitted response surfaces and Pareto charts were used to evaluate the statistical significance of the relationships between the process variables and the response variables – moduli of rupture and elasticity. The statistical analysis was used in conjunction with chemical and physical analyses, discussed in section 3.3.6, to find the optimal mechanical response of the composites by first using a step-wise experimental approach and finally a central composite design (CCD), denoted respectively by the orange triangles and blue diamonds in **Figure 2**. The optimum was finally tested and validated via chemical and physical analyses as well as comparison to literature. The FFD resulted in five composite samples, with four additional panels made during the steps-wise experiments for each of the types of lignin –

acid precipitated kraft lignin (AP-KL), black liquor (KL), and lignosulfonate (LS). The CCD was only used for the AP-KL and LS composites. All samples were made and analysed in triplicate.

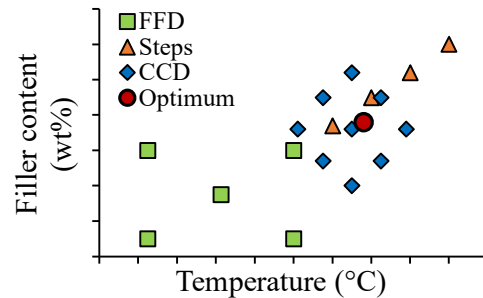


Figure 2: General design of experiments, showing the progression where an FFD was used initially based on literature. The FFD failed to contain the maximum of the response variable, thus a path of steepest ascent was determined, whereafter a CCD was set up around the range that would most likely yield optimum performance as determined by the stepwise setup.

3.3.4. Veneer application

York Timbers, situated in Mpumalanga, South Africa, supplied rotary cut *Pinus elliottii* veneer between 0.3 mm and 3 mm thick. The sheets were cut to 218 x 77 mm² to fit on top of the composite panels and left in a conditioning room at 25 °C and 65 % relative humidity for seven days, where after the moisture content was determined as 9 %. The surfaces of the composite and veneer were smoothed with 150 grit sandpaper and cleaned to remove any dust. PVA, supplied by Permoseal, was used as the resin to laminate the composites on both sides using the supplier suggested spread rate of 0.5 kg/m². The veneer composites were clamped for 24 h to ensure adequate penetration and bonding and left to dry for another 72 h at 25 °C and 65 % relative humidity. **Figure 3** shows the composite product with and without veneer.

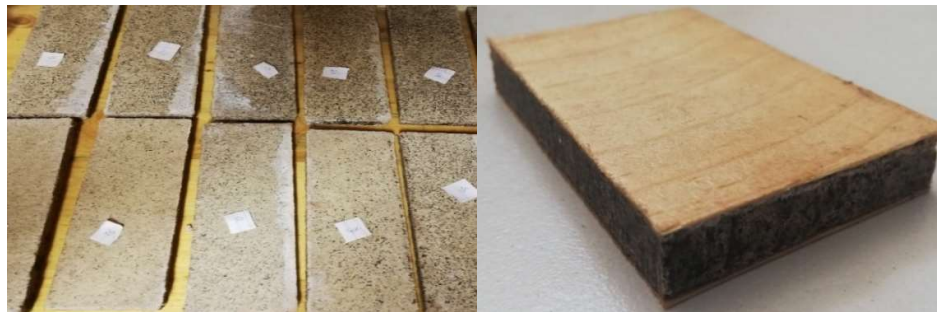


Figure 3: Composite products without and with pine veneer.

3.3.5. Composite property testing

To investigate the influences of varying process parameters on the composite physical (density and dimensional stability) and mechanical (moduli of rupture and elasticity) properties, the conditioned composite samples were tested using the methods described in this section.

The composite density was determined by weighing and measuring the samples according to the standards set out in ISO 9427 (2003). The dimensional stability was assessed via water absorption and thickness swelling according to standards given in BS EN 634-2 (2007). The samples were cut to 77x50 mm² using an angle grinder, and then weighed and the thickness accurately measured with a Vernier calliper. The samples were soaked in water for 24 h, where after they were removed, excess surface water was drained for 10 min (Mngomezulu, 2019), and the samples weighed and measured. The water absorption and thickness swelling were determined as percentages of the mass and thickness of the dry samples according to BS EN 634-2 (2007).

The mechanical properties were determined via a flexural strength test carried out on an Instron testing machine. A 5 kN load cell was fitted to the machine and the tests were performed according to standards given by ASTM D1037 (ASTM, 2012), and discussed by Amiandamhen (2017). The equipment was set to continuously increase the applied load at a fixed rate of 5 mm/min and the load-deflection curve was recorded for each sample with an accuracy of ± 0.5 % of the reading. The modulus of rupture was calculated using the maximum deflection and load before failure, while the modulus of rupture was calculated using the load/deflection slope in the normal operating range of the composite (BS EN 634-2, 2007).

3.3.6. Chemical and physical analyses of lignins and composites

The chemical and physical analyses used to determine properties of the various lignin types as well as to investigate composite interactions, both physical and chemical, are discussed in this section.

Fourier transform infrared spectroscopy (FTIR)

Lignin, PS, and composite samples were analysed with FTIR to investigate the chemical bonding mechanisms that influence composite properties. A Thermo Nicolet Nexus TM model 470 FTIR spectrometer was used for this purpose. The spectrometer was issued with ZnSE lenses against which the samples were pressed using a diamond surfaced spring loaded anvil, as well as an attenuated total reflectance module (ATR). Infrared absorption spectra, in the region of 6 000 – 400 cm⁻¹ wavenumbers, were recorded using a scanning resolution of 4 cm⁻¹ and a total of 64 scans per sample. The spectra were then baseline corrected and major absorption peaks were assigned functional groups based on literature (Dowell et al., 2013; Hajiha et al., 2014; Liu et al., 2004; Naron et al., 2017; Paauw and Pizzi, 1993; Sawpan et al., 2011; Wagh, 2013; Yang et al., 2015).

Scanning electron microscopy (SEM)

Micrographs of the samples are taken with a LEO 1430VP MERLIN FE-SEM using a magnification factor of a 1 000x. Sample preparation include adhesion of the sample to a metal stub using double-sided carbon tape, before it is placed into a S150A sputter coater at high vacuum where a thin gold layer is added to the sample for adequate conduction of the electrons to prevent bright spots on the micrographs.

Thermal gravimetric analysis (TGA) and differential scanning calorimetry (DSC)

Moisture content, volatiles, and thermal stability of the samples were determined according to the ASTM-E-1131 standard by measuring the mass change with temperature increase via thermogravimetric analysis. TGA was completed using a TA Instruments Q500 system with an inert nitrogen atmosphere, using a purge gas flow rate of 40 mL/min. Each sample, 2 – 15 mg, was carefully weighed and placed onto an aluminium sample pan. The sample mass was constantly measured while a ramp heating program of 10 °C/min was used to raise the temperature from ambient to 600 °C.

Phase transitions (glass transition, melting point) were quantified as a function of temperature using differential scanning calorimetry (DSC). A TA Instruments Q20 analysing system with an inert nitrogen atmosphere (purge gas flow rate of 50 mL/min), coupled to an RCS cooling unit, was used to perform the DSC analyses. The samples, 1 – 5 mg, were measured and placed onto non-hermetically sealed aluminium pans with a pinhole in the lid. A heating rate of 10 °C/min was used to heat the samples from ambient to 200 °C.

3.3.7. Data analysis

Experimental designs (FFD and CCD) were attained using Statistica version 13 that utilises a response surface method to determine the effects of and interactions between the experimentally varied process variables – lignin type, -content, and processing temperature – as well as to predict the reactions of the dependent variables (moduli of rupture and elasticity) to changes in the process variables. Analysis of variance (ANOVA) was used to estimate the significance of the effects that varying the process variables have on the composite properties. The means and standard deviations in data required for the statistical analysis were calculated from experimental results (done in triplicate) using Microsoft Excel 2016.

CHAPTER 4: EXPERIMENTAL RESULTS AND DISCUSSION

This chapter firstly discusses the feedstock properties that influence composite characteristics. These properties are used to investigate the change in composite performance when sludge type, lignin type, lignin content in the composite, and processing temperature are varied. Secondly, the interfacial adhesion mechanisms are investigated via physical and chemical analyses. Then, mechanical performance is optimised by altering lignin type and -content and processing temperature, and finally, as proof of technical viability, pine veneer is added to enhance composite performance and aesthetics to ultimately ensure that the new composite achieves industrial standards.

4.1. Sludge feedstock characterisation

It is well known that variations in fibre properties will cause fluctuations in the characteristics of the resulting composites (Amiandamhen et al., 2019; Chandra, 1997; Wagh, 2016). To ultimately understand the influence of the different sludge fibres used in this project, the paper and pulp mill sludges are characterised via chemical composition, functional group identification, bulk density, particle diameter, water holding capacity, and thermal stability, since these fibre properties influence composite performance (Yu et al., 2017; Zhang et al., 2020).

4.1.1. Sludge chemical composition

Paper and pulp mill sludge fibres in **Figure 4** contain cellulose, hemicellulose, lignin, and ash in varying ratios, which affect the bonding ability of the sludge (Chimphango, 2020; Davis et al., 2003). **Figure 4** indicates that MK-PS contains the most cellulose and hemicellulose (74.7 wt%), followed by SK-PS (70.9 wt%). The main difference between the kraft pulp sludges (MK and SK) are the lignin and ash contents, where MK-PS and SK-PS contain 9.1 wt% and 22.6 wt% lignin, and 16.2 wt% and 6.5 wt% ash, respectively. MS-PS, obtained via sulfite pulping, contains 29.5 wt% lignin, 24.1 wt% ash, and 46.4 wt% cellulose and hemicellulose. The composition of the sludges compare well to the compositions determined by Boshoff (2015).

Paper sludge feedstock that contain less ash content (inert material) was proven to yield better mechanical performance (Hong et al., 2018; Podschun et al., 2016; Raftery et al., 2009). This is also the case in this study, where, in section 4.3.2.2 (**Figure 16** and **Figure 18**), SK-composites (SK-sludge has the lowest ash content) had the best mechanical properties when composites with no additional lignin is considered. However, the reduced ash content results

in more hydrophilic organic material, that ultimately negatively impacted composite deformation during moisture exposure, section 4.3.2.3 and confirmed by Mngomezulu (2019).

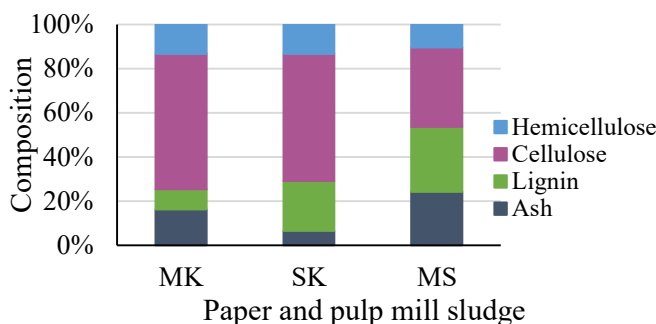


Figure 4: Chemical composition of the sludge from different mills.

4.1.2. Sludge fibre water holding capacity

Table 10 shows that SK-PS has the highest water holding capacity (WHC) of 14.6 g/g, followed by MK-PS, and MS-PS (3.0 g/g), which further suggests that SK-composites will have poor resistance to moisture deformation if the fibres are not protected from moisture via either surface modification or fibre encapsulation (Amiandamhen and Izekor, 2013).

Table 10: Sludge fibre water holding capacity.

Sludge source	WHC (g water/ g dry sludge)
MK-PS	12.5
SK-PS	14.6
MS-PS	3.0

4.1.3. Functional group identification

Figure 5 compares the FTIR absorption spectra of the sludges obtained from the Kraft (MK and SK), and sulfite (MS) pulping processes, and coincide with FTIR data obtained in other studies (Chimphango, 2020). The broad absorption peaks around 3300 cm^{-1} indicate that alcoholic and phenolic hydroxyl groups (associated with increased hydrophilicity (Amiandamhen et al., 2019)) are present in cellulose and hemicellulose fibres. The higher relative peak observed for SK-PS further supports the higher WHC shown in **Table 10**. Lower hydroxyl content, will result in increased compatibility between the natural fibres and inorganic phosphate binder (Mngomezulu, 2019; Wagh, 2013). Furthermore, the symmetric and asymmetric stretching of C-H bonds shown around 2900 cm^{-1} are common in organic material.

Peaks at 1620 cm^{-1} indicate C=C stretching as well as C=O stretching of acetyl groups in hemicellulose (Liu et al., 2004). The C=C bonds are also likely to react with other organic

substances present in the composite (Paauw and Pizzi, 1993). Aromatic structures are indicated by the peaks at $1\,500\text{ cm}^{-1}$, which suggests that lignin is still present in the sludge (Dowell et al., 2013) and is confirmed by the chemical composition analyses shown in **Figure 4**. Symmetric CH_2 bending in cellulose (Hajiha et al., 2014) and hydroxyl group (OH) bending occurs at $1\,425\text{ cm}^{-1}$. OH and CH bending in cellulose, hemicellulose, and lignin occurs at $1\,313\text{ cm}^{-1}$, whereas asymmetric stretching of C-O-C bonds in cellulose and hemicellulose arise at $1\,160\text{ cm}^{-1}$ (Yang et al., 2015), while C-C stretching of the β -glucosidic linkages between sugar units in hemicellulose and cellulose appear at $1\,032\text{ cm}^{-1}$ and 874 cm^{-1} (Hajiha et al., 2014; Sawpan et al., 2011; Yang et al., 2015). Since the C=C bonds, C=O bonds, aromatic structures, C-O-C bonds, and β -glucosidic linkages between sugar units are observed, it is concluded that although noticeable amounts of hemicellulose is removed during pulping, the cellulose and remaining hemicellulose structures are not significantly degraded, which is expected since the pulping process aims to remove or relocate lignin without destroying the cellulose structures required for further processing (Thompson et al., 2001; Zeng et al., 2017).

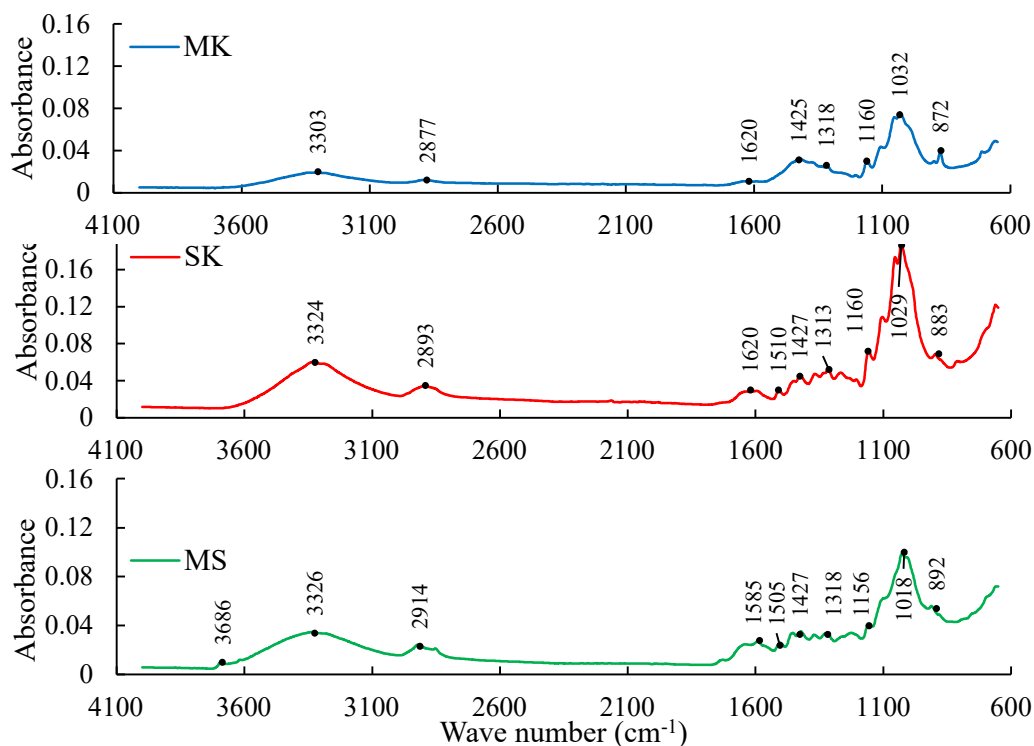


Figure 5: FTIR spectra of various sludge types.

4.1.4. Particle diameter

Particle diameter affects the bonding area around the fibres, thus influencing adhesion and distribution of shear stresses through the composite (de Alda, 2008). The Sauter mean diameters for the sludge particles were calculated, since it describes a uniform particle with the

same volume to surface area ratio as the sludge particles (Kowalczyk and Drzymala, 2016). The results for the Sauter mean diameter are summarised in **Table 11**, where MS sludge particles have the largest diameter of 408 μm , followed by MK sludge and then SK sludge (165 μm). Fibre diameters larger than 200 μm are more likely to provide adequate bonding surfaces for stress dispersion (Jeong and Wagh, 2003), hence MS-PS has an advantage, however, numerous other factors, such as the ash content and WHC already discussed, also affect composite properties.

Table 11: Sauter mean diameter for sludge particles.

Sludge source	d_{sm} (μm)
MK-PS	189
SK-PS	165
MS-PS	408

4.1.5. Bulk density

Table 12 shows the bulk density of the various sludges. Previous studies concluded that increased bulk density causes increased composite density, and *vice versa* (Chimphango, 2020; Migneault et al., 2011). This is observed when the paper sludge bulk densities in **Table 12** is compared to the densities of the composites that contain no additional lignin in **Figure 19**, section 4.3.2. According to English and Falk (1995) the fibre bulk density does not necessarily influence composite performance and the mechanical performances of the composites that contain no additional lignin, section 4.3.2, follow this observation, since MK, SK, and MS paper sludges show increasing bulk density, while SK composites (with no additional lignin) exhibit the best MOR and MOE performances (**Figure 16** and **Figure 18**), whereas MK and MS composites (without added lignin) respectively show the lowest MOE and MOR results.

Table 12: Bulk density of sludge from different paper mills.

Sludge source	Bulk density ($\text{kg}\cdot\text{m}^{-3}$)
MK-PS	43.7
SK-PS	48.9
MS-PS	389

4.1.6. Thermal stability

Paper sludge, containing mostly cellulose, hemicellulose, lignin, and inert materials (**Figure 4**), is thermally stable over a wide temperature range, and only start degrading around 260 $^{\circ}\text{C}$,

as shown in **Figure 6**. A maximum degradation rate around 320 °C is also observed, and coincide with results from Baker et al. (2012). Depending on the inert/ash content of the paper sludge, mass loss can be as high as 60 % to 80 %, which is also observed by Baker et al. (2012). The thermogravimetric analysis in **Figure 6** also indicates an initial mass loss between 50 °C and 100 °C – attributed to moisture evaporation (Toriz et al., 2002). Thus, all three paper sludge samples can be used in pressing processes that are heated to 250 °C without degradation – notable since the response surfaces in **Figure 15** and **Figure 17** show composite pressing temperatures between 115 °C and 160 °C, and there is thus no experimental evidence that paper sludge degradation will inhibit composite performance at these processing temperatures.

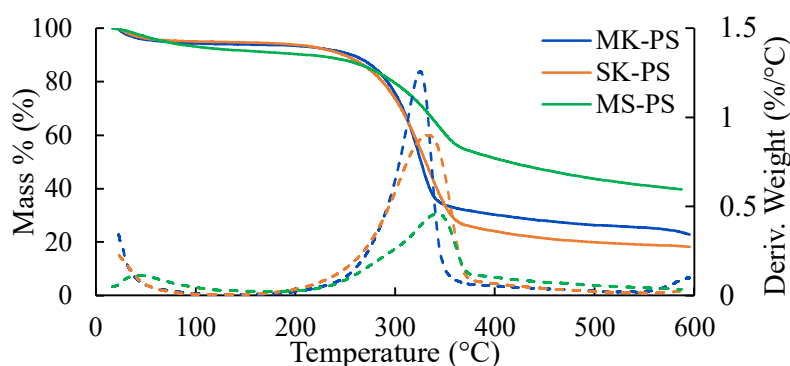


Figure 6: TGA curves for MK, SK, and MS paper sludge, The first derivative of the mass left is depicted by the dotted curves.

4.2. Lignin feedstock characterisation

To understand the lignin effects on chemical and mechanical interactions between components in the phosphate bonded paper sludge composites, this section investigates the elemental composition, functional group identification, and thermal stability of kraft black liquor, precipitated kraft lignin, and liginosulfonate.

4.2.1. Chemical characteristics of technical lignin

It is widely accepted that lignin recalcitrance to chemical modification and bonding reactions with fibrous components in composite materials is caused mainly by the hydroxyl groups (both aromatic and aliphatic) present in the lignin structure due to steric hindrances, increased hydrophilicity, and reduced chemical activity (Thielemans et al., 2002; Wool and Sun, 2011; Younesi-Kordkheili et al., 2016). Numerous studies have shown that the alteration of the hydroxyl groups is the most efficient modification mechanisms for increased usability of lignin in composite formulation (Podschn et al., 2016; Salanti et al., 2018; Wool and Sun, 2011). In this study it is proven that sulfuric acid precipitation of lignin from kraft black liquor sufficiently alters the lignin characteristics (discussed later in this section) to yield composite

materials with physical and mechanical performances that adhere to industrial standards (sections 4.3.2 and 4.4.2). However, lignosulfonate was not precipitated, since the acid precipitation is not viable due to the already low pH of lignosulfonates (Naron et al., 2017).

4.2.1.1. Average unit formulae of the monomeric units of lignin

To provide sufficient evidence that sulfuric acid chemically alters the lignin during precipitation from kraft black liquor, the average unit formulae of the monomeric phenyl propanoid units (PPU's) of lignin (obtained via elemental analysis and summarised in **Table 13**), as well as the lignin functional groups (obtained via FTIR analysis, **Figure 7** and **Table 14**) must be considered simultaneously. In **Table 13** the experimentally determined hydrogen and oxygen content per PPU compares well to what has been determined by other researchers (Gao et al., 2019; Lange et al., 2013). Furthermore, sulfuric acid precipitation of kraft lignin reduces hydrogen content, while oxygen and sulfur content are increased. To explain this observation, investigation of FTIR absorption spectra in **Figure 7** showed that hydroxyl functional group content was reduced while an increase in carbonyl groups was observed and a quantitative comparison between the lignin types, by estimating functional group quantity per lignin PPU via peak ratios (Culbertson Jr., 2017), is shown in **Table 14**.

Table 13: Estimated empirical formula for lignin from elemental analysis.

Lignin type	PPU formula	Source
MK black liquor	$C_9H_{8.28}O_{7.93}S_{0.09}$	
MK precipitated lignin	$C_9H_{8.01}O_{9.13}S_{0.49}$	
SK black liquor	$C_9H_{8.21}O_{4.06}S_{0.08}$	
SK precipitated lignin	$C_9H_{7.83}O_{6.27}S_{0.66}$	
MS lignosulfonate	$C_9H_{11.22}O_{11.14}S_{0.61}$	
Pine kraft lignin	$C_9H_{9.49}O_{2.68}S_{0.09}$	(Wool and Sun, 2011)
Hardwood kraft lignin	$C_9H_{10.03}O_{2.83}S_{0.09}$	
Softwood kraft lignin	$C_9H_{10.09}O_{3.23}S_{0.53}$	(Lange et al., 2013)
Sulfonated kraft lignin	$C_9H_{7.98}O_{5.67}S_{0.59}$	
Kraft lignin	$C_9H_{8.605}O_{2.996}S_{0.077}$	(Gao et al., 2019)
Sulfonated kraft lignin	$C_9H_{7.986}O_{5.671}S_{0.602}$	

More specifically, using the FTIR data in **Figure 7**, the number of C=O bonds and hydroxyl groups per aromatic structure in the kraft black liquor, precipitated kraft lignin, and lignosulfonate were estimated via a weak relationship between relative peak intensities at

1 720 cm^{-1} (carbonyl functional groups), around 3 350 cm^{-1} (-OH), and aromatic ring structures at 1 600 cm^{-1} . It is clear in **Table 14** that precipitated lignin has less hydroxyl and more carbonyl functional groups per PPU compared to black liquor. This is true for MK and SK samples, however SK lignin shows a final C=O content of 0.956 per aromatic ring, while MK only has 0.835 carbonyl groups per aromatic ring. As shown in “*Modulus of rupture*” in section 4.3.2, the slightly more C=O bonds present in the SK lignin results in less lignin required in the optimum composite mixture and the SK composites that contain the precipitated lignin perform marginally better than their MK counterparts.

Table 14: Relative peak intensities compared to aromatic ring structures in kraft lignin.

Relative group content	Precipitated MK lignin	MK black liquor	Precipitated SK lignin	SK black liquor
-OH	0.779	0.881	0.746	0.809
-C=O	0.835	0.552	0.956	0.556

4.2.1.2. Lignin functional groups

The lignin types shown in **Figure 7** exhibit clear similarities in the fingerprint region (1 600 cm^{-1} to 600 cm^{-1}). The peaks at 1 600 cm^{-1} indicate the vibrations of aromatic rings (Culbertson Jr., 2017), while syringal and guaiacyl ring vibrations appear at 1 180 cm^{-1} and 1 105 cm^{-1} , which also implies that the basic structure of the lignin was not altered markedly during pulping (Dowell et al., 2013) or the acid precipitation used in this study. Peaks between 1 010 cm^{-1} and 1 038 cm^{-1} are assigned to the stretching of C-O-C, C=C, and C-C-O bonds in lignin (Yang et al., 2015). Lastly, the deformation vibrations of C-H bonds in aromatic rings appear at 811 cm^{-1} for all lignin types (Younesi-Kordkheili et al., 2016). While the relative absorbance intensities at 1 3281 cm^{-1} , 1 207 cm^{-1} , and 1 104 cm^{-1} illustrate the different relative abundances of sinapyl and guaiacyl rings, as well as C=C bonds in kraft lignin and lignosulfonates (Dowell et al., 2013), they also show that sulfuric acid precipitation does not alter the main lignin structure, and that functional groups are changed only on side chains – also observed by Dowell et al. (2013) and Shen et al. (2008). Additionally, the rise in relative intensity of the peaks between 1 260 cm^{-1} and 1 150 cm^{-1} , and between 1 080 cm^{-1} and 1 010 cm^{-1} shows an increase in sulfonic content for precipitated kraft lignin (Kamoun et al., 2003). These sulfonate groups (SO_3^-) contain a free radical that could partake in reactions (Kamoun et al., 2003; Lange et al., 2013).

Furthermore, in **Figure 7** the IR absorption peaks around $3\ 350\ \text{cm}^{-1}$ are of lower relative intensity for the precipitated kraft lignin compared to kraft black liquor. Secondly, the peak at $1\ 712\ \text{cm}^{-1}$, indicative of conjugated carbonyl ($\text{C}=\text{O}$) groups (Skoog et al., 2014), showed an increase in intensity from kraft black liquor to precipitated kraft lignin, signifying the formation of these carbonyl groups (Culbertson Jr., 2017). Previous researchers in fact also found that lignin in kraft black liquor contains zero to very limited amounts of carbonyl groups since it does not show absorption at this wavenumber (Budnyak et al., 2019; Kaewtatip et al., 2010). The reduced hydroxyl group content coupled with increased $\text{C}=\text{O}$ bonds, suggest that lignin precipitation via sulfuric acid causes a condensation reaction (where the lignin and acid react to form water as a side product), and is confirmed by Kazzaz et al. (2019) and Wool and Sun (2011). These researchers state that the condensation reaction yields a free oxygen radical on the lignin structure that is, due to resonance stabilisation, observed as a double bonded oxygen in the form of a carbonyl, carboxyl, or aldehyde functional group – this is discussed in more detail by Kaewtatip et al. (2010). The free radical serves as a starting point for various lignin modifications, including amination, sulfonation, esterification, and epoxidation (Inwood et al., 2018; Kazzaz et al., 2019; Lange et al., 2013; Podschun et al., 2016; Zeng et al., 2017).

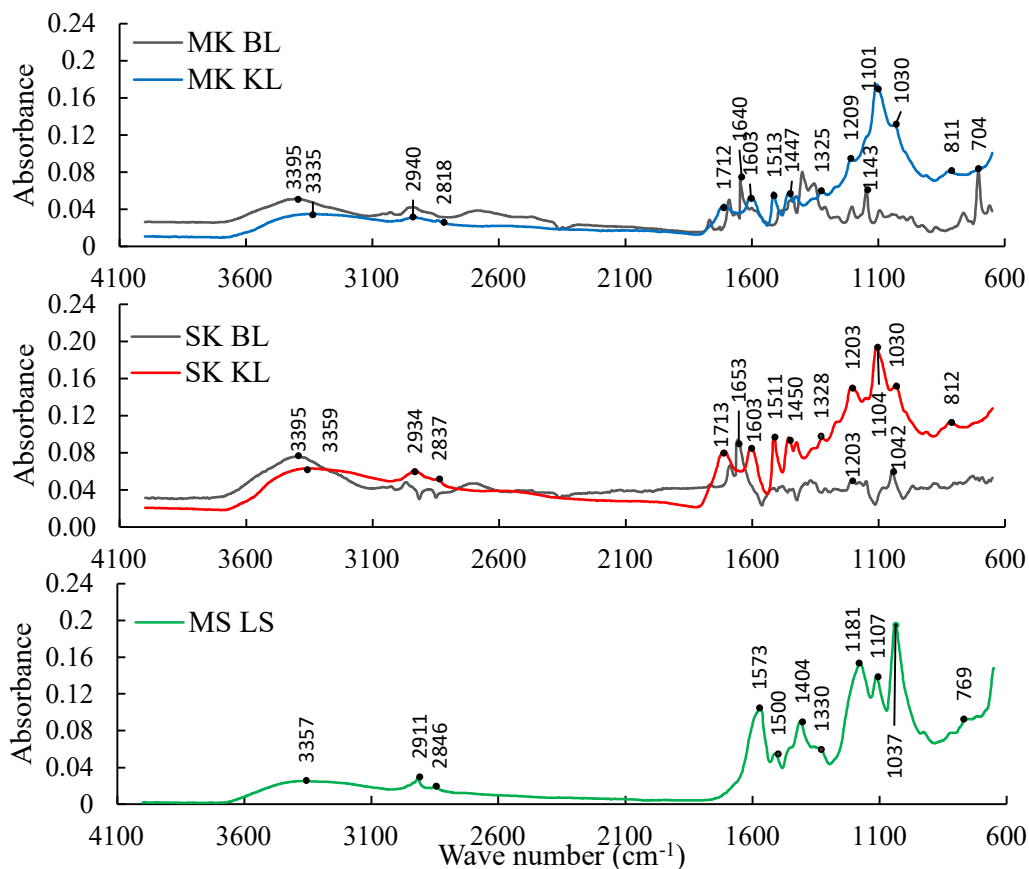


Figure 7: FTIR spectra of various lignin types.

In conclusion, sufficient evidence of the reduced hydroxyl content in precipitated kraft lignin is observed in **Table 13**, **Table 14**, and the infrared absorption spectra in **Figure 7**, and as already mentioned, altering hydroxyl groups is an efficient mechanism for increased usability of lignin in composite formulation (Podschun et al., 2016; Salanti et al., 2018; Wool and Sun, 2011). Thus, the increased performance of precipitated MK and SK composites compared to MS lignosulfonate, as well as MK and SK black liquor composites in section 4.3.2 is due to the observed lower hydroxyl and higher carbonyl content of the MK and SK precipitated lignin that influence the lignin-paper sludge interactions during composite formation – further discussed in section 4.3.1.

4.2.2. Thermal characteristics

4.2.2.1. Thermal stability

The thermal stability of a composite should be analysed to, firstly ensure that composite processing does not occur at temperatures that will result in constituent degradation, and secondly to determine the effects of increased temperature on the composite during its operational life cycle. In this section, thermal characteristics of lignin is studied to understand the possible influences lignin addition has on the composite performance and thermal stability. The temperature imposed mass changes of the MK black liquor and precipitated lignin (**Figure 8**), SK black liquor and precipitated lignin (**Figure 9**), and MS lignosulfonate (**Figure 10**) were measured via thermal gravimetric analysis (TGA). The first derivatives of the curves (dotted lines) are used to identify distinct thermal events. TGA results are largely impacted by sample mass, inert gas flow rate, and heating program (PerkinElmer Inc., 2010), thus, while the peaks in **Figure 8** and **Figure 9** are at slightly different temperatures, they indicate similar thermal events. The lignosulfonate (**Figure 10**) also exhibit similar thermal events, however the extent of mass loss differs markedly from the kraft lignin.

It is widely accepted that lignin is thermally stable below 200 °C (Brebu and Vasile, 2010; Toriz et al., 2002). Any mass loss before 200 °C is thus attributed to moisture evaporation (Brebu and Vasile, 2010). The precipitated kraft lignin shows a gradual water evaporation, starting around 50 °C and ending at 150 – 160 °C. Similarly low moisture liberation temperatures from lignin was observed by Domínguez et al. (2018) and Ház et al. (2019). Conversely, the kraft black liquor contains the moisture until 120 – 140 °C, with a maximum evaporation rate at 148 – 159 °C – hence the substantial difference in peak intensities below 200 °C between black liquor and precipitated lignin (**Figure 8** for MK, and **Figure 9** for SK). Lignin decomposition is a slow process that occurs over a wide temperature range between

200 °C and 500 °C, where a further increase in temperature results in the destruction of the degradation intermediates and the release of volatiles (Brebú and Vasile, 2010). The broad decomposition results from the various oxygen functional groups on the lignin with distinct thermal stability and scission properties.

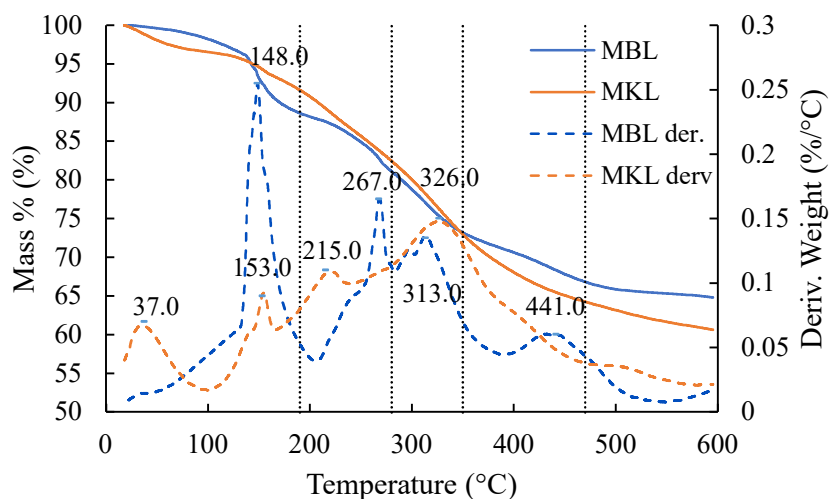


Figure 8: TGA curves for MK lignin contained within black liquor (MBL) and that underwent acid precipitation (MKL). The first derivative of the mass left is depicted by the dotted curves.

The lignin decomposition can be divided into three broad peaks – Brebú and Vasile (2010) discusses these peaks: firstly the polymer decomposition between 215 °C and 300 °C, with specific destruction of the lignin side chains between 260 °C and 280 °C; secondly, -ether links, as well as β - β and C-C links cleave between 280 °C and 350 °C; finally, the last degradation stage occurs between 350 °C and 450 °C when dimethoxy groups on the lignin undergo demethylation. Both MK and SK precipitated lignin showcase lower initial polymer degradation at temperatures cooler than 280 °C, where the precipitated lignins are thermally more stable due to improved cross-linking, better structured lignin, or increased chemical bonds (Salanti et al., 2018; Thielemans et al., 2002). Then, a larger mass loss occurs for the precipitated lignin between 330 °C and 380 °C, the result of aryl-ether and β - β links cleavage between the precipitated kraft lignin structures to form highly reactive free carbon radicals, while increased demethylation occurs within the kraft black liquor above 400 °C. Brebú and Vasile (2010) asserted that if the aryl-ether link fracture rates are slow, char forms due to the dominating cross-linking effect of the highly reactive carbon radicals. The char is thermally more stable, hence the lower demethylation rates of the precipitated kraft lignin around 450 °C compared to kraft black liquor.

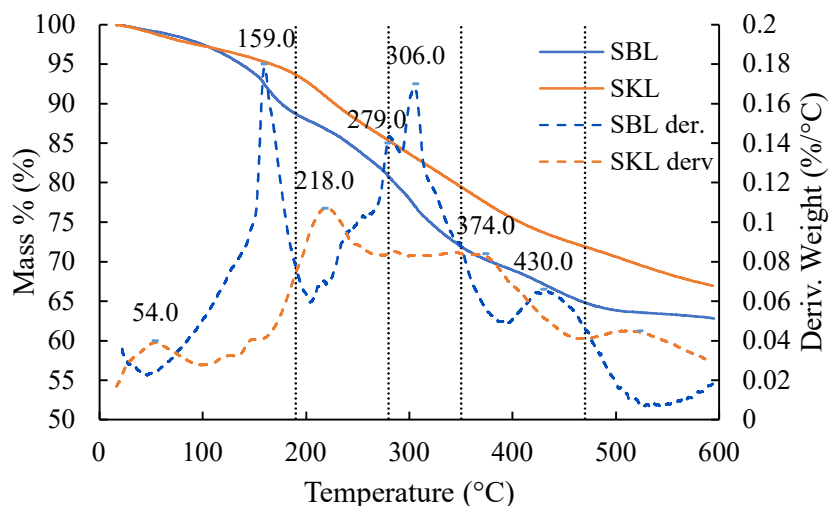


Figure 9: TGA curves for SK lignin contained within black liquor (SBL) and that underwent acid precipitation (SKL). The first derivative of the mass left is depicted by the dotted curves.

There is no pronounced difference in mass loss between the kraft black liquor and precipitated lignin below 600 °C in **Figure 8** and **Figure 9**, revealing that although the acid precipitation alters the lignin functional groups, the overall thermal stability stays relatively constant, with all kraft samples not losing more than 40 % mass at temperatures lower than 600 °C. Brebu and Vasile (2010) also observed a maximum of 40 % mass loss of kraft lignin up to 700 °C. However, the liginosulfonate exhibits larger mass loss due to polymer decomposition and propanoid side chain degradation between 200 °C and 280 °C, while almost no ether link, β - β , and C-C cleavage occurred between 300 °C and 350 °C, and, similar to the kraft samples, the liginosulfonate in **Figure 10** had a 42 % mass loss.

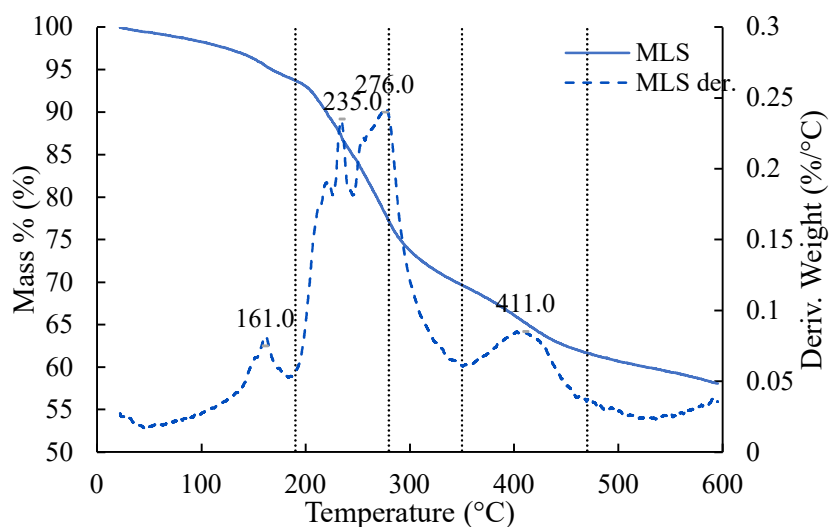


Figure 10: TGA curves for MS liginosulfonate (MLS). The first derivative of the mass left is depicted by the dotted curves.

The samples analysed in **Figure 8**, **Figure 9**, and **Figure 10** exhibit similar degradation stages to that shown by pure lignin samples studied by previous researchers (Brebú and Vasile, 2010; Domínguez et al., 2018; Ház et al., 2019) – this, in conjunction with the FTIR data in **Figure 7** that, as discussed in section 4.2.1.2, show sample peaks comparable to pure lignin, suggests that the organic part of the precipitated samples from black liquor is in fact lignin. The kraft black liquor and precipitated kraft lignin, as well as the lignosulfonate samples are all thermally stable at temperatures cooler than 200 °C. All the lignin samples degrade slowly over a wide temperature range, and lignin improves the apparent thermal stability of the composites formulated in this study (investigated in section 4.3) compared to composites that only contain paper sludge and the phosphate ceramic as binding agent, since previous researchers have proven that the phosphate rapidly degrades between 90 °C and 130 °C (Ma et al., 2014; Vinokurov et al., 2019; Wagh, 2016). These observations regarding the relatively high thermal stability of lignin and comparably lower thermal stability of the phosphate ceramic is considered in section 4.3.1.2 (*Thermal gravimetric analysis* of composites), where a trade-off between lower temperatures for low phosphate degradation and high processing temperatures for adequate lignin softening (next section 4.2.2.2) is shown and ultimately used to explain the experimentally determined optimum processing temperatures as per section 4.3.2.

4.2.2.2. Thermal softening of precipitated kraft lignin

The thermal softening (also referred to as glass transition) of the precipitated kraft lignin samples was investigated via differential scanning calorimetry (DSC) to determine if it aids in fibre encapsulation and mechanical interlocking – well known adhesion mechanisms in composite materials (Matthews and Rawlings, 1999; Zhang et al., 2016). Only the precipitated kraft lignin samples were analysed via DSC, since the kraft black liquor and lignosulfonate were added into the composites in solution form as received from the paper and pulp mills.

As discussed in 4.2.2.1, moisture evaporation from lignin occurs at a range of temperatures cooler than 180 °C and that the precipitated kraft lignin does not hold onto water until 180 °C before evaporation starts, rather the moisture is released at temperatures below 100 °C (Domínguez et al., 2018; Ház et al., 2019). This thermal event is also shown by the peaks between 60 and 75 °C of the DSC curves in **Figure 11**. The DSC curves measure the heat flow to and from the sample to ultimately identify thermal events that do not revolve around mass change - glass transition, melting, and chemical reduction that does not involve mass change (PerkinElmer Inc., 2010). Nevertheless, significant mass changes affect the heat flow via an alteration in sample heat capacity, however, from **Figure 8** and **Figure 9** the mass loss for MK

and SK samples (black liquor and precipitated lignin) between 130 °C and 175 °C is only 2.3 %, hence, the peaks at this temperature range in **Figure 11** are due to a phase change, more specifically a softening/glass transitioning or melting of the lignin – Culbertson Jr. (2017) stated purified softwood kraft lignin undergoes glass transition between 154 °C and 166 °C; Brodin (2009) showed that isolated softwood and hardwood kraft lignin exhibited glass transition around 148 °C and between 119 °C and 162 °C, respectively; and Toriz et al. (2002) studied lignin that undergoes glass transition between 140 °C and 170 °C.

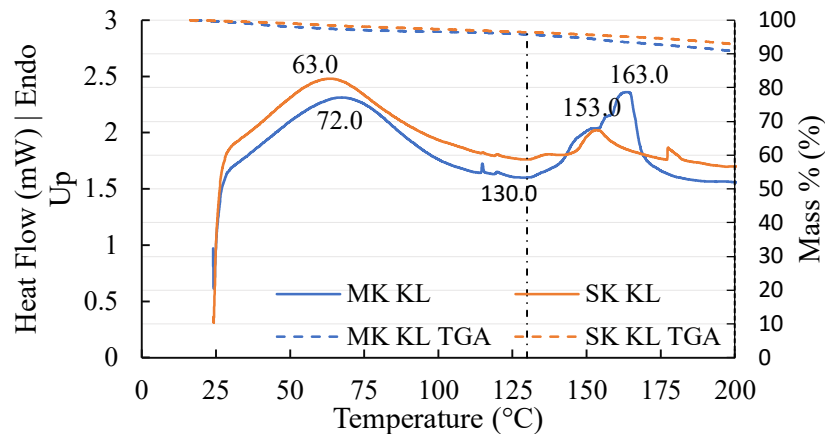


Figure 11: DSC curves for MK and SK acid precipitated lignin. The TGA responses are denoted by the dotted curves, while the softening onset temperature at 130 °C is highlighted by a dashed line.

Ultimately, during composite formulation, the observations above that (i) lignin does not degrade below 200 °C (**Figure 8**, **Figure 9**, and **Figure 10**), (ii) the precipitated lignin undergoes glass transition between 150 °C and 170 °C (**Figure 11**), and (iii) the phosphate binder significantly degrades between 90 °C and 130 °C (Ma et al., 2014; Vinokurov et al., 2019; Wagh, 2016) justify the temperature range of 100 °C to 160 °C chosen in the experimental design utilized in section 4.3.2 to find the optimal process conditions for maximum composite performance.

4.3. Composite performance

The composite performances are investigated for various sludge and lignin types, lignin content in composites, and composite processing temperatures. This section investigates the mechanisms that result in improved physical and mechanical performance, while also finding optimal lignin type, -content, and processing temperature for maximum mechanical properties by firstly screening to determine which processing variables (lignin type, -content, processing temperature, -pressure, and composite density) had the biggest effects on composite performance, and subsequently were chosen for central composite design (CCD) optimization.

4.3.1. Constituent interactions

To simplify discussions regarding observations and conclusions made from the composite properties in the following sections, this section investigates the interactions between constituent particles and the binder matrix to understand the effects lignin and processing temperature have on the composite properties. The composites examined in this section are, unless otherwise stated, produced from the optimum process conditions as obtained from section 4.3.2, summarised in **Table 17** as around 40 wt% precipitated kraft lignin, 20 wt% kraft black liquor, 20 wt% liginosulfonate, and at temperatures of 118 °C (MK – black liquor and precipitated lignin), 133 °C (SK – black liquor and precipitated lignin), and 155 °C (MS).

The interactions between constituent particles and the phosphate matrix occur at the surface interfaces between different phases, and include mainly mechanical interlocking, chemical bonding, and proximity affinity – weak chemical forces when compounds are in close contact (Emblem and Hardwidge, 2012; Wagh, 2016) – and depend on chemical compatibility, contact area, interface roughness, and availability of active surface chemical groups (Zhou et al., 2016). In this section chemical compatibility and surface chemical groups are investigated via FTIR, while TGA analysis is used to compare thermal stability of the various composites to infer changes in interfacial adhesion. SEM is utilized to examine the interfacial contact between constituents.

4.3.1.1. Fourier transform infrared spectroscopy (FTIR)

Figure 12 compares the composites that contain no lignin, kraft black liquor (denoted by BL composite), precipitated kraft lignin (denoted by KL composite), and liginosulfonates. The broad absorption peaks around 3 300 cm^{-1} indicate that alcoholic and phenolic hydroxyl groups are present in the composites. The symmetric and asymmetric stretching of C-H bonds found between 2 700 cm^{-1} and 3 000 cm^{-1} are common in organic material. The peaks around 1 410 cm^{-1} and 1 445 cm^{-1} indicate CH_2 bending of cellulose (Hajiha et al., 2014) and the presence of ionic carbonate from the filler (Skoog et al., 2014). The peaks at 1 320 cm^{-1} are assigned to OH and CH bending, while C-O-C asymmetric stretching of cellulose bonds occur at 1 153 cm^{-1} (Gao et al., 2019), and vibrations of glycosidic linkages in hemicellulose and ionic carbonate appear at around 870 cm^{-1} . The peaks between 1 585 cm^{-1} and 1 611 cm^{-1} are assigned to the stretching of C=C bonds during aromatic skeletal vibrations of lignin (Culbertson Jr., 2017), and naturally show increased peak intensity in composites containing additional lignin, be it precipitated kraft lignin, kraft black liquor, or liginosulfonates.

The infrared spectra shown in **Figure 12** also shed light on the chemical interactions between sludge fibres and lignin particles in the composites. Firstly, the decrease in relative peak intensity around $3\ 300\ \text{cm}^{-1}$ for precipitated kraft lignin composites show reduced OH content compared to lignin-free-, kraft black liquor-, and lignosulfonate composites, which has a twofold effect: improved chemical compatibility between the organic constituents and inorganic matrix for improved interface interaction (Wagh, 2013), and reduced hydrophilicity that will ultimately result in less water absorption and smaller composite deformation, proven in section 4.3.2.3 (*Physical properties*) and substantiated by Amiandamhen et al. (2017, 2019).

This observed reduction in OH content is a direct result of acid precipitation induced condensation reaction that form free oxygen radicals that are resonance stabilised as C=O bonds due to the relatively large lignin molecules, as discussed in section 4.2.1 above. A comparison between **Figure 7** and **Figure 12** show that the C=O bonds (resulting in infrared peaks between $1\ 680\ \text{cm}^{-1}$ and $1\ 730\ \text{cm}^{-1}$) present in precipitated kraft lignin disappear when the lignin is added into the composites. Furthermore, comparing the absorption spectra of composites containing no lignin and containing the precipitated kraft lignin (**Figure 12**) highlights an increased relative peak intensity between $1\ 050\ \text{cm}^{-1}$ and $1\ 120\ \text{cm}^{-1}$ when precipitated lignin is added into the composites, which indicates increased ether links (C-O-C) (Gao et al., 2019; Skoog et al., 2014). It is thus determined from the observable formation of these ether links in **Figure 12** that the acid precipitation, causing increased C=O groups in lignin, results in an improved bonding reaction between the lignin and cellulose/hemicellulose. Thielemans et al. (2002) and Zeng et al. (2017) discussed similar binding mechanisms between lignin and cellulose/hemicellulose fibres. Promisingly, ether links are also the most common linking mechanisms found in lignin polymers (Lange et al., 2013; Wool and Sun, 2011). This observed bonding mechanism, where lignin C=O groups bind with paper sludge via ether links, will be used in section 4.3.2.2 to rationalise changes in composite properties, more specifically the increased mechanical strength (section 4.3.2.2) and reduced overall water absorption (section 4.3.2.3).

As will be discussed under “*Dimensional stability*” in section 4.3.2.3, the composites that contain lignosulfonate are affected by moisture to an extent that they ultimately lose all structural integrity when submerged in water for 24 h, and the FTIR results in **Figure 12C** show that lignosulfonate composites exhibit increased OH content (at $3\ 360\ \text{cm}^{-1}$) compared to composites containing no added lignosulfonate. It is thus concluded that higher OH content results in raised hydrophilicity and is substantiated by Amiandamhen (2017, 2019).

Furthermore, increased sulfonic content for lignosulfonate composites is indicated by higher relative peak intensities between $1\ 034\ \text{cm}^{-1}$ and $1\ 180\ \text{cm}^{-1}$, and will increase the apparent polarity of the constituents (Kazzaz et al., 2019). The increased polarity coupled with the resonance stabilisation due to the aromatic rings in lignin (Lange et al., 2013) should improve Van der Waal's forces (vdW) at the adhesion interfaces to increase mechanical strength of the composites (Leite et al., 2012; Zhou et al., 2016). However, vdW forces are not as strong as chemical bonding (Emblem and Hardwidge, 2012; Wagh, 2016) and, as discussed in section 4.3.2, lignosulfonate will not enhance mechanical performance as much as precipitated kraft lignin, while the increased hydrophilicity due to the lignosulfonate will also diminish the dimensional stability of the composite compared to lignin-free- and kraft lignin composites.

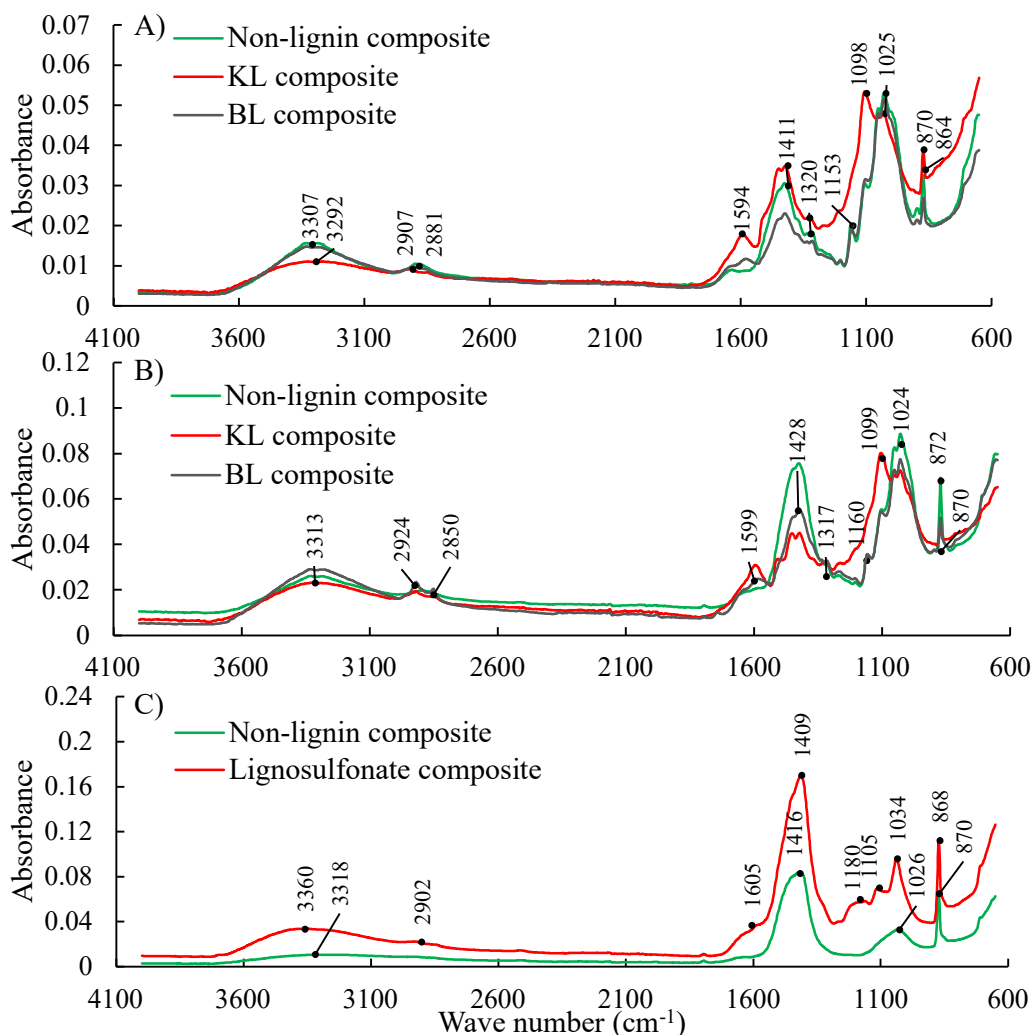


Figure 12: FTIR spectra for A) MK, B) SK, and C) MS composites.

4.3.1.2. Thermogravimetric analysis (TGA)

This section aims to investigate thermal characteristics of the composites, by determining if lignin addition yields composites with improved thermal stability via TGA. It is important to understand the thermal characteristics of the composite to avoid fabrication temperatures that are higher than the degradation temperatures of the composite.

The TGA results are shown for MK black liquor- and precipitated lignin composites (**Figure 13A**), SK black liquor- and precipitated lignin composites (**Figure 13B**), and composites containing MS lignosulfonate (**Figure 13C**). Since the composites in this study are novel, there are limited comparable results in literature, but similar thermal events were observed by Mngomezulu (2019) for phosphate bonded composites that contained pine-, black wattle-, and bagasse fibres. Additionally, a study of the thermal degradation mechanisms of paper sludge (between 250 °C and 350 °C, **Figure 6** in section 4.1.6) and lignin (section 4.2.2) suggests that the composite thermal stability results in this section are reasonable. All composites release moisture between 50 °C and 100 °C, however, the composites that contain kraft black liquor had slightly more evaporation induced mass loss of 9.6 % – 10.2 % compared to the moisture loss of 7.9 % – 8.1 % of the precipitated kraft lignin composites. After evaporation the mass loss of the kraft composites in **Figure 13A** and **Figure 13B** is nearly zero until the degradation onset temperatures, around 200 °C, are reached, while the MS composites in **Figure 13C** show a gradual mass loss until 200 °C. Then, the most prominent thermal degradations for the MK, SK, and MS composites occur between 200 °C and 350 °C, where after degradation happens at a slower rate until 600 °C.

When precipitated kraft lignin is used in the composite instead of kraft black liquor, the overall mass loss of the kraft composites in **Figure 13A** and **Figure 13B** is reduced from 40 % to 30 %, while lignosulfonate composites in **Figure 13C** showed mass loss of 35 %. Thus, composites containing precipitated kraft lignin, compared to kraft black liquor composites, have increased thermal stability. This further substantiates that the precipitated kraft lignin chemically binds to the paper sludge, as concluded from the observed changes of the carbonyl groups into ether linkages in **Figure 12**, section 4.3.1.1, since it is widely accepted that increased chemical bonding between composite constituents results in improved thermal stability (Wool and Sun, 2011; Salanti et al., 2018; Wang et al., 2019). In section 4.3.2, the improved chemical bonding between the precipitated kraft lignin and paper sludge, compared to the kraft black liquor and lignosulfonate, is used to explain the differences in performance of the composites that contain the precipitated lignin, kraft black liquor, and lignosulfonate.

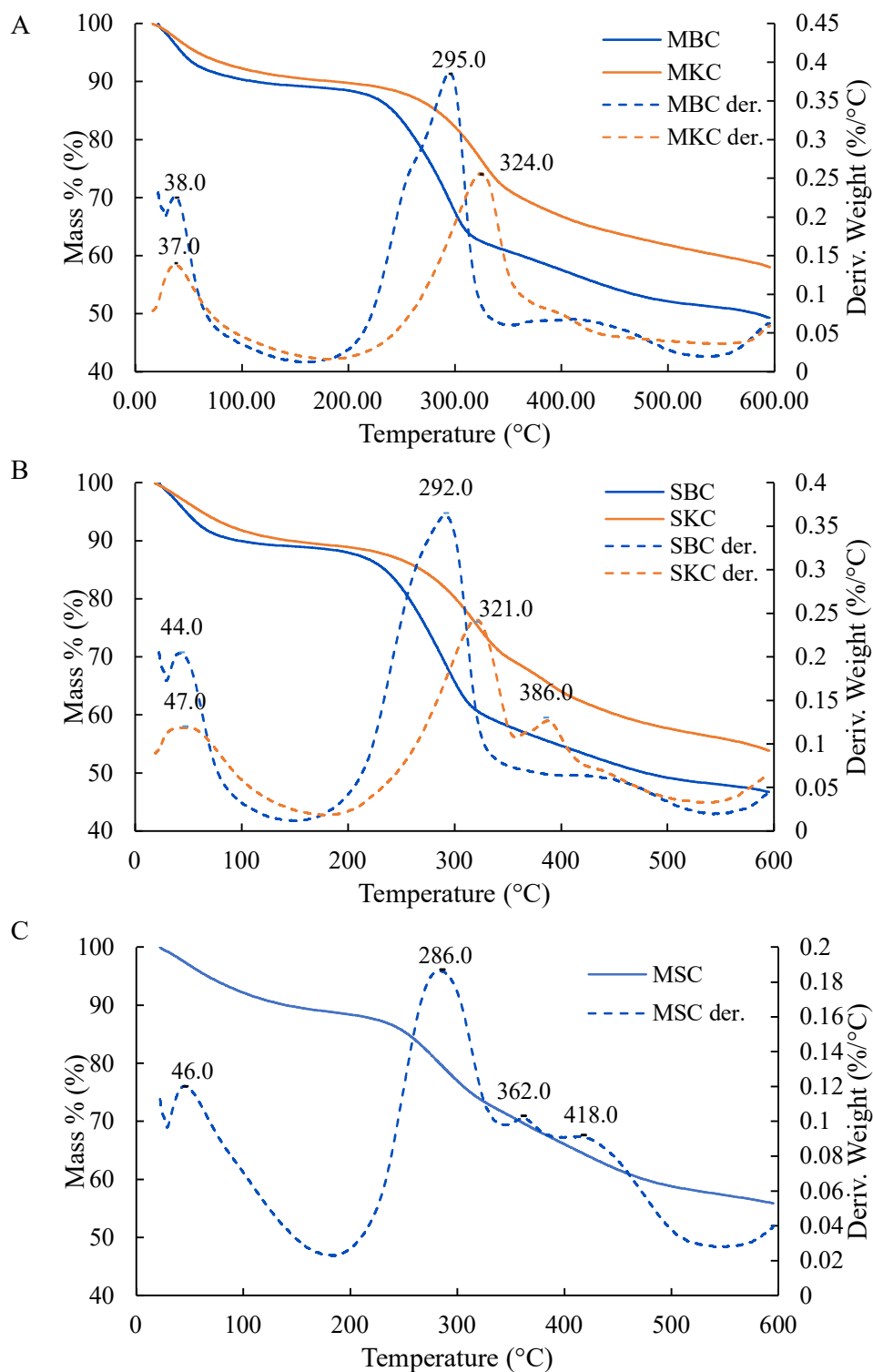


Figure 13: TGA curves for composites containing: (A) MK; (B) SK kraft black liquor (MBC and SBC) and precipitated kraft lignin (MKC and SKC); and (C) MS lignosulfonate (MSC). The first derivative of the mass left is depicted by the dotted curves.

4.3.1.3. Scanning electron microscopy (SEM)

To understand the failure process and gain insight into the adhesion mechanisms the focus of the micrographs in **Figure 14** is mainly on the fracture surface of the composites after destructive testing.

The small crystalline structures visible in all composites (red circles 1) are attributed to the presence of the magnesium potassium phosphate ceramic and calcium carbonate filler – the formation of these microstructures is extensively discussed by Viani et al. (2019). These crystalline structures clump together to form more complex constructions – the matrix that covers the elongated paper sludge fibres. Furthermore, in **Figure 14G** the glassy phase (red circle 2) shows the effect of heating and cooling of the acid precipitated kraft lignin (as discussed via the foregoing thermal analyses in section 4.2.2) and the deformation of the lignin around other particles is visible. Mechanical attachment depends on the binder flowing into and around the fibres (Giles et al., 2005) and it is thus concluded that the lignin softening (as per section 4.2.2) due to processing temperatures around 130 °C improved mechanical interlocking, supplementary to the chemical bonding as discussed previously (FTIR results in section 4.3.1.1). This mechanical interlocking and chemical bonding are the main adhesion mechanisms used to discuss the observed variations in composite properties in the following section 4.3.2.

Kraft black liquor yields composites with increased fibre dispersion (**Figure 14D**) but still insufficient fibre encasement (**Figure 14C**). Conversely, composites containing lignosulfonates show improved fibre encapsulation (**Figure 14E**), however, clean fibre pullout is visible in **Figure 14F** (red circle 3), which suggests a lack of interfacial adhesion (de Lemos et al., 2017). Finally, composites containing the precipitated kraft lignin shows a solid, continuous matrix structure that fully encases the fibres (**Figure 14H**) that will improve composite performance (observed in section 4.3.2). The importance of a continuous binding matrix that must envelope fibres is highlighted by Amiandamhen et al. (2019). Additionally, these precipitated kraft lignin composites did not fail due to fibre pullout, but rather due to fibre failure (4) and matrix fracture (red circle 5), while the fibre stayed firmly embedded within the binding matrix to prove good adhesion for interfacial stress transfer (Wang et al., 2019).

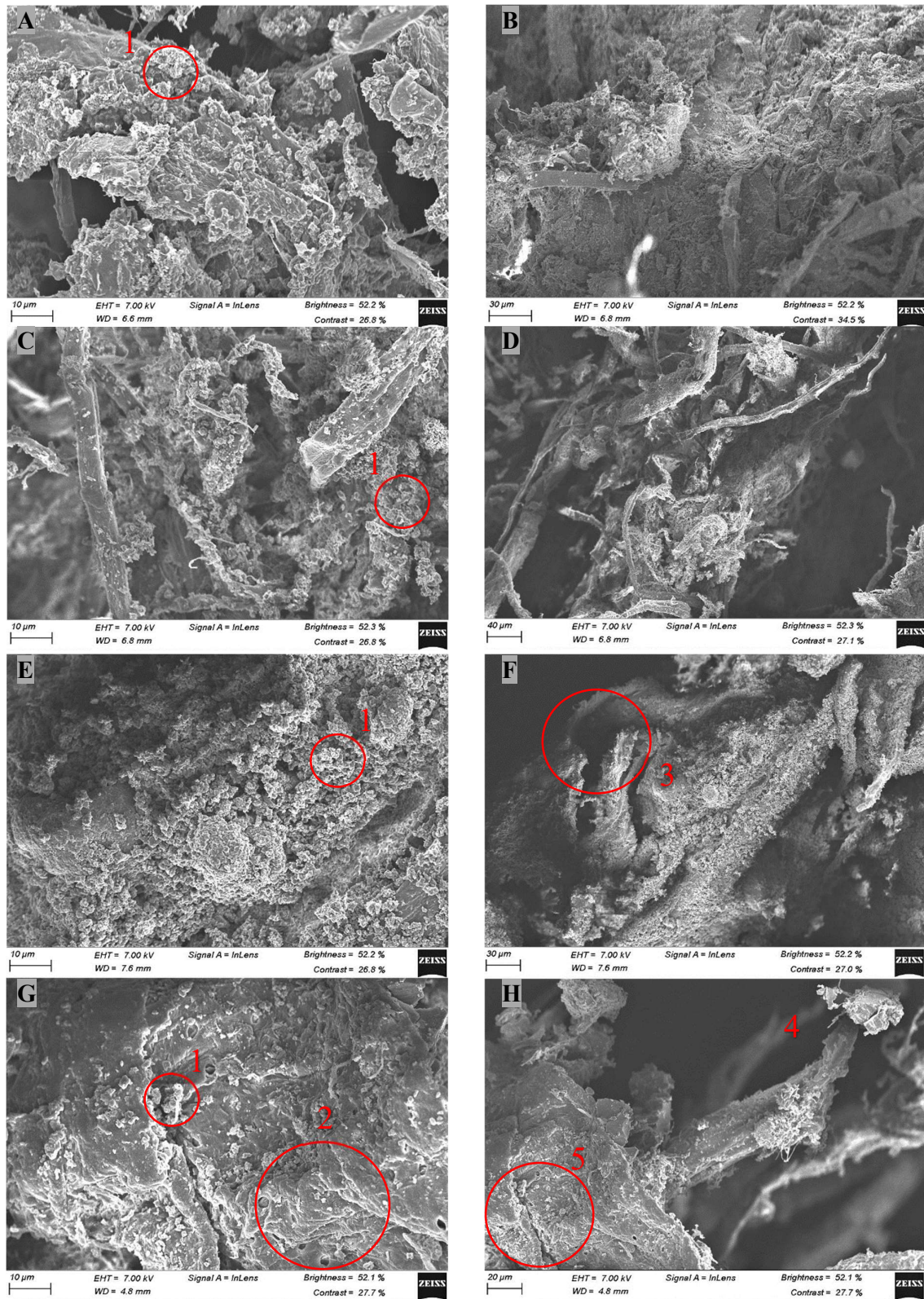


Figure 14: Micrographs of composites that contain no additional lignin (A and B); 20 wt% kraft black liquor (C and D); 20 wt% liginosulfonate (E and F); and 40 wt% precipitated kraft lignin (G and H). The micrographs on the left were taken at a larger zoom factor than on the right.

4.3.2. Composite properties

In this section, the effect of different lignin-paper sludge formulations and processing temperatures for composite production were evaluated in terms of their influence on the physical and mechanical properties of the composites to obtain optimised performances. The composite performances are also compared in terms of the interfacial adhesion mechanisms (from section 4.3.1) likely to be responsible for these differences among formulations.

4.3.2.1. Composite formulation

Firstly, the optimum phosphate to paper sludge ratio of 1:1.94, as obtained from Chimphango (2020), was verified by producing composites with three levels of phosphate to paper sludge ratios, as shown in **Table 15**, and the mechanical performances of these composites are summarized in APPENDIX A.1, where composites not containing the optimum ratio of 1:1.94 showed inferior performance compared to composites that contained this ratio. Next, composites were produced using a full factorial experimental design (FFD), where after a set of composites were made from statistically determined paths of steepest ascent (for mechanical performance). From these results, rational ranges for the most significant process conditions were determined and utilized in a central composite design (CCD) to finally obtain maximum mechanical performances that were statistically and experimentally confirmed and rationalised with the constituent interactions as discussed in the previous section 4.3.1. The process conditions for the FFD, experimental setup for the pathway steepest ascent, and CCD are shown in **Table 16**. The measured moduli of rupture and elasticity for these composites are summarised in APPENDIX A.1, while for the purpose of clarity in this section, only four composites with significantly different properties from each of the paper and pulp mills are discussed to clearly show the lignin and temperature influences on composite performance – firstly, zero lignin (green) composites serve as the basis for comparisons. Secondly, 5 wt% lignin (orange) composites were chosen as the low lignin iteration., with the middle lignin the optimal mechanical performance as per section 4.3.2.2 (red bars), and high lignin (yellow bars) of 20 wt%, 40 wt%, and 60 wt% for black liquor, lignosulfonate, and precipitated lignin.

Table 15: Verify optimum phosphate to paper sludge ratio obtained by Chimphango (2020).

Mill	Lignin content (%)	Temp (°C)	Density (kg.m ⁻³)	Phosphate : paper sludge		
				Low phosphate	Medium phosphate ^a	High phosphate
MK	20.0	100.0	1 000	1:3	1:1.94	1:1
SK	20.0	100.0	1 000	1:3	1:1.94	1:1

^a Optimum ratio from Chimphango (2020)

Table 16: Summary of the three experimental setups completed for each of the paper mills.

FFD for MK, SK, and MS						
Variable	Variable magnitude					
	Base	Minimum	Low	Medium	High	Maximum
Lignin content (%)	0.0	NA	5.0	13.0	20.0	NA
Temp (°C)	100.0	NA	25.0	63.0	100.0	NA
Density (kg.m ⁻³)	1 000	NA	900	NA	1 200	NA
Path of steepest ascent						
Pathway steps	MK		SK		MS	
	Lignin content (%)	Temp (°C)	Lignin content (%)	Temp (°C)	Ligno-sulfonate content (%)	Temp (°C)
1	40.0	130.0	40.0	130.0	30.0	150.0
2	50.0	170.0	50.0	170.0	40.0	200.0
3	60.0	200.0	60.0	200.0		
CCD						
	Variable	Variable magnitude				
		Minimum	Low	Medium	High	Maximum
MK	Lignin content (%)	16.0	25.0	32.0	38.0	47.0
	Temp (°C)	70.0	90.0	105.0	120.0	140.0
SK	Lignin content (%)	17.0	25.0	31.0	37.0	45.0
	Temp (°C)	70.0	90.0	105.0	120.0	140.0
MS	Ligno-sulfonate content (%)	11.0	17.0	24.0	30.0	37.0
	Temp (°C)	70.0	90.0	125.0	160.0	180.0

4.3.2.2. Mechanical properties

Mechanical performance is the most important composite property (Amiandamhen et al., 2019), and was thus used for optimisation purposes. The moduli of rupture (MOR) and elasticity (MOE) are the main mechanical responses measured in this study. Previous work investigated the sludge fibre to binder ratio as well as the filler type and content that will produce composites with optimum performance (Amiandamhen, 2017; Chimphango, 2020; Mngomezulu, 2019). It was therefore decided that to prove the value of lignin addition, these previously determined optimum process parameters will be used to ultimately highlight the lignin effects. It was determined in section 4.3.1.2 that processing temperature also significantly influenced the constituent interactions. Consequently, as discussed above, lignin content and process temperature were varied in this study inside the ranges following the logic of **Table 16** to find the optimal mechanical responses for composites and to understand how constituent interfacial adhesion is affected by varied lignin content and processing temperature.

Modulus of rupture

When comparing the composites that contain no additional lignin in **Figure 16** to previous work, MOR results from this study (1.0 MPa to 1.6 MPa) were observed to be similar to MOR results of phosphate bonded composites observed by Amiandamhen (2017) (between 0.6 and 1.4 MPa), and by Chimphango (2020) (between 1.2 and 2.5 MPa). However, by increasing lignin content and processing temperature, MOR results are markedly increased to a maximum, where further escalations in lignin content and temperature result in lower MOR results. These peaks in MOR responses are observed for precipitated kraft lignin (MK and SK) and lignosulfonate (MS) composites in **Figure 15** as 5.3 MPa, 7.2 MPa, and 3.3 MPa. The improvement in MOR performance due to lignin addition is also shown in **Figure 16** by the MOR results of four various lignin contents for different lignin types, where the lowest and highest MOR experimental responses are respectively given as 1.0 MPa and 5.3 MPa (MK); 1.6 MPa and 7.2 MPa (SK); and 1.4 MPa and 3.3 MPa (MS). These increases in MOR are statistically significant, with p-values smaller than 0.05 (MK: 0.0018; SK: 0.006; and MS: 0.009). Additionally, the Pareto charts in **Figure 15** indicate that lignin content, processing temperature, and their interaction all have significant effects on MOR for composites containing precipitated kraft lignin, while the lignosulfonate-temperature interaction has a statistically insignificant effect on the MOR response of MS composites ($p > 0.05$).

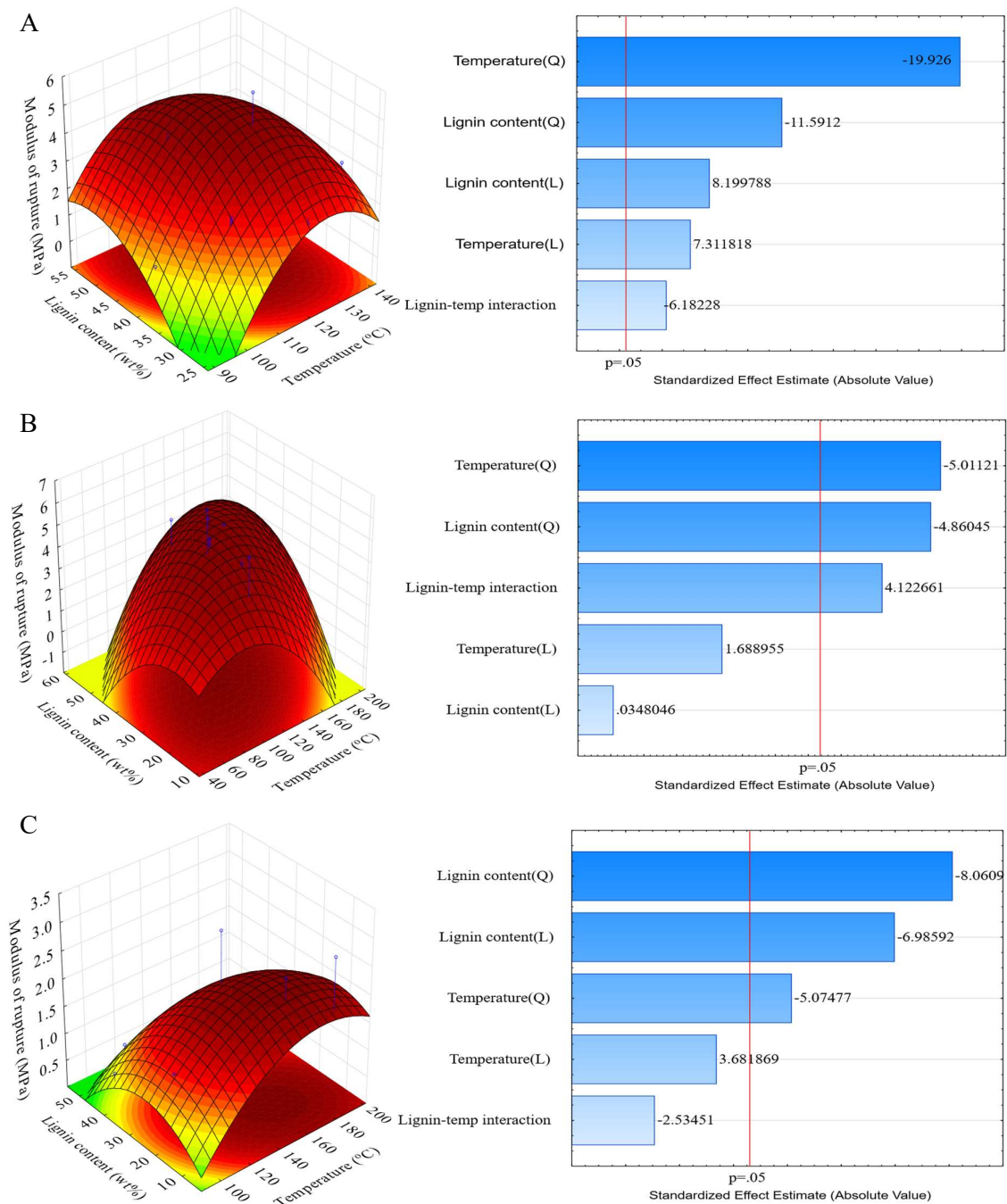


Figure 15: Fitted response of modulus of rupture as a function of lignin content and process temperature for A) MK composites, B) SK composites, and C) MS composites.

The increased MOR performances when precipitated kraft lignin and liginosulfonate were added into the composites are due to the suggested chemical binding between the lignin (precipitated kraft or liginosulfonate) and paper sludge fibres (*Constituent interactions*, section 4.3.1), as well as the lignin that moulds around the paper sludge due to the observed glass transition of precipitated kraft lignin between 130 °C and 175 °C (section 4.2.2.2) to increase interfacial adhesion and ultimately stress transfer between phases (Wang et al., 2019; Zhou et

al., 2016). Moreover, the peak in MOR as processing temperature is varied is due to a trade-off between sufficient moisture evaporation, lignin softening, and phosphate degradation: temperatures higher than 100 °C is required to remove excess water, since intermolecular hydrogen bonds form between the organic constituents and water that ultimately impedes intimate intermolecular contact with the hydrophobic matrix (Wang et al., 2019), however, temperature is limited by degradation of the ceramic binder, that already occurs around 90 °C – 130 °C, hence the optimal processing temperatures are 118 °C, 133 °C, and 155 °C for MK, SK, and MS composites, respectively.

Figure 16 clearly indicates the large improvement in MOR responses when precipitated kraft lignin is used (430 % for MK and 350 % for SK), compared to kraft black liquor (no notable change) and lignosulfonates (136 %). Additionally, the best performing lignosulfonate composite (MS) only achieves an MOR between 48 % and 63 % that of the precipitated kraft lignin composites (MK and SK). Hence, to achieve maximum MOR performance, precipitated kraft lignin should be used rather than kraft black liquor or lignosulfonate. The larger observed improvements in composite MOR when precipitated kraft lignin is used compared to lignosulfonate is due to the chemical bonding that takes place between the kraft lignin and paper sludge but not between lignosulfonate and the paper sludge in section 4.3.1.

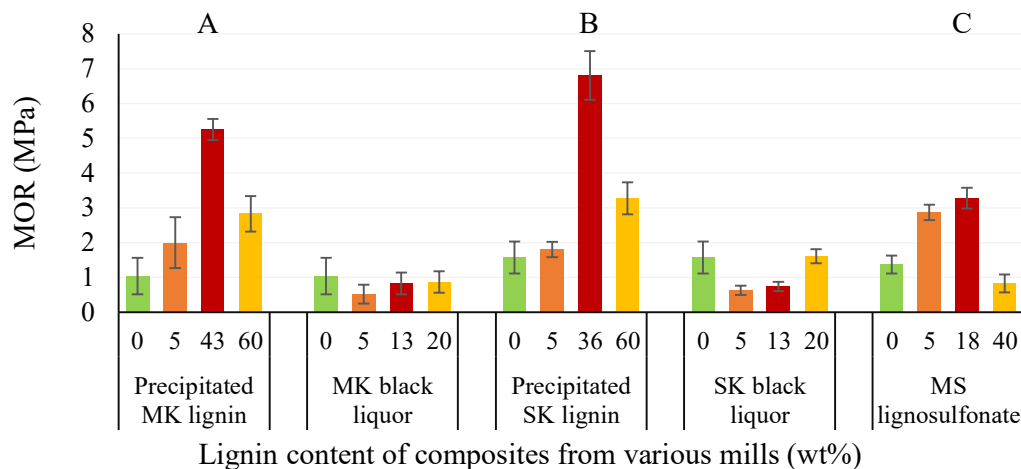


Figure 16: MOR for various lignin types and contents, split between different paper and pulp mills.

Modulus of elasticity

Figure 17 shows that maximum MOE responses occur for certain combinations of lignin content and processing temperature. **Figure 18** compares four sets of lignin content for the various lignin types, where the significantly improved MOE performance is highlighted for composites containing precipitated kraft lignin. The lignin-free composites are within ranges

of MOE performance obtained by other researchers, ranging between 464 MPa and 1 290 MPa (Amiandamhen, 2017; Chimphango, 2020), while optimum lignin content yields MOE responses between 1 734 MPa and 2 793 MPa, and are as much as double the best performing composites without lignin built by these researchers. The Pareto charts in **Figure 17** show that processing temperature significantly influences all the composites, while lignin content significantly influences the MOE results of MK and MS composites, and a lignin-temperature interaction only shows statistically significant effects on the MOE of MK composites.

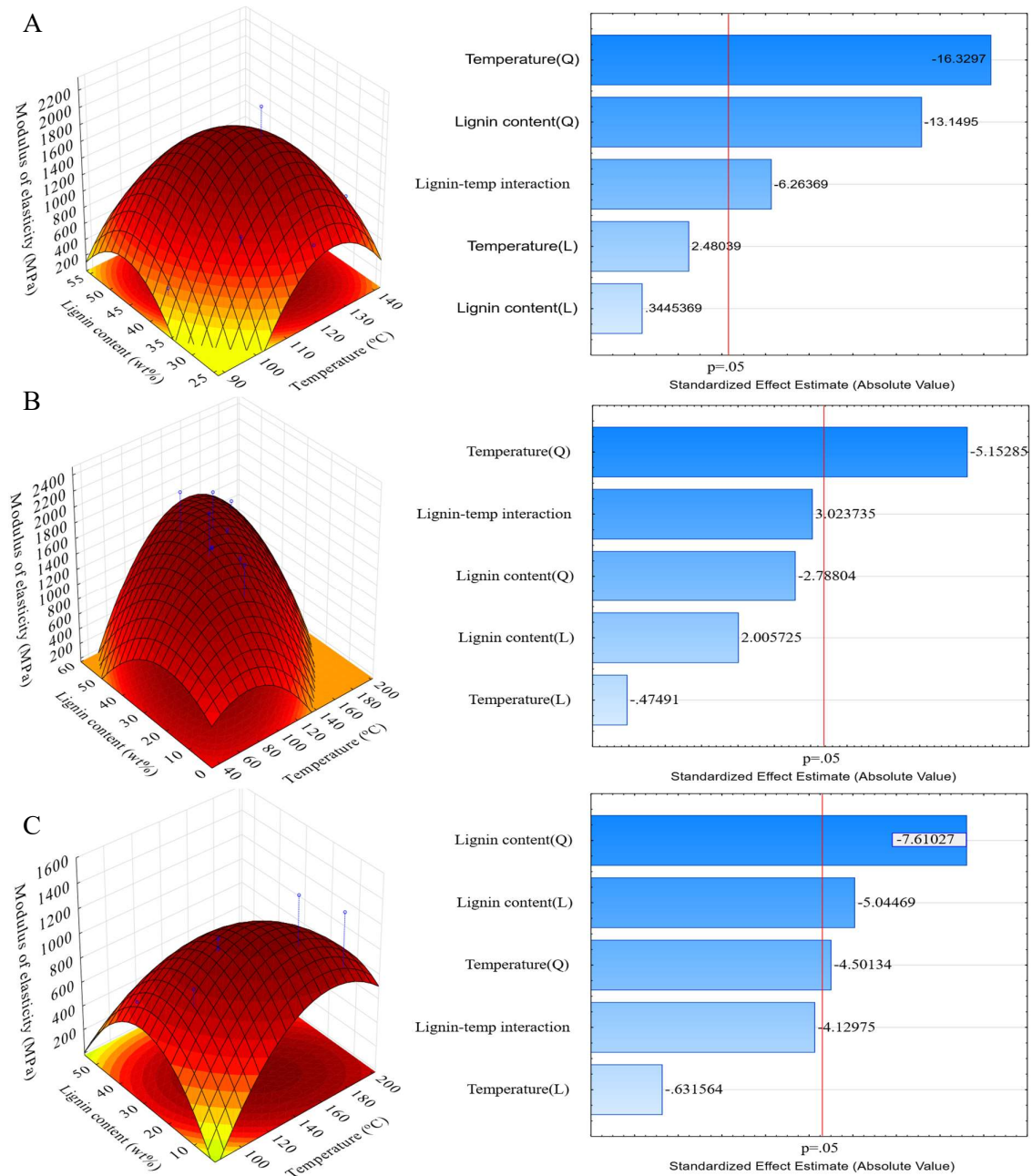


Figure 17: Fitted response of modulus of elasticity as a function of lignin content and process temperature for A) MK composites, B) SK composites, and C) MS composites.

The press temperature and lignin content process conditions that yield maximum MOE results coincide with the conditions for maximum MOR performance. For maximum MOE, the temperatures for MK, SK, and MS composites are 119 °C (118 °C for MK MOR), 131 °C (133 °C for SK MOR), and 157 °C (155 °C for MS MOR), while the lignin loadings are 43 % (also 43 % for MK MOR), 38 % (36 % for SK MOR), and 19 % (18 % for MS MOR), respectively. Hence, in this study the addition of precipitated kraft lignin as well as lignosulfonate into their respective paper sludge composites result in simultaneous improvements in MOR and MOE. This is in contrast to the general trend observed in previous studies where a trade-off between MOR and MOE exists when lignin substitutes a binding compound during composite formation (Paauw and Pizzi, 1993; Toriz et al., 2002; Wool and Sun, 2011; Zeng et al., 2017). These researchers claimed that reduced bonding caused by the chemical incompatibility between the lignin and other constituents inhibited mechanical performance, whereas in this study the precipitated kraft lignin chemically bonds to the paper sludge (section 4.3.1.1) and moulds around the paper sludge fibres due to processing temperatures close the glass transition temperature of the precipitated lignin (section 4.2.2.2). This observation is firstly rationalised by the fact that FTIR results (section 4.3.1.1) show possible chemical bonding while the MOR and MOE responses in **Figure 16** and **Figure 18** show significant improvements when precipitated kraft lignin is added compared to lignosulfonates and composites that contain no additional lignin, and secondly supported by claims in literature that interfacial adhesion improves mechanical performance (Fuentes et al., 2014; Sun et al., 2016; Toriz et al., 2002; Wang et al., 2019; Zeng et al., 2017).

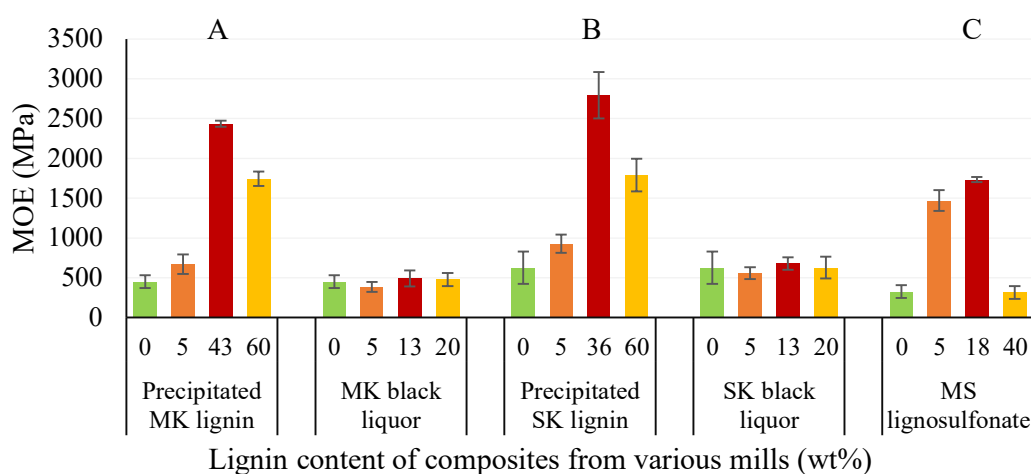


Figure 18: MOE for various lignin types and contents, split between different paper and pulp mills.

In **Figure 18** the MOE of the composites increase with increased lignin content until a maximum is achieved (red). However, the kraft black liquor composites data (MK and SK)

suggest that maximum MOE, around 13 wt% lignin, is not significantly different compared to the MOE achieved by the 0 wt% black liquor composites, with t-tests ($\alpha = 0.05$) for the statistically significant differences between lignin-free and black liquor composites yielding p-values of 0.145 and 0.302 for MK and SK, respectively. Conversely, the MOE results of the precipitated kraft lignin and lignosulfonate composites are significantly improved compared to the corresponding 0 % lignin composites, with MOE results increasing from between 327 MPa and 627 MPa to between 1 734 MPa and 2 793 MPa. The inadequate MOR and MOE performances of the kraft black liquor composites compared to precipitated kraft lignin composites is argument enough for the lignin precipitation as part of composite production.

Optimum process conditions for maximum MOR and MOE performance

The response surface models shown in **Figure 15** and **Figure 17** were obtained from statistical analyses of the MOR and MOE data obtained from the CCD in **Table 16** and the model parameters together with a summary of the predicted and experimentally observed optimal processing conditions are given in Appendix A. The statistically determined optimum process conditions are verified by the experimentally measured MOR and MOE performances, as shown by absolute MOR and MOE responses as well as the errors and acceptable R^2 -values in Appendix A.4. It must be noted that experimentally, the composite performances had larger and more sudden increases in MOR and MOE performance, whereas the statistical models showed less intense peaking. This resulted in accurate predictions of the process parameters, but a conservative prediction in all MOR and MOE results, however, the process parameters are confirmed experimentally, and is summarised in **Table 17**. Furthermore, the optimum lignin content in this study, ranging between 18 wt% (lignosulfonate) and 43 wt% (precipitated kraft lignin), is within reasonable limits since previous research showed that modified lignin can attribute between 20 wt% and 40 wt% of the mass in formaldehyde particleboards (Podschun et al., 2016), replace around 50 wt% formaldehyde resin (Cetin and Özmen, 2002), and even contribute up to 85 wt% of thermoplastic composites (Wool and Sun, 2011).

Table 17: Process conditions for optimum composite properties.

	Temperature (°C)	Lignin content (%)	CaCO ₃ content (%)	Fibre content (%)	Binder content (%)
MK	118	43.0	10.0	31.0	16.0
SK	133	36.0	10.0	35.6	18.4
MS	155	18.0	10.0	47.5	24.5

4.3.2.3. Physical properties

The influence of process temperature and lignin content on composite density, water absorption, and thickness swelling is discussed in this section. The interfacial adhesion mechanisms, as discussed in section 4.3.1, is then used to explain these observed effects. The physical properties of the kraft black liquor composites were not investigated since it clearly showed inferior mechanical performances compared to precipitated kraft lignin composites in the previous section 4.3.2.2 – MOR in **Figure 16** and MOE in **Figure 18**.

Composite density

The density standard for cement-based composites is $\geq 1\,000\text{ kg.m}^{-3}$ (ISO 16893:2016). From **Figure 19**, the addition of precipitated kraft lignin increases composite density from below 1000 kg.m^{-3} to around $1\,400\text{ kg.m}^{-3}$, with statistical analyses yielding p-values between 0.001 and 0.003, while the addition of lignosulfonate does not significantly change the composite density (p-values > 0.05). Furthermore, when the composites that contain no additional lignin (green bars in **Figure 19**) are studied, a significant variation in composite density is observed between composites that contain different paper sludge types, with MK, SK, and MS composites having densities of $1\,054\text{ kg.m}^{-3}$, 942 kg.m^{-3} , and $1\,354\text{ kg.m}^{-3}$, respectively. This observation is in accordance with observations made by Amiandamhen and Izekor (2013), Chimphango (2020), and Migneault et al. (2011) that proved the effect of various bio-based fibres on composite density, since the MS paper sludge, with the highest bulk density of 389 kg.m^{-3} compared to MK and SK paper sludge (around 45 kg.m^{-3}), resulted in composites (with no additional lignin) with the highest measured densities. It is therefore concluded that sludge content and -type, as well as lignin content and -type are the main influencers of composite density in this study.

No literature was found that previously proved the influence of precipitated kraft lignin on phosphate bonded composites. However, adopting the logic that constituents with higher bulk densities cause increased composite density (as shown with the various paper sludges above and substantiated by Amiandamhen and Izekor (2013), Chimphango (2020), and Migneault et al. (2011)), it is concluded that raised precipitated kraft lignin content, among other factors not measured in this study, is at least partially responsible for initially increased composite density – since MK and SK precipitated kraft lignin exhibit bulk densities around 825 kg.m^{-3} and 674 kg.m^{-3} , compared to their corresponding paper sludges that show bulk densities around 44 kg.m^{-3} and 49 kg.m^{-3} , respectively.

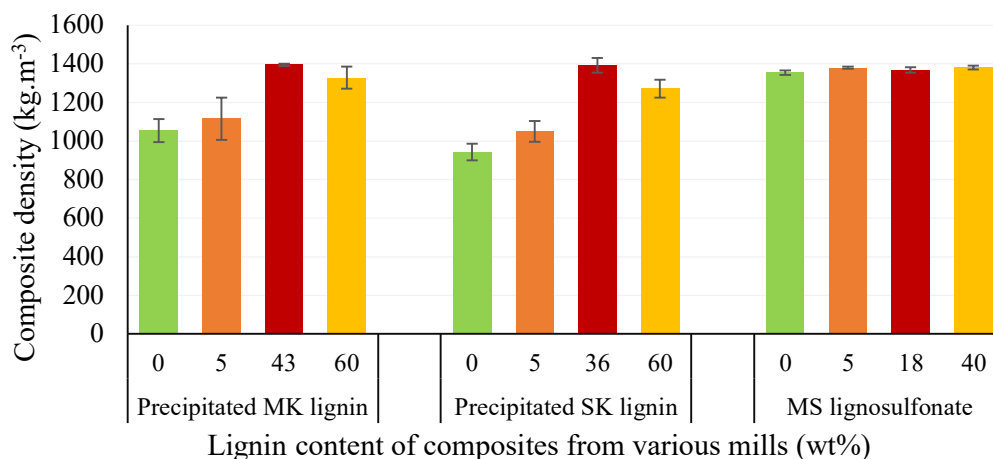


Figure 19: Density at different lignin contents for the composites from the different mills.

Dimensional stability

The dimensional stability of the composites is investigated via composite water absorption (WA) and thickness swelling (TS). The values shown in **Figure 21** compare well to previous studies that investigated paper sludge phosphate ceramics where WA ranged between 23 % and 30 % (Chimphango, 2020) and 57 % and 80 % (Amiandamhen, 2017). Comparing various lignin contents and -types for different paper and pulp mill composites in **Figure 21**, it is observed that the addition of precipitated kraft lignin reduced the WA of the MK and SK composites respectively from 34.0 % to 14.7 %, and from 46 % to 12.5 %. By adding precipitated kraft lignin into the composites there is an overall reduction in hydrophilic hydroxyl group content, since the paper sludge fibre content is effectively reduced via the additional precipitated kraft lignin that shows reduced hydrophilic properties as a result of sulfuric acid precipitation that lower the hydroxyl content of the lignin as discussed in section 4.2.1. Furthermore, the precipitated kraft lignin chemically binds to the paper sludge via ether links (discussed from FTIR data in section 4.3.1.1) and undergoes glass transitioning (section 4.2.2.2) at the experimentally determined optimum processing temperatures (section 4.3.2.2) around 130 °C to ultimately encase the paper sludge fibres (visible in **Figure 14H**, section 4.3.1.3) and further reduce WA. No previous work was found that exploits the reduced hydrophilicity of the kraft lignin caused by the acid precipitation to improve the WA results of a phosphate bonded composite material, nevertheless Amiandamhen et al. (2019;) and Wagh (2016) showed that by increasing the content of hydrophobic materials in composites and the encapsulation of the natural fibres, reduced composite WA is obtained compared to composites that contain less hydrophobic materials and more exposed fibres. However, the addition of lignosulfonate to MS composites contradicts these observations, since it seems to also reduce

composite WA in **Figure 21**, although being hygroscopic (section 4.3.1.1). This is easily explained by a visible loss of structural integrity in **Figure 20** for composites containing lignosulfonate, as well as the reduced dry mass of MS composites after wet testing was completed, summarized in **Table 18**.

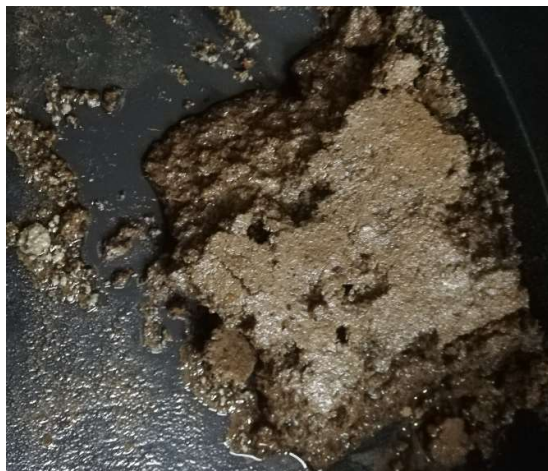


Figure 20: Visible loss in structural integrity of MS composites that contain 40 wt% lignosulfonate.

Table 18 quantifies the reduced structural integrity by showing the change in dry mass of the composite after the wet tests were completed and the samples were dried. The small changes in dry mass with magnitudes less than 1.5 % is attributed to natural variation in equilibrium moisture content of the composites, and small changes in mass due to material handling, and is considered negligible. However, the MS composites containing lignosulfonate show mass loss of more than 7.0 %, which is due to the observed failure in composite structure, where the composites break apart for lignin content higher than 5 wt%, and could even be due to “leaching” of the lignin from the composite. The results in **Table 18** prove that the measured reduction in WA for lignosulfonate composites is not due to reduced water absorption, but rather due to a loss in composite constituents. Hence, increasing the content of hydrophilic lignin types do not reduce WA absorption, but rather has a detrimental effect on composite integrity when exposed to excess moisture. This observation stands in accord with the effects of increased hydrophilic hydroxyl content on composites as discussed by Wagh (2016).

Table 18: Percentage change in dry mass before and after water absorption test.

Lignin content	Precipitated	Precipitated	MS
	MK lignin	SK lignin	lignosulfonate
% increase in dry mass			
0 wt% (green)	1.2	-0.4	0.8
5 wt% (Orange)	0.8	0.5	-7.3
Medium loading (red)	-0.6	0.3	-14.8

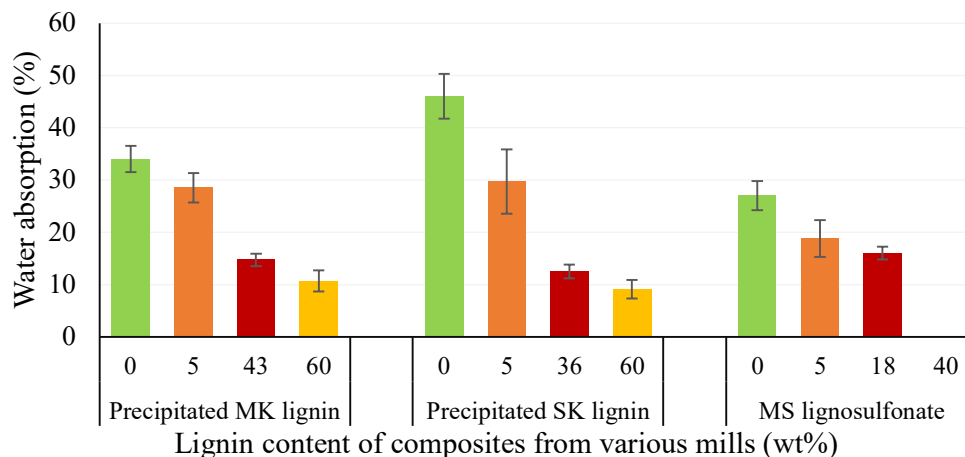


Figure 21: Water absorption at different filler contents for the composites from the different mills.

To further investigate the effects of lignin content on the WA of phosphate bonded composites, the WA of lignin-free composites (green bars from **Figure 21**) is compared to the WA of medium/optimum lignin content composites (red bars from **Figure 21**) as a function of the water holding capacity (WHC) of the paper sludge in **Figure 22**. Before lignin is added to the composites, it is observed that sludge fibres with a higher WHC yields composites with increased WA. However, by increasing lignin content the WHC of the fibres affects the composite WA to a smaller extent, since the WA for the lignin composites remain nearly constant around 14 %, regardless of the sludge WHC. The reduced effects of sludge properties (WHC) on WA is further proof that the sludge fibres are more properly encased by the precipitated kraft lignin and binder. Furthermore, SEM micrographs and thermal analyses in section 4.3.1, together with increased composite density, in **Figure 19**, indicated that the glass transition of precipitated kraft lignin reduced composite void volume and increased constituent contact, which ultimately reduced bound water absorption (Amiandamhen, 2017; Mngomezulu, 2019).

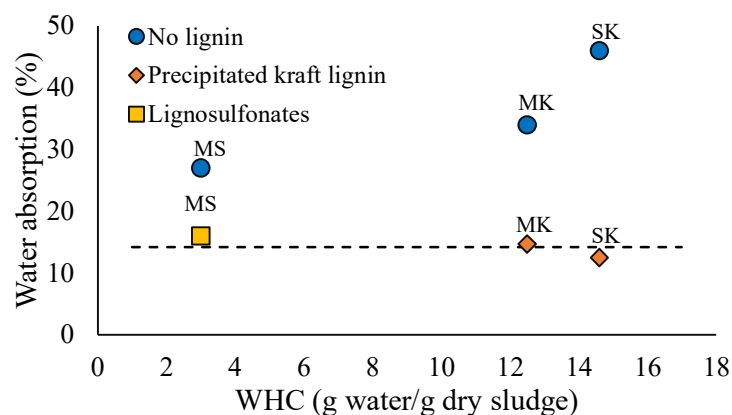


Figure 22: Effects of sludge WHC on composite water absorption.

The thickness swelling (TS) results for composites containing different ratios of various lignin types are shown in **Figure 23**. The TS of the composites that contain no additional lignin (green) compare well to TS results between 1.2 % and 15.7 % obtained by previous researchers for phosphate bonded composites (Amiandamhen, 2017; Chimphango, 2020). Regardless of lignin type, TS in **Figure 23** is significantly reduced by between 24 % (MK) and 78 % (MS) when optimal lignin content (red) is used compared to lignin-free composites (green) with statistical analysis yielding p-values between 0.003 and 0.01 ($p < 0.05$). An increase in precipitated kraft lignin content naturally results in a reduction in paper sludge content, as well as moulding around the paper sludge fibres, as shown by SEM micrographs in **Figure 14H** and suggested by glass transition of the precipitated lignin at process temperatures around 130 °C (shown in **Figure 11**, section 4.2.2.2), improving encasement of the fibres, and finally inhibiting fibre swelling. This mechanism is rationalised by conclusions from Amiandamhen (2017) and Mngomezulu (2019) that an increase in phosphate binder content results in reduced TS due to improved fibre encapsulation.

However, no binding reaction occurs between the paper sludge and lignosulfonates (MS), as per FTIR results in **Figure 12**, section 4.3.1. The lignosulfonate is also hydrophilic due to relatively high hydroxyl group content (**Figure 7**, section 4.2.1), yet reduced TS is observed for the MS composites which contradicts observations made for precipitated kraft lignin composites, as well as observations made by other researchers (Amiandamhen, 2017; Mngomezulu, 2019). This is most likely due to the noticeable loss in structural integrity and dry mass of the MS samples when exposed to water, as observed in **Figure 20** and **Table 18**.

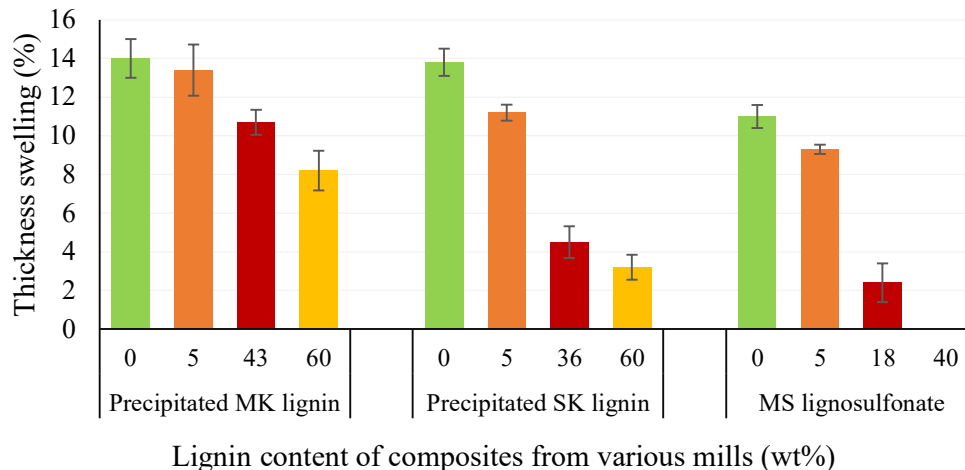


Figure 23: Thickness swelling at different filler contents for the composites from the different mills.

4.3.3. Binder reduction

Previous studies have shown that lignin can be used as filler in polymeric composites (Wool and Sun, 2011), or as a partial binder replacement with negative to limited positive impact on composite properties by substituting polypropylene resin (Toriz et al., 2002), phenols in phenol-formaldehyde resin (Cetin and Özmen, 2002; Younesi-Kordkheili et al., 2016), and epoxy resins (Salanti et al., 2018). However, this project highlights the significant improvements of sludge/phosphate composite properties when precipitated kraft lignin is used to partially replace the phosphate ceramic. **Table 19** summarises the reduction in phosphate binder content due to the experimentally optimised lignin content. This binder reduction, together with improved composite performance, emphasises the necessity of precipitated kraft lignin to improve the techno-economic viability of sludge/phosphate composites. However, section 4.4 discusses the addition of veneer to further improve the mechanical properties to finally reach industrial standards as set out in **Table 22**.

Table 19: Binder and filler reduction due to the addition of lignin.

Mill	Composite type	Lignin content (%)	Binder content (%)
MK	Lignin-free	0.0	27.2
	Lignin	43.0	16.0
	% change		-41.2
SK	Lignin-free	0.0	27.2
	Lignin	36.0	18.4
	% change		-32.4
MS	Lignin-free	0.0	27.2
	Lignosulfonate	18.0	24.5
	% change		-9.9

4.4. Composite performance enhancements to reach industrial standards

To sufficiently valorise paper and pulp mill waste, this proposed bio-composite project should be technically and economically viable. This section investigates performance enhancements by adding veneer to the composite material to ultimately achieve industrial standards as final proof of the technical viability of the lignin composite material, while the economic viability of the composite is investigated in CHAPTER 5.

4.4.1. Performance enhancements via the addition of pine veneer

Due to the observed maxima in MOR and MOE performance in section 4.3.2, it is concluded that additional variation in the specified process conditions – press temperature, and lignin type and content – will not yield further improved composites. Instead, in this section the effects of 0.35 mm and 2.0 mm pine veneer on the lignin composites are investigated, since it is widely accepted that the addition of overlayers such as veneer improves the performance and aesthetic properties of composite materials (Stark et al., 2010). The veneer was added to composites that were produced under optimal process conditions as found in section 4.3.2, to highlight that veneer, as the only new variable in process conditions, affects composite performance.

4.4.1.1. Experimental setup

As proof of a well understood concept, the pine veneer (0.35 mm and 2 mm) was attached to the lignin composites using PVA wood resin with a manufacturer recommended spread rate of 0.5 kg.m⁻². The rotary cut pine veneer was obtained from York Timbers, Mpumalanga, South Africa, with density 380 kg.m⁻³, and moisture content 9 %. **Table 20** shows the experimental setup where no veneer, 0.35 mm veneer, and 2.0 mm veneer were added to composites produced under optimal conditions as defined in **Table 17**, section 4.3.2.

Table 20: Experimental design to showcase the effects of veneer on composite performance.

	Veneer	Temperature (°C)	Lignin content (%)	CaCO ₃ content (%)	Fibre content (%)	Binder content (%)
MK	No	118	43.0	10.0	31.0	16.0
	0.35 mm					
	2.0 mm					
SK	No	133	36.0	10.0	35.6	18.4
	0.35 mm					
	2.0 mm					
MS	No 2 mm	155	18.0	10.0	47.5	24.5

4.4.1.2. Performance comparison

This section compares the dimensional stability and mechanical performance of the composites containing no lignin and optimum lignin (as discussed in section 4.3.2) as well as 0.35 mm veneered, and 2 mm veneered composites. **Table 21** is a summary of the various composites where the recommended veneered composite product for each of the mills is shown in bold.

Table 21: Physical and mechanical properties of optimum lignin and lignin-free composites, as well as optimum lignin content composites with pine veneer.

Composite type	Density kg.m ⁻³	WA %	TS %	MOR MPa	MOE MPa
MK composites					
Lignin-free	1 054 ± 45	34.0 ± 0.5	11.0 ± 1.7	1.0 ± 0.1	452 ± 17
Lignin	1 395 ± 60	14.7 ± 1.2	10.7 ± 0.6	5.3 ± 0.3	2 435 ± 38
0.35 mm veneer	1 301 ± 30	14.3 ± 1.0	9.5 ± 0.4	17.4 ± 1.7	3 882 ± 171
2 mm veneer	1 099 ± 21	19.4 ± 0.9	5.2 ± 0.8	22.1 ± 0.7	3 616 ± 167
SK composites					
Lignin-free	942 ± 26	46.1 ± 1.1	13.8 ± 5.6	1.6 ± 0.2	627 ± 66
Lignin	1 392 ± 38	12.5 ± 1.3	4.5 ± 0.8	7.2 ± 0.7	2 793 ± 293
0.35 mm veneer	1 216 ± 10	17.8 ± 4.0	3.6 ± 0.4	19.9 ± 2.7	2 909 ± 95
2 mm veneer	1 059 ± 16	23.8 ± 2.4	3.3 ± 0.3	17.7 ± 1.9	2 101 ± 123
MS composites					
Lignin-free	1 354 ± 14	27.0 ± 3.4	10.9 ± 4.5	1.4 ± 0.1	327 ± 26
Lignosulfonate	1 368 ± 14	16.0 ± 2.0	2.4 ± 1.0	3.3 ± 0.3	1 302 ± 31
2 mm veneer	1 021 ± 20	31.6 ± 1.0	3.3 ± 1.4	6.4 ± 0.6	1 602 ± 200

Mechanical properties

Glued veneer is a vital part in mechanical performance improvements of natural fibre composites (Evans, 2013; Mngomezulu, 2019; Stark et al., 2010) and is observed in **Table 21**, where the addition of veneer significantly enhances the MOR from between 3.3 MPa and 7.2 MPa for unveneered composites to between 6.4 MPa and 22.1 MPa for veneered composites. Slightly less impressive, but still relatively large improvements in MOE is also shown in **Table 21** where veneered composites exhibit MOE responses around 1.3 times that of unveneered composites. These MOR and MOE improvements are of similar magnitude to that observed by Mngomezulu (2019). The overall performance enhancements due to the addition of lignin (section 4.3.2.2) and pine veneer (**Table 21**) ensure the technical viability of the composite material, as discussed in section 4.4.2.

In **Table 21**, there is a clear improvement in MOR and MOE when veneer is added to the composites. However, there is an observable decrease in MOE and MOR when veneer thickness is increased. To understand this phenomenon, we have to study the mathematical

equations used to calculate the MOR and MOE results given by Equation 15 and Equation 16, as well as the subsequent change in m and F used to calculate the MOE and MOR results as a function of the change in veneer thickness. The composite cores were formed to have a thickness of 13 mm and is considered in conjunction with the varying veneer thicknesses in Figure 24 and Figure 25.

$$MOE = \frac{L^3}{4wt^3} m ; m = \frac{\Delta F}{\Delta d} \quad 15$$

$$MOR = \frac{3LwF}{2t^2} \quad 16$$

The equations highlight that MOR and MOE are dependent on sample size, and in both equations an increase in thickness will reduce calculated results if all other variables remain constant. It is clear from Figure 24 and Figure 25 that although the composites can withstand higher applied loads and deflects less per unit force as veneer thickness increases, the fact that F and m do not increase in similar ratios to t^2 and t^3 (decreasing slopes in Figure 24 and Figure 25) provides the explanation as to why the MOR and MOE results decreases in **Table 21**.

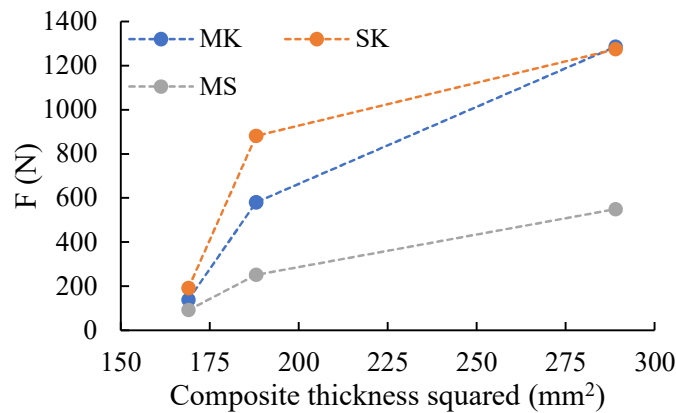


Figure 24: The maximum force before rupture used to calculate MOR is compared to t^2 from Equation 16.

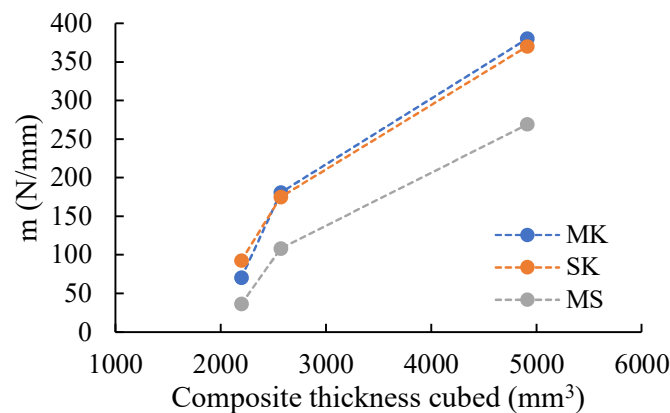


Figure 25: The force per deflection parameter used to calculate MOE compared to t^3 from Equation 15.

Dimensional stability

The dimensional stability of a composite is quantified via water absorption and thickness swelling after submersion in water for 24 h. In **Table 21** the addition of 0.35 mm veneer changes the WA and TS to a smaller extent than 2.0 mm veneer that increases the WA of the MK, SK, and MS composites by 32.0 % (from 14.7 % to 19.4 %), 90.4 % (from 12.5 % to 23.8 %), and 97.5 % (from 16.0 % to 31.6 %), respectively. The resulting increased WA's are larger than the acceptable limits stated by the industrial standards shown in **Table 22**. Conversely, the 2.0 mm veneer reduces the MK and SK composite TS respectively by 51.4 % (from 10.7 % to 5.2 %) and 26.7 % (from 4.5 % to 3.3 %), while increasing the MS composite TS by 37.5 % (from 2.4 % to 3.3 %) – however still markedly less than industrial standards (**Table 22**). It must be noted that the water absorption and thickness swelling of the pine veneer are 89.5 % and 1.8 %, respectively. The general trend is that these properties influence the overall composite performance in opposite fashion and that the thicker veneer results in greater changes in WA and TS, since it contributed more to the total composite mass and volume. A similar observation was made by Mngomezulu (2019).

4.4.2. Composite classification

The new composites formulated in this study should be classified and compared to industry standards before it can enter a competitive market for inexpensive materials. This section aims to define and compare the composites to industrial standards, based on literature as discussed in section 2.9.

4.4.2.1. Classification

The composites in this study utilize paper sludge fibres that are obtained from a chemical pulping process. Infra-red absorption spectra in section 4.1.3 indicate that the kraft pulping process did not deteriorate the fibres, and only removed natural lignin. The fibres also have an average diameter smaller than 0.5 mm (section 4.1.4). Furthermore, the phosphate ceramic contributes only between 16 wt% and 24.5 wt% of the material mass (**Table 19** in section 4.3.3), and is therefore seen as a ceramic adhesive and not a ceramic cement, since it does not encapsulate the paper sludge fibres (Stark et al., 2010). Moreover, the addition of acid precipitated kraft lignin to a content around 40 wt% is within the reasonable expected ranges for lignin content in composite materials (Cetin and Özmen, 2002; Podschun et al., 2016; Wool and Sun, 2011). The lignin acts as a thermoplastic adhesive under pressure and heat (“*Thermal softening of lignin*” in section 4.3.1), and was shown as an adhesive replacement in section

4.3.3. Stark et al. (2010) substantiates the notion that lignin can act as a binder replacement. It is therefore concluded that the new composite material (core before veneer is added) should be classified as a paper sludge fibre reinforced lignophosphate composite.

4.4.2.2. Standards

The new lignin composites must adhere to standards for use if it is to be technically viable to pursue this project. **Table 22** shows the standards for various types of composite, as well as the properties of the unveneered and veneered composites produced during this study.

The MK, SK, and MS composites (veneered and unveneered) composites exhibit physical properties that adhere to the standards shown in **Table 22**. These composites have densities larger than $1\,000\text{ kg}\cdot\text{m}^{-3}$ (EN 634-2-2007; ISO 16893:2016), while having a maximum TS of 10.7 % - that still adheres to the standard maxima of 15 % (EN 634-2-2007), 19 % (ISO 16893:2016), and 25 % (ASTM D1037-99, 1999). Similarly, the composites also exhibit smaller WA than the maxima set by the standards, with only the 2 mm veneered SK (19.4 %) and MS (31.6 %) composites not satisfying the ISO standards for general purpose particleboard (19 %), however still meeting the European (35 %) and American standards (60 %) (ASTM D1037-99, 1999; EN 634-2, 2007). Phosphate bonded paper sludge composites studied by Chimphango (2020) showed similar densities to that exhibited in this study by the phosphate composites that contain lignin. Conversely, the composites investigated by Chimphango (2020) had larger WA results than permitted by all of the standards shown in **Table 22**.

The MOE performances of the unveneered Kraft composites (MK and SK) satisfy some standards, while the MOR results do not. However, when veneer is applied to the Kraft composites, all of the ISO and ASTM standards for MOR are satisfied, with MK and SK yielding MOR results of 22.1 MPa and 19.9 MPa, respectively, implying that the veneered composites could even be used in heavy duty load bearing structures in dry conditions. Although both veneered MK and SK composites also achieved MOE performances greater than 2 900 MPa – the minimum required for heavy duty load bearing structures (ISO 16983:2006) – the researcher suggests that only furniture and non-loadbearing wall structures should be fabricated until further performance testing, ageing studies, and investigation on failure mechanisms ensure safe operation if the composites are used in load-bearing structures. Furthermore, the mechanical properties of the unveneered MS composites do not achieve the set standards, and while the addition of veneer increases the MOR and MOE to 6.4 MPa and 1 602 MPa, respectively, it is still not enough to satisfy the standards. It must be noted that

apart from achieving the required performance standards, the kraft lignin composites of this study markedly improved the mechanical performance of the paper sludge composites formulated by Chimphango (2020) with maximum MOR and MOE results of 1 290 MPa and 4.12 MPa, respectively.

Table 22: Standards for various composites compared to the properties of the new veneered and unveneered composites.

Standard		Density kg.m ⁻³	WA %	TS %	MOR MPa	MOE MPa
(N 634-2, 2007	Cement bonded particleboard. Furniture.	> 1 000	< 35	< 15	> 9 > 11	> 4 000 > 1 600
ISO 16893:2016 (Particleboard)	Load bearing. Heavy duty load bearing in dry conditions.				> 15 > 18	> 2 100 > 2 900
ISO 16893:2016	General purpose particleboard.	> 1 000	< 19	< 19	> 15	> 2 200
ASTM D1037-99 (1999)	Particleboard for standard use.		< 60	< 25		
AAAMSA Group (2004)	Fibre reinforced cement board	1 260 – 1 500			> 7.5	> 3 974
Composite properties						
Mill	Veneer type	Density kg.m ⁻³	WA %	TS %	MOR MPa	MOE MPa
MK	No veneer	1 395	14.7	10.7	5.3	2 435
	2.0 mm pine veneer	1 099	19.4	5.2	22.1	3 616
SK	No veneer	1 392	12.5	4.5	7.2	2 793
	0.35 mm pine veneer	1 216	17.8	3.6	19.9	2 909
MS	No veneer	1 368	16.0	2.4	3.3	1 302
	2.0 mm pine veneer	1 021	31.6	3.3	6.4	1 602

CHAPTER 5: TECHNO-ECONOMIC ANALYSIS

5.1. Introduction

This section aims to determine the economic viability of the kraft composites with veneer that show better performance compared to composites that contain no additional lignin and the composites that contain lignosulfonate. To show the economic advantage of adding the precipitated kraft lignin, even though there are additional expenses such as the purchase of acid, cooling utilities, and unit process equipment expenses, it is compared to composites that were formed using lignosulfonate (spent pulping liquor from sulfite pulp mill) as well as composites that contain no additional lignin as part of the project sensitivity analysis.

Firstly, the proposed process is discussed, then the mass balance based on annual sludge emission is done to finally size and cost the major unit operations from which the fixed capital investment is predicted. Next, the total operating cost is projected based on the annual flow rates. Finally, the fixed capital investment and total production costs are used to determine the economic viability parameters.

5.2. Process flow diagrams

The process flow diagrams (PFDs) shown in **Figure 26**, **Figure 27**, **Figure 28**, and **Figure 29** indicate the unit operations required to convert paper and pulp sludge into laminated composites. The overall process is divided into three main stages: lignin preparation, composite production, and lamination.

5.2.1. Lignin preparation plant

Two lignin preparation plants were designed based on whether the spent liquor is obtained from the Kraft process (MK or SK) or sulfite process (MS). It must be noted from **Figure 26** and **Figure 27** that the acid precipitation requires more processing equipment and will also have more utility expenses.

5.2.1.1. Kraft lignin precipitation

CHAPTER 4 discusses the precipitated kraft lignin (via sulfuric acid) qualities that prove to aid in the performance of phosphate composites. It is thus necessary to consider this lignin precipitation process in the economic analysis, since extra processing results in higher operating costs. Kraft lignin can be precipitated from the spent liquor via pH reduction. In **Figure 26** 70 wt% sulfuric acid is added to the spent liquor (M-101) and left to form precipitate

for 24 h (R-101) before filtering to remove the acid water (F-101) where after the lignin is dried (D-101) and milled (C-101).

5.2.1.2. Lignosulfonate preparation

Lignosulfonates from the sulfite process cannot be precipitated via acid reduction (Naron et al., 2017). **Figure 27** indicates that water is either added (M-101) or removed (D-101) from the spent liquor depending on the solids content of the liquor obtained from the paper and pulp mill and the required solids content of the lignin stream that will be used during composite production. This stream will contain all the water required for composite production and no water will be added in the composite production plant.

5.2.2. Composite production plant

Figure 28 shows the process used to produce the bio composites by mixing sludge as fibre, calcium carbonate as filler, magnesium potassium phosphate as the binder, and lignin as a partial binder replacement (M-201). The mixture is then pre-pressed (PP-201) and pressed (P-201) before it is left to cure (CO-201), and finally cut to size and sanded (FI-201).

5.2.3. Lamination plant

Figure 29 shows the lamination process, where PVA resin is used to add veneer onto the composites via application of pressure (P-301), left to set (CO-301), after which the composites are sanded to a smooth surface and stacked and stored, ready for shipping (FI-301).

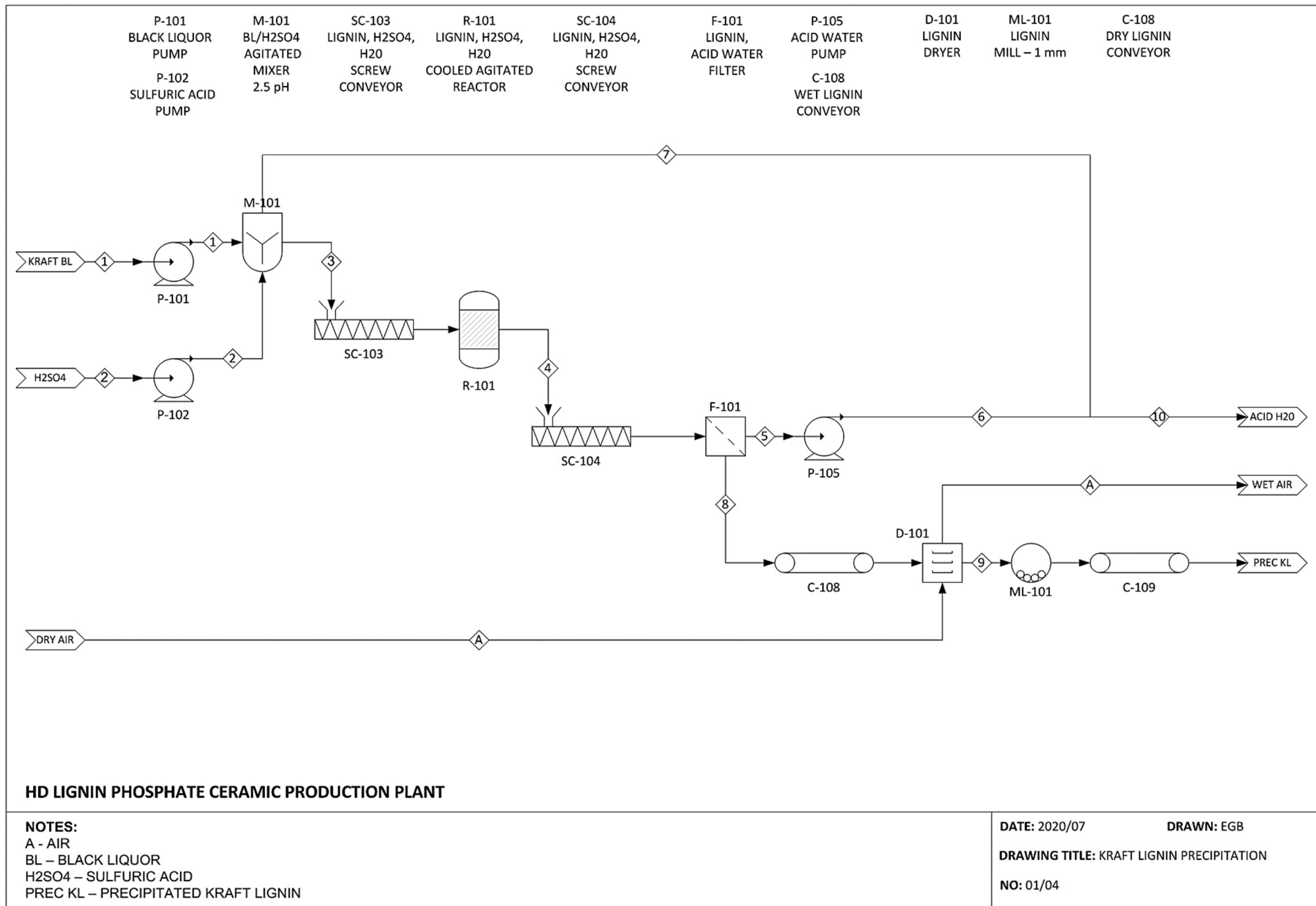


Figure 26: Kraft lignin precipitation plant. This plant prepares the lignin for use during composite production.

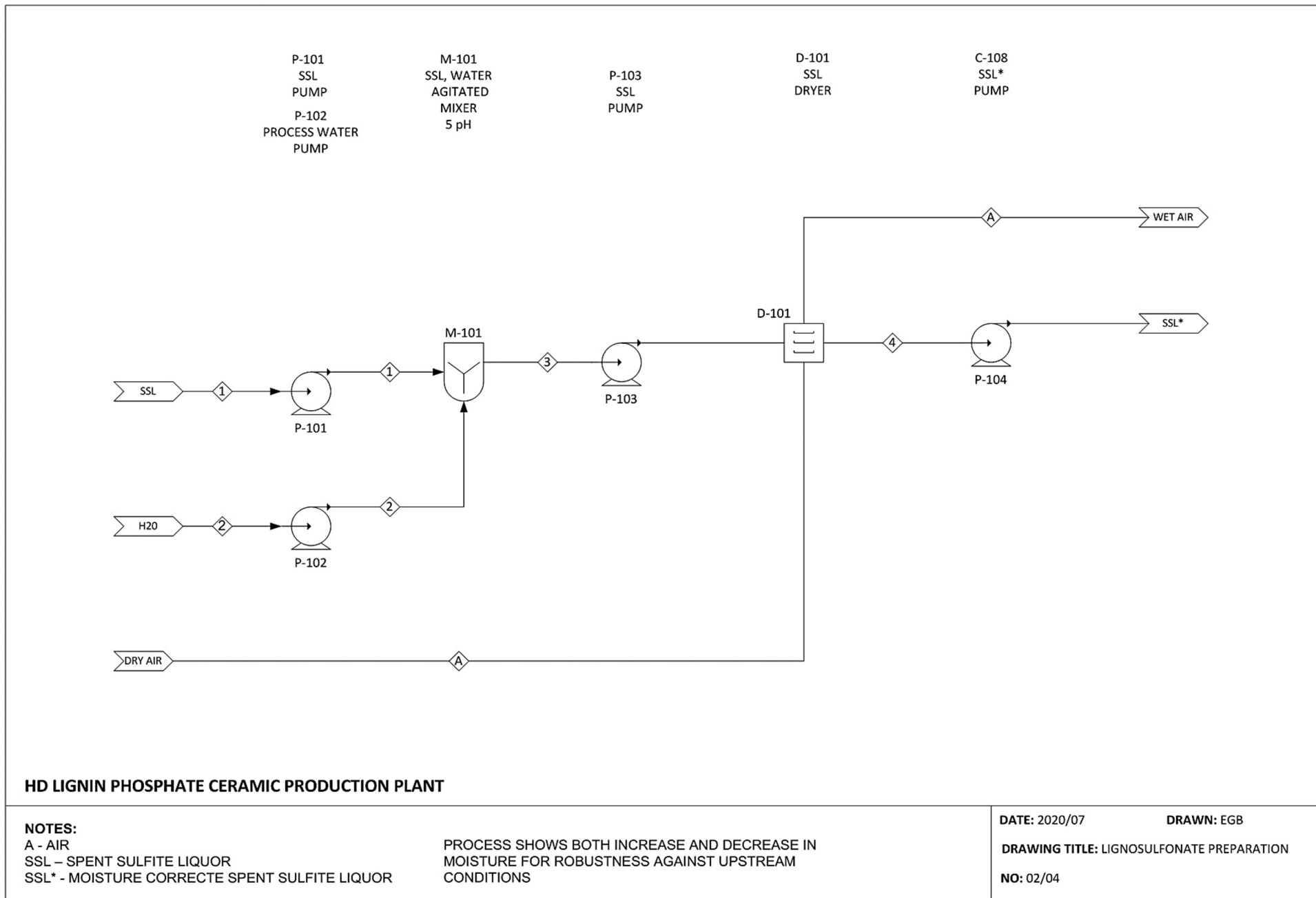


Figure 27: Lignosulfonate preparation plant. This plant prepares the lignosulfonate for use during composite production.

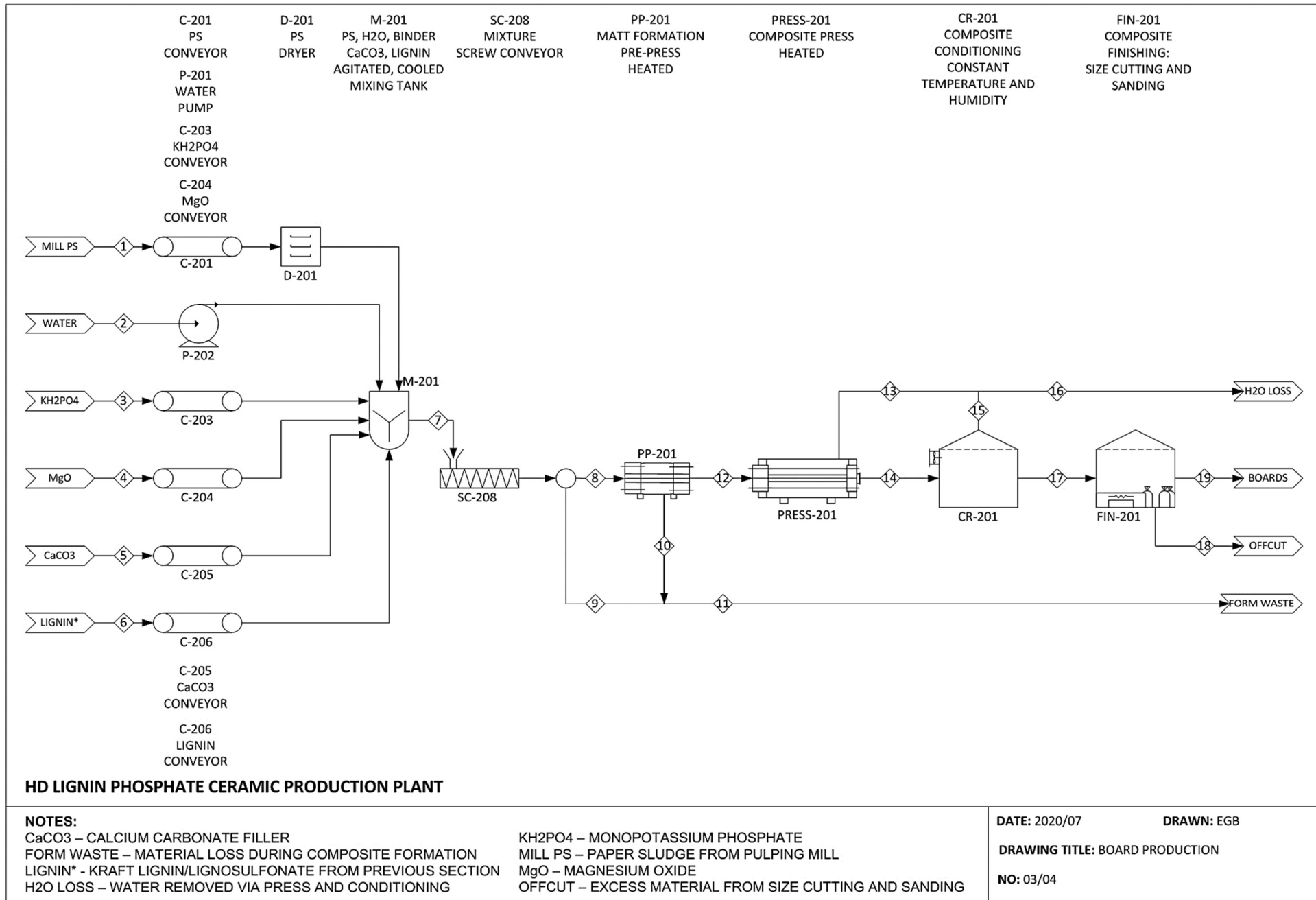


Figure 28: Composite production plant.

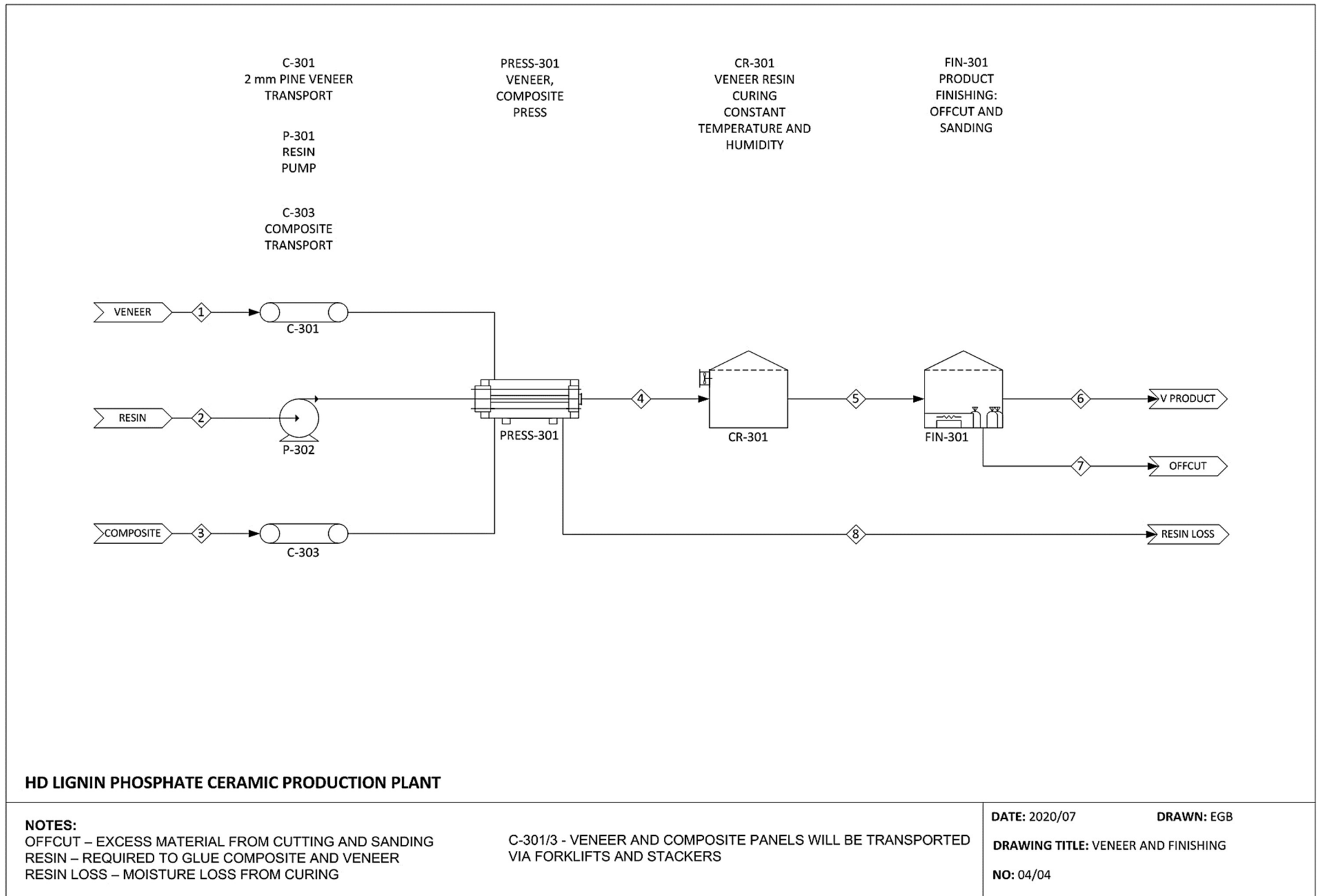


Figure 29: Lamination plant. This plant adds veneer onto the composites produced. It is assumed that veneer and resin is bought instead of produced on-site.

5.3. Plant capacity

Plant capacities are based on the annual amount of paper and pulp mill sludge formed by each of the mills as given by Boshoff (2015) and is summarised in **Table 23**. It is assumed that all other feedstock material will be available in abundance, thus the composite production rate is limited by the annual sludge emission, where the other materials are acquired to achieve the required composition as determined during composite optimisation in CHAPTER 4, summarized in **Table 24** for convenience. The total mass flow through each unit operation was ultimately used to size the equipment.

Table 23: Annual sludge formation (Boshoff, 2015).

Mill	Process	Lignin type	Sludge formation dry ton/year	Sludge moisture content %
Mondi (Richards Bay)	Kraft	Precipitated Kraft lignin	12 500	64
Sappi (Ngodwana)	Kraft	Precipitated Kraft lignin	15 000	80
Mpact (Piet Retief)	Sulfite	Lignosulfonate solution	500	70

Table 24: Summary of optimised process conditions for composite production from the three pulp mills.

Composite	Temperature (°C)	Lignin content (%)	CaCO ₃ content (%)	Fibre content (%)	Binder content (%)
MK	118	43.0	10.0	31.0	16.0
SK	133	36.0	10.0	35.6	18.4
MS	155	18.0	10.0	47.5	24.5

5.3.1. Mass balance

To fully specify the mass balance of the entire process, the assumptions in **Table 25** were made. From these assumptions, the overall mass flow rates, as well as flow rates over individual unit operations were calculated to finally determine the required equipment size. The overall flow rates are summarised in **Table 26**. Some important calculations regarding feedstock flow rate is summarized in Appendix B.1.

It is clear from **Table 26** that increased sludge formation results in increased composite panel production, with MK, SK, and MS having the potential to produce around 770 000, 840 000, and 20 000 panels per annum, respectively. Increased panel production increases the amount of magnesium potassium phosphate binder required, but as per usual, increased production should result in less expensive products. Both MK and SK mills also have the added advantage of lignin that reduces the required amount of binder; however, the cost of sulfuric acid should not outweigh the savings in reduced binder.

Table 25: Assumptions made to fully specify the mass balance of the process.

Plant section	Unit operation	Assumption	Reason/Reference
Kraft preparation; Composite production; lamination	Pumps, belt conveyors, screw conveyors	0 % mass loss.	Simplifies mass balance; mass loss is considered within other unit operations; Chimphango (2020).
	Storage	15-day feedstock supply and product storage.	Adequate storage without exaggerated influence on capital investment.
Kraft lignin preparation	Filter (F-101)	Filter cake (precipitated lignin) has 30 % moisture content.	Experimental work done by this researcher.
Composite production	Pre-press (PP-201)	6 % material loss due to matt formation.	Chimphango (2020).
	Press (P-201)	Heated by either steam or electricity, the model will choose the least expensive option.	Hot oil will be extra capital cost and must constantly be reheated by steam or other hot process streams.
		Press duration of 30 min.	From experimental work.
	Conditioning (CO-201)	8% moisture loss due to composite curing.	Chimphango (2020).
	Finish (FI-201)	6 % material loss due to cutting and sanding.	Chimphango (2020).
Lamination	Press (P-301)	Press duration of 4 h.	Sufficient curing time for PVA resin.
	Finish (FI-301)	6 % mass loss due to sanding.	Chimphango (2020).

Table 26: Flow rates over the entire process.

Stream	Unit	MK	SK	MS
IN				
Lignin preparation				
Spent liquor	ton/year	45 370	44 671	1071
70 % Sulfuric acid	ton/year	6 502	6 402	NA
Water	ton/year	0	0	0
Composite production				
Sludge	ton/year	30 673	66 429	1 660
Water	ton/year	18 750	22 500	0
Monopotassium phosphate	ton/year	1 075	1 292	43
Magnesium oxide	ton/year	5 376	6 461	215
Calcium carbonate	ton/year	4 032	4 213	105
Lamination				
Veneer	m ² /year	4 598 712	5 001 716	119 070
Resin	ton/year	2 300	2 501	60
OUT				
Lignin preparation				
Acid water	ton/year	25 946	25 547	NA
Moisture in air	ton/year	6 823	6 718	395
Composite production				
Moisture in air	ton/year	30 840	67 186.46	1 225
Total material loss due to processing	ton/year	6 321	7 002	162
Lamination				
Resin loss	ton/year	230	250	6
Total material loss due to processing	ton/year	2 511	2 731	65
Laminated composites	panels/ year	772 400	840 100	19 950

5.3.2. Equipment sizing and cost calculation

After the flow rates were calculated, the required size of all major equipment was determined to estimate the cost of equipment. At least two cost values were obtained for most of the required equipment, where after the most expensive option was chosen in order to obtain a conservative prediction for the total capital expense. The determined equipment sizing parameters are given in Appendix B.2.

Sinnott (2005) shows a cost estimation method for generic process equipment and is summarised here. **Equation 17** is adapted from the equation given by Sinnott (2005) to adjust for date and currency exchange rate.

$$C_e = CS^n \left(\frac{CEPCI_{2019}}{CEPCI_{2004}} \right) \left(\frac{R}{£} \right) \quad 17$$

C_e is the equipment purchase cost (R); C , S , and n the cost constant, size parameter, and equipment specific index from **Table 27**; and CEPCI the chemical engineering plant cost index to adjust for date.

Table 27: Parameters used in Equation 17 (Sinnott, 2005).

Equipment	Size paramter	Unit	Cost constant (£)	index
	S		C	n
Conveyors				
1 m wide belt	2 – 40	m	1 800	0.75
Crushers				
Cone	20 – 200	ton/h	2 300	0.85
Pulverisers	20 – 200	kg/h	2 000	0.35
Dryers				
	5 – 30	m ²	21 000	0.45
Filter				
Plate and frame	5 – 50	m ²	5 400	0.60
Vacuum drum	1 – 10	m ²	21 000	0.60
Reactors				
	3 – 30	m ³	9 300	0.40
Storage tanks				
	50 – 8000	m ³	1 400	0.55

Equipment more specific to composite formation processes were sized and costed based on previous studies (Hollaway et al., 1994; Koenigshof, 1978). Equation 18 (Sinnott, 2005) is then used to predict equipment cost by adjusting for size and date of the previously costed equipment.

$$C_e = C_{pre} \left(\frac{S_e}{S_{pre}} \right)^{0.6} \left(\frac{CEPCI_e}{CEPCI_{pre}} \right) \quad 18$$

The subscripts e and pre denote the newly predicted and previously calculated values, respectively. C denotes the equipment purchase cost, and S the size parameter used for adjustment. Table 28 shows the sizing factor and design specifications for some composite formation equipment.

Table 28: Composite formation equipment design specifications and sizing factors.

Equipment	Sizing factor	Units	Design specifications
Composite production			
Pre-press	Mass flow	kg/h	Non-heated press with low pressure capability to form composite matt
Press setup			
Press (nr of presses based on panels/h)	Mass flow	kg/h	30 min/cycle; 30 panels per cycle; Panel size: 4ft x 8ft; Heated; 15 MPa pressure
Loading and unloading	Mass flow	kg/h	Machinery to handle 30 panels per cycle
Conditioning			
Forklifts and carts	Mass flow	kg/h	
Storage banks	Mass flow	kg/h	24 hr residence period for composite curing
Finishing			
Saw line	Panels	panel/h	
Sander	Panels	panel/h	
Storage banks	Panels	panel/h	15 days of panel storage
Lamination			
Press setup			
Press (nr of presses based on panels/h)	Panels	panel/h	4 hr press time; 30 panels per cycle; Panel size: 4ft x 8ft; No heating; 2 MPa pressure
Loading and unloading	Panels	panel/h	Machinery to handle 30 panels per cycle
Conditioning			
Forklifts and carts	Panels	panel/h	
Storage banks	Panels	panel/h	24 h residence period for PVA setting
Finishing			
Sander	Panels	panel/h	
Packaging and strapping	Panels	panel/h	
Storage banks	Panels	panel/h	15 days of panel storage

5.4. Capital and operating expense

The capital (CAPEX) and operating expenses (OPEX) predicted for the paper and pulp mills are shown in **Figure 30**. The CAPEX and OPEX increase with increased sludge feed rate; however, increased sludge flow will result in increased panel production and ultimately sales income. The prediction of CAPEX and OPEX is explained in section 5.4.1 and section 5.4.2, respectively, and the results are given in Appendix B.3. and B.4., respectively.

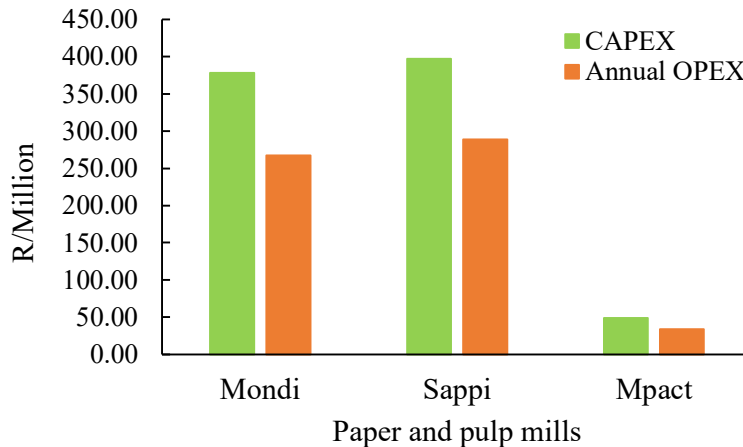


Figure 30: Comparing capital and operating expenses of different paper and pulp mills.

The capital expense was compared to previously costed composite mills, where these mills were roughly resized with the six tenth rule to a production rate of 770 000 panels per year – similar to the projected rate for MK and SK. Koenigshof (1978) projected a CAPEX of R 406 million to produce COM-PLY panels with veneer; and Spelter (1994) suggested a capital investment of \$ 0.5/ft² wood based composite – which translates to around R 367 million to produce 770 000 panels 4ft x 8ft in size. **Table 29** indicates that the CAPEX for MK and SK is R 378 million and R 397 million, respectively, which coincides with the values predicted by Koenigshof (1978) and Spelter (1994).

Furthermore, **Table 29** illustrates that increased paper and pulp mill waste utilization reduces the CAPEX and OPEX required to convert one ton dry waste per year into usable bio-composite material. The addition of lignin has a large effect on CAPEX and OPEX per annual ton of waste conversion. **Table 29** also indicates that the ratio between CAPEX and OPEX is reduced with increased production, since SK (with the largest PS emission) has a CAPEX/OPEX ratio of 1.38, while MS (with a relatively low PS emission of 500 ton/year) has a ratio of 1.52. This is the general behaviour of production scaling, since OPEX increases with higher production rates, while CAPEX becomes less expensive per production unit (Robus et al., 2016).

Table 29: Comparing CAPEX and OPEX per unit annual waste feed rate.

		MK	SK	MS
Dry sludge	ton/year	12 500	15 000	500
Lignin	ton/year	19 100	18 809	215
Total waste	ton/year	31 600	33 809	715
CAPEX	R/million	378.03	397.14	51.63
CAPEX/sludge	R/(ton/year)	30 242	26 476	103 260
CAPEX/ total waste	R/(ton/year)	11 963	11 747	72 210
OPEX	R/year/million	267.18	288.78	33.87
OPEX/sludge	(R/year)/(ton/year)	21 375	19 252	67 742
OPEX/ total waste	(R/year)/(ton/year)	8 455	8 542	47 372
CAPEX/OPEX		1.415	1.375	1.524

5.4.1. Capital expense

The CAPEX (Appendix B.3.) is determined by calculating the total purchase cost for all process equipment (section 5.4.1.1) and determining additional capital required (section 5.4.1.2).

5.4.1.1. Equipment cost

Figure 31a shows the purchase cost for the major process equipment, divided into lignin preparation, composite production, and lamination, while **Figure 31b** shows purchase cost for smaller process equipment as well as additional material and labour required for installation. The individual equipment purchase costs are obtained as described in section 5.3.2. The additional material and labour costs are estimated as per **Table 30**.

It is clear that the press operation requires the most capital, while product finishing (cutting and sanding) and mixing and reaction tanks require the least amount of capital. Also, most of the mixing and reactor capital is due to the precipitation of kraft lignin. “Additional material” envelope installation material such as concrete for foundation and steel for support structures and pipe racks, instrumentation, and insulating material. “Other equipment” groups smaller unit operations such as dryers, milling equipment, filters, and conditioning areas. The high equipment cost for MK and SK projects are due to the relatively high paper sludge flow rates around 15 000 ton/year, compared to the low 500 ton/year sludge flow from the MS mill.

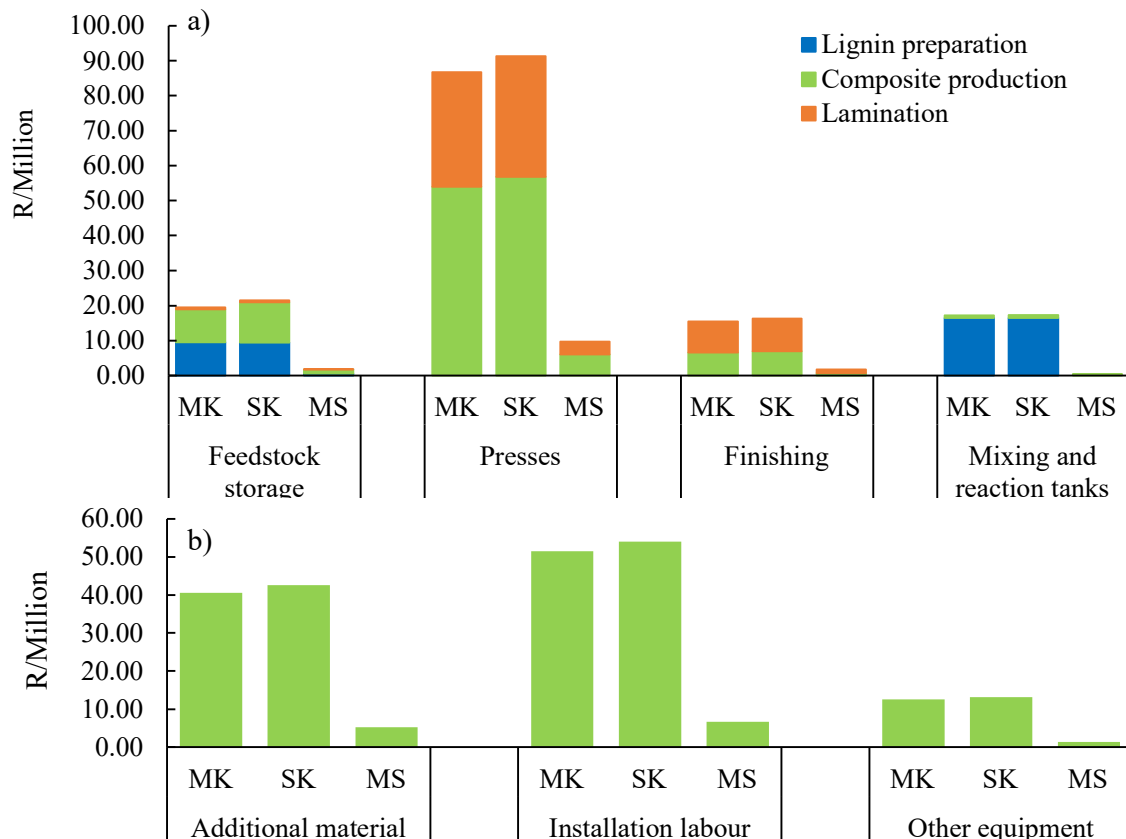


Figure 31: Equipment cost for a) major unit operations divided between lignin preparation, composite production, and lamination for each of the paper and pulp mills, and b) additional equipment, material, installation labour, and other unit operations.

5.4.1.2. Additional capital required

Table 30 shows how the total fixed capital investment is calculated. This includes the cost for additional material, installation labour cost, indirect costs such as transport and cleaning, and contingency factors as percentages of the equipment cost.

5.4.1.3. Economic benefit of production scaling

The CAPEX and minimum required selling price (MRSP) are plotted against plant capacity for various dry sludge flow rates in **Figure 32**. A threefold increase in sludge flow rate only results in a capital investment 1.88 times that for the original sludge flow rate from the kraft mills. This, also depicted by the deviation from the straight lines in **Figure 32A**, together with the reduction in MRSP as production capacity is increased in **Figure 32B** shows the economic benefits of upscaling. This is the case even if variable production cost increases with higher production, since fixed operating costs will reduce per unit product and CAPEX does not increase linearly with production capacity. The economic benefit of upscaling is an accepted occurrence and is also observed by other researchers (Chimphango, 2020; Robus et al., 2016).

Table 30: Break down of total fixed capital investment (Westney, 1997).

Equipment cost	Sum of equipment in section 5.4.1.1	100.0
Additional material	% of equipment cost	27.0
Pipe work		1.5
Concrete		8.5
Steel		0.5
Instrumentation installation		2.2
Electricity for installation		16.0
Paint and Insulation		0.5
Total material costs		127.0
Installation labour	27 % of total material cost	34.3
		161.3
Indirect costs	29 % of material and labour costs	46.8
Sub total		208.1
Contractors fee and contingency	18 % of the subtotal	37.5
Total fixed investment		245.6

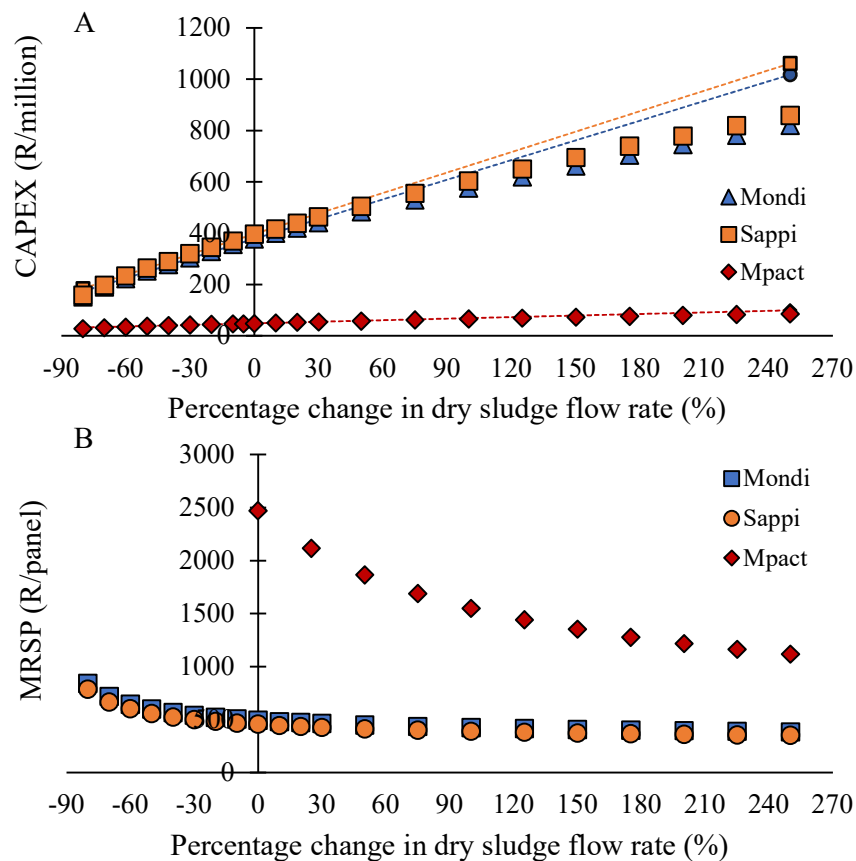


Figure 32: Economics of production scale is investigated by plotting A) CAPEX and B) MRSP against various plant capacities. A zero per cent change implies current sludge production as observed by Boshoff (2015).

5.4.2. Operating expense

The operating expenses are calculated by firstly determining the annual feedstock cost, annual salaries, operating utility expenses, and annual depreciation of equipment. The total operating expense (total annual production cost) is then predicted as per **Table 35**.

5.4.2.1. Cost of feedstock

Table 31 shows the cost per unit mass of the required feedstock material, while **Figure 33** depicts the total cost of feedstock for each of the paper and pulp mills. The MK and SK projects show the highest annual feedstock expense due to increased material throughput. The sulfuric acid is not a major expense when compared to the cost of binder (MgO and KH_2PO_4).

Table 31: Cost per unit mass of feedstock.

Material	Cost R/ton	Reference
Sulfuric acid	1 900	Humbird et al. (2011)
Fresh water	17	Chimphango (2020)
Calcium carbonate	3 200	Chimphango (2020)
Magnesium oxide	4 850	Chimphango (2020)
Monopotassium phosphate	9 060	Chimphango (2020)
PVA resin	17 000	Yuefang Chem (2020)
Veneer	17 R/(4ft x 8ft)	Timbercity Woodstock (2020)

The feedstock expenses are significantly higher for the kraft mills than for the lignosulfonate mill due to the large difference in dry sludge flow rates from each mill, while the added cost of sulfuric acid is less than 10 % of the overall feedstock cost.

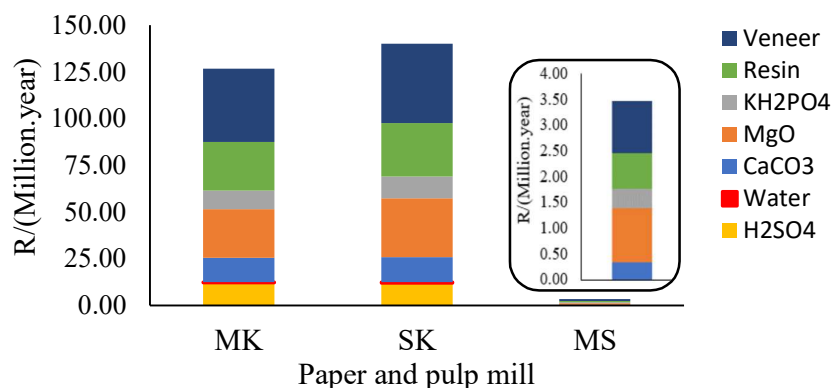


Figure 33: Cost of feedstock for different paper and pulp mills.

5.4.2.2. Sludge disposal and lignin fuel replacement

Transport cost and landfill charges are expenses that result from the removal of paper sludge from site. These costs were determined, from values given by Robus et al. (2016), as R 210 per

ton and R 780 per ton, respectively. Since the paper sludge will be used in this proposed project, that is assumed to become part of an existing paper and pulp mill, and not removed to landfill, these costs are considered as negative expenses in the discounted cash flow calculations, to quantify the reduced removal costs of the paper sludge compared to current situations where paper sludge is removed to landfill. Furthermore, lignin – with a calorific value of about 26 500 MJ/ton (Bruijninx et al., 2016) – is used as a fuel during the kraft pulping process and should be replaced when utilised in the proposed composite products. Coal and natural gas were considered as replacements, and ultimately coal was chosen due to its low cost of R 0.02/MJ as determined from Motlang and Nembahe (2018). It is evident that the kraft lignin has an effective cost between R 19.51 and R 31.17 per unit composite product, but in total comprise only about 89 % of the annual savings from the reduction of paper sludge disposal.

5.4.2.3. Salaries

Labour include managing staff, operators, engineers, and admin staff. The salaries in **Table 32** are suggested by Chimphango (2020); however, a contingency of 10 % is added.

Table 32: Salary expense to operate the suggested process, adapted from Chimphango (2020).

Position	Nr of staff	Salary	
		R/year/staff member	R/year
Production			4 636 000
Craftsmen	6	84 000	
Shift operators	3	170 000	
Maintenance technician	3	175 000	
Maintenance supervisor	1	243 000	
Shift supervisor	2	347 000	
Lab manager	1	360 000	
Plant manager	1	460 000	
Plant engineer	2	670 000	
General			1 340 000
Clerks	2	95 000	
Secretary	1	118 000	
Accountants	2	258 000	
Administrator	1	516 000	
10 % contingency			597 600
Total			6 573 600

5.4.2.4. Depreciation

Straight-line depreciation was assumed over the lifespan of the project. **Table 33** shows how the annual depreciation is calculated.

Table 33: Annual depreciation.

	Value	Unit
Project lifespan	15	Years
Annual depreciation	$\frac{\text{Fixed capital investment}}{\text{Project lifespan}}$	R/year

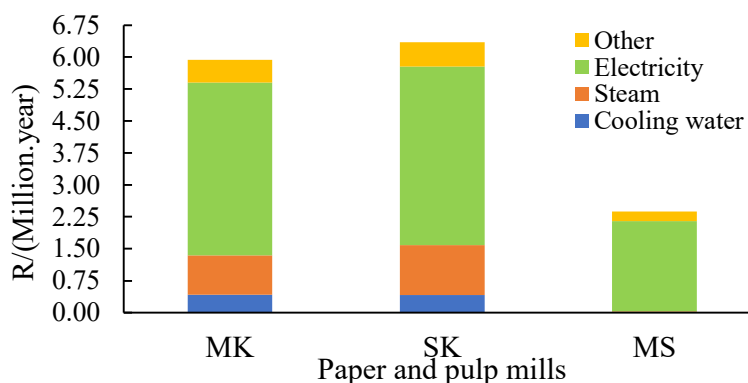
5.4.2.5. Utilities

Utility expenses include the use of cooling water to prevent overheating during lignin precipitation via acidification, steam to heat the material during composite pressing, and electricity for mechanical operation of the pumps, conveyors, agitators, and auxiliary lights.

Table 34: Cost per unit for operating utilities required.

Utility	Unit	Cost	Reference
Cooling water	R/ton	17	
Steam	R/ton	140	Chimphango (2020)
Electricity	R/kWh	0.84	

Figure 34 depicts the total annual utility cost for each of the paper and pulp mills, with electricity contributing the most to the utility cost. Although MS composites require heating to 155 °C, because of the small material throughput, steam contributes a negligible amount towards the total utility cost. It should be noted that saturated steam at 5 bar (151 °C) will be used for all composites except for MS composites where saturated steam at 8 bar will be used to maintain the required 20 °C temperature difference for adequate heat transfer. “Other” utility costs in **Figure 34** refer to electricity use for air conditioning, office lighting and allows for unforeseen usage of cooling water or steam. Cooling water is used during kraft lignin acidification to prevent excess heat generation, while this is not a necessity for liginosulfonate composites from MS.

**Figure 34:** Utility expenses for different paper and pulp mills.

5.4.2.6. Total production cost

Table 35 illustrates other costs that should be considered when OPEX is calculated, which include administration, distribution and marketing, research and development, and overhead costs (Westney, 1997). The values predicted by this method are only estimations, and the costs they represent should be determined again after the process is fully designed and developed.

Table 35: Annual operating expenses (Westney, 1997).

Direct production costs (DPC)		
Var	Feedstock material	From section 5.4.2.1
Fix	Salaries	From section 5.4.2.3
Var	Utilities	From section 5.4.2.5
Fix	Maintenance	6 % of fixed capital investment (FCI)
Fix	Consumables	15 % of Maintenance
Fix	Lab fees	10 % of Salaries
Var	Patents and royalties	5 % of Production cost (PC)
Total		DPC
Fixed production costs (FPC)		
Fix	Depreciation	From section 5.4.2.4
Fix	Local tax	2 % of FCI
Fix	Insurance	1.5 % of FCI
Total		FPC
Plant overhead cost (POC)		
Fix	Overhead costs	50 % of (Salaries and Maintenance)
Production cost (PC)		DPC + FPC + POC
General costs (GC)		
Fix	Administration costs	50 % of salaries
Var	Distribution and marketing	4 % of PC
Fix	Research and development	4 % of PC
Total		GC
Subtotal		PC + GC
Allowance for contingency		5 %
Total cost excluding tax		Annual operating expense

5.4.3. Cash flow calculations

Cash flow calculations are used to determine the profitability of the proposed process and is shown in Appendix B.5. Annual cash flow is predicted by considering production capacity, sales income, overall production costs (divided into fixed and variable costs, as denoted by *FIX* and *VAR* in **Table 35**), depreciation, tax on profit, working capital, fixed capital investment, sludge disposal cost elimination, and lignin fuel replacement expense.

Table 36: Assumptions regarding the annual cash flow of the proposed project, adapted from Chimphango (2020).

Parameter	Value	Unit	Reference
Project lifespan	15	years	Chimphango (2020)
Construction period	2	years	
1 st year	60	% of FCI	
2 nd year	40		
Working capital	5	% of FCI	
Ramp up production capacity			
1 st year	70	% of production capacity	(Robus et al., 2016)
2 nd year	80		
3 rd year	90		
onwards	100		
Annual production hours	6 600	h	Chimphango (2020)
Depreciation			
Straight line			
Period	15	years	
Salvage value	0	R	
Income tax	28	% of taxable income	Chimphango (2020)
Inflation rate	5.7	%	Chimphango (2020)
Minimum acceptable rate of return (Discount rate)	20	%	York timber (2018)

5.5. Profitability indicators

Key economic indicators such as payback period, net present value (NPV), and internal rate of return (IRR) are used to investigate the economic viability of a proposed project (Robus et al., 2016). After the cash flow of the project over its lifespan was predicted, these profitability indicators, as well as minimum required selling price (MRSP), were calculated to determine the economic viability of the proposed project.

5.5.1. Market research

5.5.1.1. Product selling price

To determine the profitability of the proposed project, a selling price must be selected. **Table 37** summarises the wholesale market prices achieved by various composites with diverse finishing. The selling price increases from around R 300/panel to over R 500/panel when veneer or laminates are added. Furthermore, the type of finishing affects final selling price, since melamine laminated boards are less expensive than wood veneered boards, while expensive laminates such as the gloss board and moisture resistant laminates drastically

increase selling price. Since a new product is proposed, an intermediate wholesale selling price of R 636 is assumed when the profitability indicators in this section is determined, while a low selling price of R 509, this intermediate selling price of R 636, and a high selling price of R 850 will be used during the sensitivity analysis.

Table 37: Market price from different sources.

Supplier	Product type	Selling price (R/panel) Size: 4ft x 8ft
Boardmaster	Plain chipboard	330
	Melamine on chip	405
	Melamine on Supawood	513
	Pine veneer chipboard	636
	Pine veneer on Supawood	708
	Gloss board on chip	939
BUCO	Melamine chipboard	456
Builders Warehouse	Melawood	522
	Plywood	545
	Laminated pine shelf	1 118
Cashbuild	Chipboard (no veneer)	300
	MDF Supawood (no veneer)	342
	Melamine board	506
	Countertop – moisture resistant finishing on chipboard	1 470
DIY shop	Laminated particleboard	850
PG Bison	Melamine particleboard	509
Alibaba	Melamine faced chipboard	490

5.5.2. Minimum required selling price

The minimum required selling price (MRSP) is calculated based on a minimum acceptable rate return (discount rate) of 20 %. **Figure 35** compares the MRSP to high and low market prices chosen from **Table 37**. The MRSP of MK and SK products is only 4 % lower than the low market price, while the MRSP of MS composites is around 400 % higher than the low selling price. This suggests that the MK and SK projects will get the minimum acceptable rate of return of 20 % even at a low market price, while MS cannot achieve a 20 % rate of return even at a high selling price. The high MRSP for MS composites is due to the low sludge flow rate that results in low product output, while fixed operating costs and capital investment is still relatively high as seen in **Table 29**.

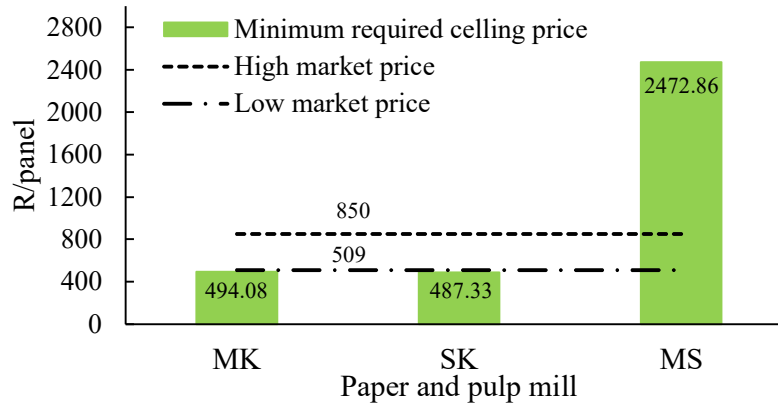


Figure 35: The minimum required selling price is compared to a minimum market price of R509 and a high market price of R850.

5.5.3. Payback period

The payback period is taken as the period required for the cumulative annual cash flow to become positive after capital investment. This however is a rough estimation of the viability of the project since the time value of money is not considered.

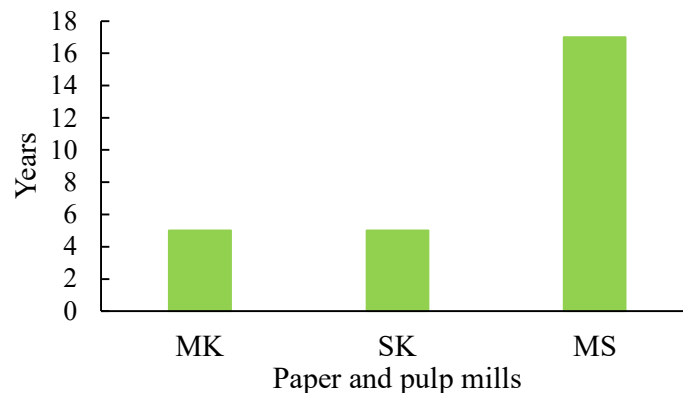


Figure 36: Payback period when a selling price of R636 is assumed.

Considering the 15 year lifespan of the project and assuming an intermediate selling price of R636/unit, a five year payback period (MK and SK mills) depicted in **Figure 36**, suggests that these paper and pulp mills should invest in this project; however, the fact that the payback period for MS is more than 15 years indicates that over the lifespan of this project, MS will only suffer a loss in investment.

5.5.4. Net present value

Unlike the payback period, the net present value (NPV) of a project considers the time value of money. A present value is determined for each annual cash flow total, the sum of which gives the NPV. A minimum percentage return on investment of 20 % is used to determine the

NPV. **Figure 37** compares the NPV of the three mills, where the large positive NPVs predicted for MK and SK indicate economic viability, while the negative NPV predicted for MS suggests that this project will result in a loss on investment. Higher NPVs for mills with higher sludge flow rates can be attributed to the economies of scale (Robus et al., 2016).

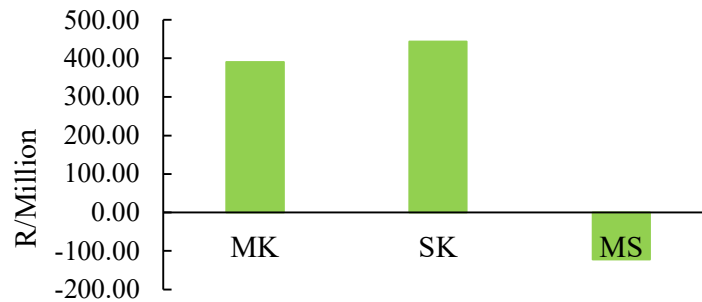


Figure 37: NPV at intermediate market price (R636/panel).

5.5.5. Internal rate of return (discounted cash flow percentage)

The internal rate of return (IRR) is seen as the percentage return on investment when the NPV is zero. Thus, if the IRR is larger than the required rate of return, the proposed project will be economically viable. The IRRs shown in **Figure 38** coincides with the NPVs shown in **Figure 37**. Because of the relatively large difference between MRSP for composites produced by MS and actual market price, the IRR is negative, implying that the future value of money must be higher than the current value of money if this project is to be economically viable. An IRR of 20 % is targeted to ensure positive return on capital despite loss in investment interest, and possible interest payable due to financing, while an inflation rate of 5.8 % is considered in the calculations of the annual cash flow. **Figure 37** and **Figure 38** indicate that a larger plant capacity will result in increased return on investment, and MS should consider increasing the proposed plant capacity by adding sawdust or other lignocellulosic waste, or sell the paper sludge to another mill for utilization in composite production.

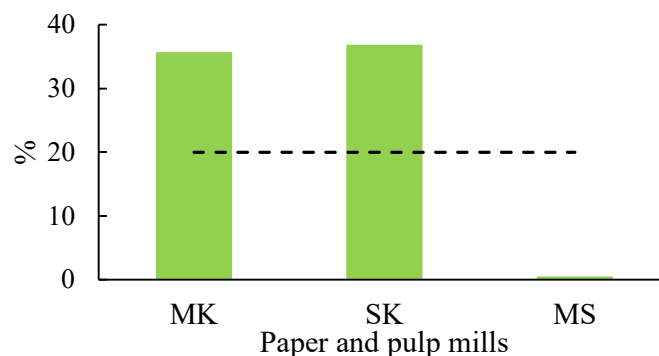


Figure 38: Discounted cash flow percentage obtained by the paper and pulp mills if market price of R636 is assumed.

5.6. Sensitivity analysis

To determine the effects of certain parameters on the economic viability of the project, CAPEX, overall OPEX, individual operating expenses, selling price, plant production capacity, sludge emission rate from the paper and pulp mills, and lignin and veneer usage was varied. A product standard size of 4ft x 8ft is assumed for all comparisons in this section.

5.6.1. Deviation in product selling price

Figure 39 indicates the sensitivity of the model for different selling prices (SP) – R 509, R 636, and R 850, and MRSP (orange) per unit product. Even at low SP, the composites from the MK and SK mills show economic viability, since the IRR is still between 22 % and 26 %, while the fact that even at R 850 per unit product MS still loses on investment suggests that this project will not be viable for MS unless the waste used in the composite drastically increases as discussed in section 5.6.4.

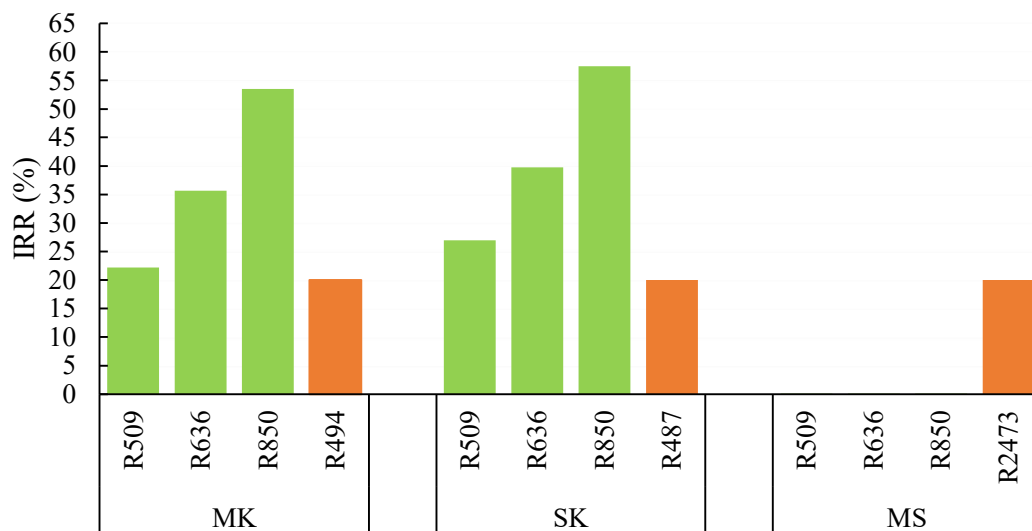


Figure 39: The IRR for various product selling prices (green) and the minimum required selling price (orange).

5.6.2. Deviation in CAPEX and OPEX

The effect of a 25 % deviation in CAPEX, OPEX, and working capital on IRR is shown in **Figure 40**. A 25 % deviation in working capital does not meaningfully influence the IRR. An increase in 25 % in either CAPEX or OPEX still results in an IRR of more than 25 % for the MK and SK projects. MS still has a zero IRR even if the CAPEX and OPEX are reduced by 25 %. This observation together with **Table 29** (CAPEX/sludge), **Figure 33** (Feedstock), **Figure 34** (Utilities), and **Figure 41** (deviation in individual OPEXs) leads to the conclusion that regardless of the cost of feedstock – e.g. sulfuric acid for kraft lignin isolation – and utilities

– e.g. cooling operations for said acidification – the CAPEX per unit sludge is the overwhelming cause for the unfeasibility of the MS project.

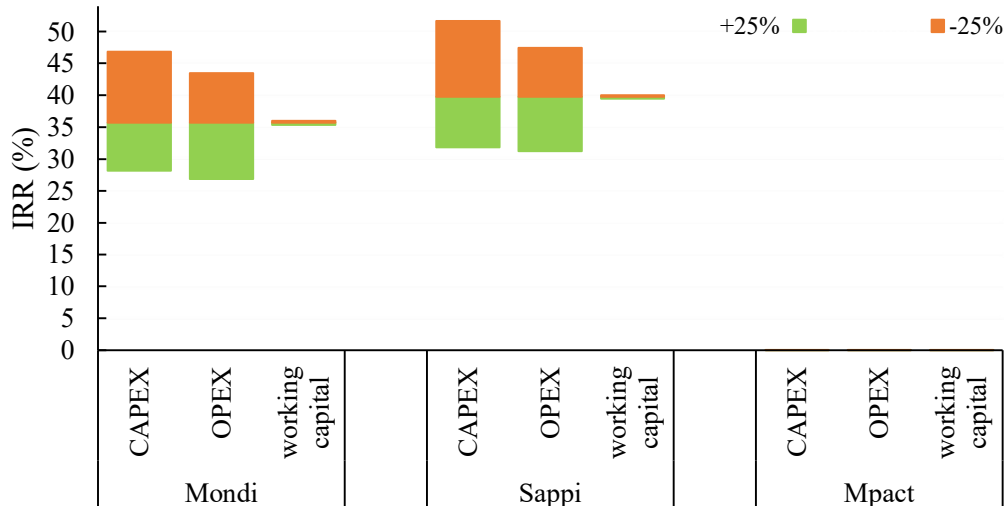


Figure 40: The effects of a 25 % deviation in capital expenses, overall annual operating expenses, and working capital on the IRR.

5.6.3. Deviation in individual operating expenses

Figure 41 compares the cost of feedstock, salaries and utilities to determine the contribution of individual operating expenses to the overall OPEX. The deviation in purchase of feedstock contributes the most to OPEX variation. Thus, the most effort must be focused on reducing the purchase cost of feedstock material. However, a 25 % increase in feedstock cost still results in an IRR larger than 30 % for MK and SK. The influence of the operating expense deviation cannot be observed for MS, since the IRR is smaller than zero.

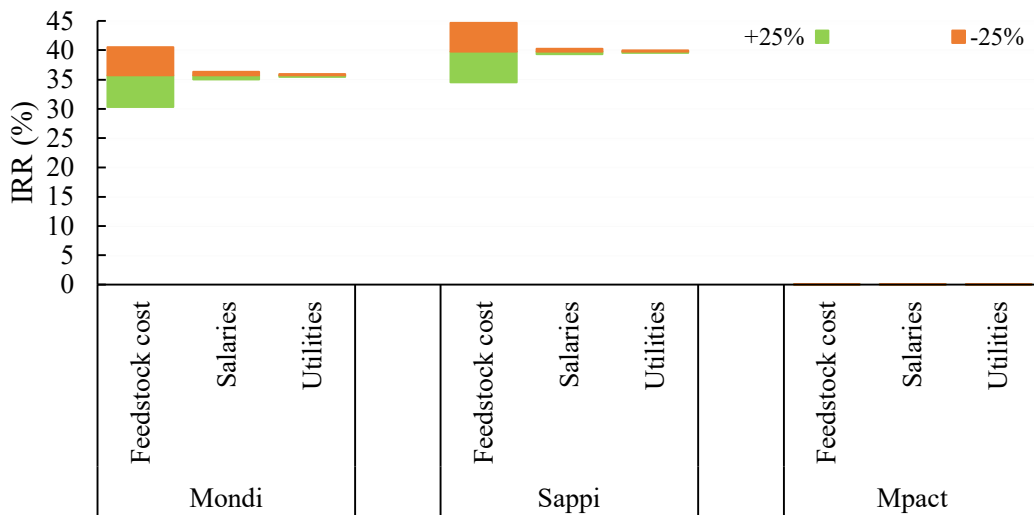


Figure 41: The effects of feedstock cost, salaries, and utilities on IRR.

5.6.4. Deviation in sludge emission from paper and pulp mills

Figure 42 indicates that paper and pulp mills with increased sludge emission will ultimately have a higher IRR - indicating a larger return on investment, with 20 % being the minimum acceptable rate of return. Increase in IRR with higher sludge flow rates are attributed to the fact that capital expenses will decrease proportionally with larger magnitudes of production and composite sales (Robus et al., 2016). This is also evident in the fact that SK achieves a slightly higher IRR than MK, since SK and MK have sludge flow rates of 15 kton/year and 12.5 kton/year, respectively.

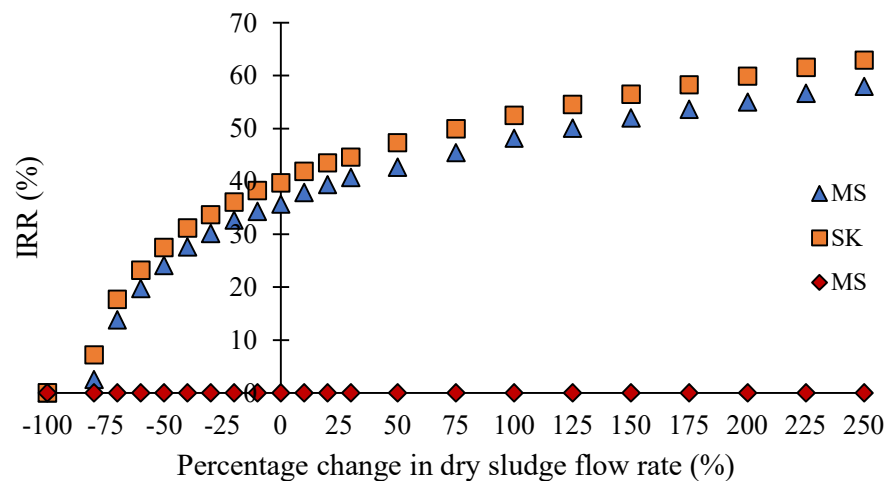


Figure 42: Effects of deviation in dry sludge emission from the paper and pulp mills on IRR.

An IRR of 20 % is achieved even if a new plant is built that utilizes only 40 % of sludge emitted by MK and SK. Furthermore, a 1 160 % increase (500 to 6 300 dry ton/year) in sludge flow from MS will result in an IRR of 20 % at a selling price of R 636. Increased sludge flow can be achieved by partnerships between paper and pulp mills to mix the respective sludge streams, or merely by adding additional waste such as sawmill dust produced when logs are cut and chipped.

5.6.5. Reduced production capacity

Unlike in the previous section, where the IRR is calculated for different plant capacities, in this section, the influence of reduced production on IRR is shown for plants with capacities as designed in section 5.3. Reduced production could result either from reduced sludge flow from paper and pulp mills, or a reduced market for bio composites. **Figure 43** indicates the robustness of the projects against reduced production due to a decreased market, since even at 73 % and 66 % operating capacity, the MK and SK projects will yield an IRR of 20 %.

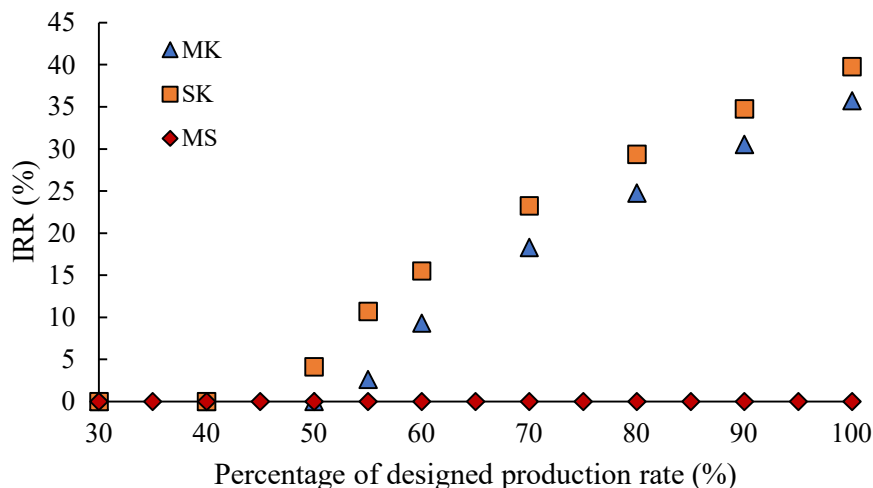


Figure 43: The effect of reduced production rate on DCF%.

5.6.6. Various lignin contents utilised in composite production

Lignin is normally burnt by paper and pulp mills for chemical and energy recovery. This might cause a limitation on the amount of lignin that can be used during composite production. The lignin content designed for in previous sections are bolded in **Figure 44**. If less kraft lignin is added to the composites, MK and SK still have sufficient return on investment with a minimum IRR of more than 30 %. Deviation in lignin content does not markedly alter the IRR, however, from an economic point of view, it is not recommended that lignin content between 0 and 8 wt% is used, since the added operating cost and investment will actually result in reduced IRR, because additional equipment and operating expenses will be more than the income generated by adding lignin. It should be clear that increased liginosulfonates content will not yield IRR larger than zero for MS.

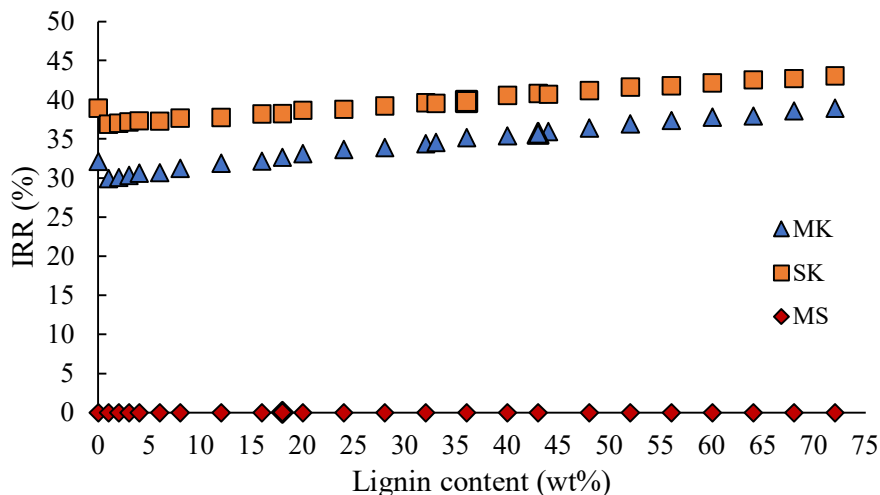


Figure 44: The effect of lignin content used to produce the composites on IRR.

5.6.7. Various fractions of veneered product

Markets for both veneered and unveneered composites exist. **Figure 45** shows the effect of the split between veneered and unveneered products on IRR. If no veneered products are produced, MK and SK will still achieve a IRR of 23 % and 29 %, respectively. The reduced capital investment and operating cost by not adding veneer, still does not yield a IRR larger than zero for MS, since unveneered panels are sold for only R330/panel. It is not recommended that between zero and 10 % of the products be veneered, since additional capital investment and operating expenses are not covered by increased selling income. Furthermore, to maximise IRR, the trend in **Figure 45** shows that all of the composites must be veneered.

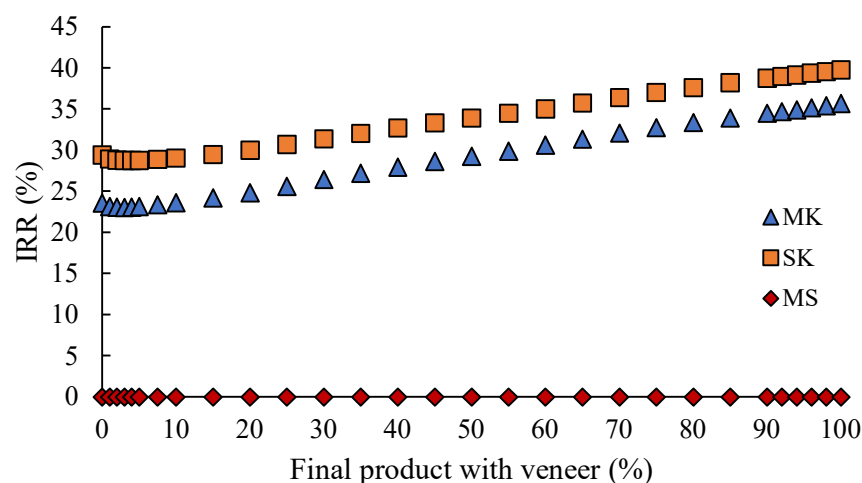


Figure 45: The effect of the fraction of product to be veneered on IRR.

5.7. General discussion

Numerous techno-economic studies have shown the possible benefits from utilising paper sludge in bioethanol production (Robus et al., 2016), and composite production (Chimphango, 2020), as well as the utilisation of lignin in value-adding processes (Thielemans et al., 2002; Wool and Sun, 2011). This study, however, combines the use of paper sludge and lignin in a single, easily produced green composite that could be used as inexpensive construction material. And by considering the impact of utilisation of paper sludge and lignin on the economics of the existing mills, it is found that the added expense of a fuel-replacement for lignin that will not be burnt for energy recovery is only 89 % of the savings due to reduced transport and landfill cost for paper sludge removal. Furthermore, the possible revenue from the green composite also adds to the attractiveness of the proposed project.

Robus et al. (2016) found that for a paper sludge flow rate of 5 500 ton/year the IRR could be around 25 % for the paper mill expansion towards bioethanol production from paper sludge,

whereas this project shows a possible IRR between 21 and 25 % for a similar paper sludge flow rate, however, the investigated kraft mills have dry sludge flow rates of more than 12 000 ton/year to yield an IRR of over 35 %. Furthermore, Chimphango (2020) showed that unveneered, non-loadbearing paper sludge composites have a minimum required selling price at least 50 % more than the average market price due to high energy requirements and limitations on production capacity, while the proposed composites that contain additional lignin and have a veneer finish have a minimum required selling price that is only 95 % of the low-end market price of R 509/4 x 8 ft² panel. The reduction in MRSP is caused by improved production capacity since lignin increases usable waste feedstock, to take advantage of the economy of scale, as well as reducing binder cost.

This leads to the conclusion that the MK and SK mills should invest in the proposed project, since it is shown to be viable even at increased capital and operating expenses, reduced production capacity, and lower than predicted selling price. The project is deemed not viable for the MS mill, since a loss in investment is predicted, as well as a non-viable selling price of R2 521/panel. Numerous factors could improve the possible economic viability of the project for MS, some solutions being: 1) a 20 % reduction in CAPEX and OPEX by utilising equipment for more than one operation (e.g. only one press to intermittently form the composite as well pressing the veneer), and reducing feedstock cost either via supplier discount or inhouse production of chemicals; and 2) increase in waste fibre flow rate from 500 ton/year dry sludge to 3 000 ton/year dry sludge and sawmill dust, which will increase panel production from 20 000 to 120 000 panels/year and reduce the minimum required selling price from R 2 521 to R 650/panel for a return on investment of 20 %. However, it is recommended that all paper and pulp mills should consider cost minimisation via heat exchange networks that would reduce heating requirements, and reduction in water usage by not completely drying the sludge before mixing to form the composite.

CHAPTER 6: CONCLUSIONS AND RECOMMENDATIONS

6.1. Conclusions

This study was aimed at the valorisation of paper and pulp waste by producing a composite that utilises an eco-friendly phosphate ceramic in conjunction with technical lignin to bind paper sludge fibres obtained from three South African paper and pulp mills. The conclusions of this study are summarised and discussed according to the project objectives.

I. Determine the characteristics of different types of technical lignin that could be useful in phosphate ceramic composites.

Desired properties of the technical lignin include low hydroxyl content and hydrophilicity, high reactivity towards hydrocarbons and thermal stability, while also possibly softening. These properties will result in composites with low water absorbance and deformation, and good mechanical performance due to improved interfacial adhesion via chemical bonding and enhanced mechanical interlocking. These lignin properties were identified via chemical (Fourier transform infrared spectroscopy), morphological (scanning electron microscopy), and thermal (thermogravimetry and differential scanning calorimetry) analyses to have substantial influence on final composite performance. The kraft black liquor and lignosulfonate showed relatively high hydroxyl content with between 0.81 and 0.88 hydroxyl groups per phenylpropanoid lignin monomeric structure that led to detrimental effects of moisture-induced deformation. Both lignin types did not chemically react with the paper sludge to improve interfacial adhesion, and any increase in mechanical performance was attributed to the softening of the lignin between 150 °C and 165 °C that improved mechanical interlocking, one of the interfacial adhesion mechanisms. Furthermore, the lignin exhibited better thermal stability than the phosphate ceramic, only degrading at temperatures hotter than 200 °C.

II. Determine if acid precipitated kraft lignin will yield significant improvements compared to kraft black liquor and lignosulfonate.

The composite mechanical performance, measured by the moduli of rupture (MOR) and elasticity (MOE), did not significantly improve when black liquor was added – composites that contained no additional lignin had MOR and MOE results of 1.0 MPa – 1.6 MPa and 327 MPa – 452 MPa, respectively, while composites that contain black liquor showed MOR and MOE performances of 0.83 MPa – 0.74 MPa and 491 MPa – 679 MPa. Conversely, the addition of acid precipitated kraft lignin significantly improved MOR and MOE results to

5.3 MPa – 7.2 MPa and 2 435 – 2 793 MPa, respectively. These improvements are the results of improved lignin properties. The sulfuric acid precipitation had a secondary effect on the lignin by reducing hydroxyl content – between 0.74 and 0.78 hydroxyl groups per phenylpropanoid unit (PPU) – via free oxygen radical formation that was observed as an increase in carbonyl groups on the PPU. This chemical alteration reduces the lignin hydrophilicity while increasing its reactivity towards hydrocarbons. However, the thermal stability of the precipitated lignin remained fairly unchanged, with similar glass transition and degradation temperatures compared to kraft black liquor and lignosulfonate.

III. Determine the effects of lignin on the interfacial adhesion mechanisms that control composite properties

The interfacial adhesion mechanisms are mechanical interlocking, van der Waal's forces, and chemical bonding. The kraft black liquor and lignosulfonate had similar effects on the adhesion mechanisms – high lignin hydrophilicity increased composite water absorbance of the composites. These effects caused increased water-induced deformation, measured by thickness swelling, while the kraft black liquor composites even showed reduced MOR results. The lignosulfonate increased MOR and MOE results compared to composites that contain no additional lignin and suggest improved mechanical interlocking. However, these improvements were not as prominent as the performance increase caused by the addition of precipitated kraft lignin that, due to the chemical alterations of the lignin, chemically bonded to the paper sludge via the formation of ether links. The alteration of the hydroxyl groups to carbonyl groups ($-C=O$) also reduced hydrophilicity. Furthermore, the precipitated lignin softened upon heating to around 130 °C to mould around the sludge fibres. The chemical bonding to and encasement of the paper sludge fibres by the precipitated lignin resulted in less water absorption (from 34.0 - 46.1 % to 12.5 - 14.7 %), reduced thickness swelling (from 11.0 – 13.8 % to 4.5 – 10.7 %), and superior mechanical performance (MOR from 1.0 – 1.6 MPa to 5.3 – 7.2 Mpa; MOE from 452 – 627 MPa to 2 435 – 2 793 MPa).

IV. Determine the technical viability of the lignin composites by evaluating the performance against previous research and industry standards.

Pine veneer was added to the composites to further improve the performance results as well as to increase the aesthetics of the new material that will finally raise selling price. This performance increase of MOR and MOE to 17.4 – 22.1 MPa and 2 909 – 3 882 MPa, respectively, ultimately yielded precipitated kraft lignin composites that adhere to industry

standards stipulated by the ISO, ASTM, and EN standards organisations for composite materials that may be used for interior purposes, such as furniture, cupboards, solid door cores, and non-loadbearing partitioning walls. Although the performance of the lignosulfonate composites also improved, it was to a lesser extent, since the resin used reacted differently to the various sludges.

V. Determine the economic competitiveness of the new lignin composite in a competitive market of inexpensive construction materials.

Precipitated kraft lignin composites showed economic viability due to reduction in phosphate binder cost and relatively high production rate, between 750 000 and 850 000 panels sized 1.2 x 2.4 m² and 13 mm thick. The lignosulfonate composites are not viable unless plant capacity is increased either via saw dust utilisation or sourcing of kraft lignin from elsewhere. Cost minimisation must be investigated via heat exchange networks, reduction in water utilisation, and possible supplier discount for feedstock. Assuming a competitive product selling price of R 220/m², the economic viability of the kraft lignin composites are supported by the estimated internal rate of return being between 35.7 % and 36.9 % for a sludge emission rate between 12 500 ton/year and 15 000 ton/year. The high IRR suggests that this project is a more attractive investment for kraft mills than continuing with sludge disposal, even with the addition of fuel costs to replace lignin. Conversely, due to the low sludge flow rate of 500 ton/year of the MS sulfite pulping mill, an internal rate of return of only 20 % is achieved at the unrealistic selling price of R 858/m². Economics of scale is evident from the predicted data that show the kraft mill expansion into green composite production could yield attractive investment, while the lignosulfonate composite plant will result in a loss in investment.

In conclusion, the stated objectives were met to valorise paper and pulp mill waste via the production of a bio composite on the way to a lower carbon economy.

6.2. Recommendations

I. Phosphate content variation for sludge-lignin combinations

The paper sludge and lignin from various mills contain different amounts of minerals. Some of these minerals partake in the acid-base reaction that form the phosphate ceramic. In this study, the phosphate ceramic to sludge fibre ratio was kept constant when lignin content was optimised. However, after lignin content optimisation, this ratio was altered by increasing the phosphate content to further improve mechanical strength but negatively impacting the modulus of elasticity, showing that this ratio might be influenced by the mineral content of the various sludge and lignin mixtures, and a tailored ratio per mill could cause improved composite performance.

II. Effects of impurities on composite performance

It is necessary to further investigate the effects of impurities on composite performance, since minerals, such as calcium carbonate, in the paper sludge and technical lignin can react with the phosphate ceramic to enhance composite performance, while other inert impurities such as plastics or silica can inhibit contact between lignin and sludge for adequate chemical bonding and will limit performance. Washing and filtration can be used to purify the components before composite production, however, the higher resulting costs must be considered.

III. Precipitation techniques for lignosulfonate

Before the kraft lignin is precipitated via sulfuric acid, it also shows undesirable properties such as high hydroxyl content. The sulfuric acid precipitation technique does not work for lignosulfonates and it is recommended that a precipitation treatment with similar altering effect is researched to reduce the hydroxyl groups of the lignosulfonates if it is to be used in composite production.

IV. Chemical modification to improve thermal incompatibilities

The thermal trade-off between phosphate degradation and lignin glass transition for improved mechanical interlocking is discussed in this project. However, it is possible to alter the glass transition temperature of lignin via changes in molecular weight, degree of cross-linking, and breaking of very stable, rigid chemical bonds within lignin monomeric structures. Lowering the glass transition temperature to a range where the phosphate does not degrade, can improve composite performance by mitigating the trade-off effect.

REFERENCES

- AAAMSA Group. (2004), *General Specification for Drywall Partitions and Lightweight Internal Walls*, Midrand.
- Akbari, H., Mensah-biney, R. and Simms, J. (2015), “Production of Geopolymer Binder from Coal Fly Ash to Make Cement-less Concrete”, pp. 1–8.
- de Alda, J.A.G.O. (2008), “Feasibility of recycling pulp and paper mill sludge in the paper and board industries”, *Resources, Conservation and Recycling*, Vol. 52 No. 7, pp. 965–972.
- Amiandamhen, S.O. (2017), “Phosphate bonded wood and fibre composites”, Stellenbosch : Stellenbosch University, available at: <http://scholar.sun.ac.za/handle/10019.1/100912> (accessed 3 March 2019).
- Amiandamhen, S.O. and Izekor, D.N. (2013), “Effect of wood particle geometry and pre-treatments on the strength and sorption properties of cement-bonded particle boards”, *Journal of Applied and Natural Science*, Vol. 5 No. 2, pp. 318–322.
- Amiandamhen, S.O., Meincken, M. and Tyhoda, L. (2016), “Magnesium based phosphate cement binder for composite panels: A response surface methodology for optimisation of processing variables in boards produced from agricultural and wood processing industrial residues”, *Industrial Crops and Products*, Vol. 94, pp. 746–754.
- Amiandamhen, S.O., Meincken, M. and Tyhoda, L. (2017), “Calcium phosphate bonded wood and fiber composite panels: production and optimization of panel properties”, *Holzforschung*, Vol. 71 No. 9, pp. 725–732.
- Amiandamhen, S.O., Meincken, M. and Tyhoda, L. (2019), “Phosphate bonded natural fibre composites: a state of the art assessment”, *SN Applied Science*, Vol. 1 No. 910.
- Amiandamhen, S.O., Montecuccoli, Z., Meincken, M., Barbu, M.C. and Tyhoda, L. (2018), “Phosphate bonded wood composite products from invasive Acacia trees occurring on the Cape Coastal plains of South Africa”, *European Journal of Wood and Wood Products*, Vol. 76 No. 2, pp. 437–444.
- ANSI/AHA A135.4. (1995), “Basic hardboard, ANSI/AHA A135.4”, American National Standards Institute/American Hardboard Association, Palatine.
- ANSI/AHA A194.1. (1985), “Cellulosic fiberboard, ANSI/AHA A194.1-1985”, American

- National Standards Institute/American Hardboard Association, Palatine.
- ANSI A208.1-1993. (1993), “Particleboard, ANSI A208.1-1993”, American National Standards Institute, Gaithersburg.
- ANSI A208.2-1994. (1994), “Medium density fiberboard (MDF), ANSI A208.2-1994”, American National Standards Institute, Gaithersburg.
- ANSI A208. (1999), “Particleboard, American National Standard, Composite Panel”, *Association, Gaithersburg (1999)*.
- Aro, T. and Fatehi, P. (2017), “Production and Application of Lignosulfonates and Sulfonated Lignin”, *CHEMSUSCHEM*, Vol. 10, pp. 1861–1877.
- ASTM. (2012), “Standard Test Methods for Evaluating Properties of Wood-Base Fiber and Particle Panel Materials - ASTM:D1037-12”, *ASTM International*, pp. 1–8.
- ASTM. (2013), *ASTM D1037-13 Standard Test Methods for Evaluating Properties of Wood-Base Fiber and Particle, Annual Book of ASTM Standards*, available at:<https://doi.org/10.1520/D1037-06A.1.2>.
- ASTM C208-94. (1994), “Standard specification for cellulosic fiber insulating board, ASTM C208-94”, American Society for Testing and Materials, Philadelphia.
- ASTM D1037-99. (1999), “Particleboard, American National Standard, Composite Panel Association”, Gaithersburg.
- Bajpai, P. (2011), “Biotechnology for pulp and paper processing”, *Biotechnology for Pulp and Paper Processing*, Vol. 9781461414, pp. 1–414.
- Baker, G.A., Ravula, S., Zhao, H. and Jones, J. (2012), “PEG-functionalized ionic liquids for cellulose dissolution and saccharification”, *Green Chemistry*, Vol. 14 No. May 2016, pp. 2922–2932.
- Bayvel, L.P. and Jones, A.R. (1981), “Methods of Measuring Particle Size Distribution”, *Electromagnetic Scattering and Its Applications*, Dordrecht.
- Bentz, D.P., Ferraris, C.F., Jones, S.Z., Lootens, D. and Zunino, F. (2017), “Limestone and silica powder replacements for cement: Early-age performance”, *Cement and Concrete Composites*, Vol. 78, pp. 43–56.
- Berlin, A. and Balakshin, M. (2014), “Industrial Lignins: analysis, properties, and

- applications”, *Bioenergy Research: Advances and Applications*, pp. 315–336.
- Bhaskar, J., Haq, S., Pandey, A.K. and Srivastava, N. (2012), “Evaluation of properties of propylene-pine wood plastic composite”, *Journal of Materials and Environmental Science*, Vol. 3 No. 3, pp. 605–612.
- Bledzki, A.K. and Gassan, J. (1999), “Composites reinforced with cellulose based fibres”, *Progress in Polymer Science (Oxford)*, Vol. 24 No. 2, pp. 221–274.
- Börjesson, M.H. and Ahlgren, E.O. (2015), *Pulp and Paper Industry*, available at:<https://doi.org/10.1016/B978-0-12-803408-8.00006-8>.
- Boshoff, S. (2015), *Characterization and Fermentation of Waste Paper Sludge for Bioethanol Production*.
- Brebu, M. and Vasile, C. (2010), “Thermal Degradation of Lignin - A Review”, *Cellulose Chemistry and Technology*, Vol. 44 No. 9, pp. 353–363.
- Brodin, I. (2009), *Chemical Properties and Thermal Behaviour of Kraft Lignins*, KTH Royal Institute of Technology.
- Bruijninx, P., Weckhuysen, B., Gruter, G.-J. and Engelen-Smeets, E. (2016), “Lignin Valorisation: The Importance of a Full Value Chain Approach”, p. 22.
- BS EN 634-2. (2007), “Cement-bonded particleboards –Specifications- Part 2: Requirements for OPC bonded particleboards for use in dry, humid and external conditions”, *British Standard (2007)*.
- Budnyak, T.M., Pylypchuk, I. V, Lindstro, M.E. and Sevastyanova, O. (2019), “Electrostatic Deposition of the Oxidized Kraft Lignin onto the Surface of Aminosilicas: Thermal and Structural Characteristics of Hybrid Materials Electrostatic Deposition of the Oxidized Kraft Lignin onto the Surface of Aminosilicas : Thermal and Structu”, *ACS Omega*, available at:<https://doi.org/10.1021/acsomega.9b03222>.
- Cai, J. ming and Panteki, J. (2016), “Using Calcium Carbonate Whisker in Engineered Cementitious Composites”, *Proceedings of the 9th International Conference on Fracture Mechanics of Concrete and Concrete Structures*, pp. 1–11.
- Cai, Z. and Ross, R.J. (2010), “Mechanical Properties of Wood-Based Composite Materials”, *Wood Handbook - Wood as an Engineering Material*, U.S. Department of Agriculture.

- Carll, C. (1986), *Wood Particleboard and Flakeboard: Types, Grades, and Uses*, Madison, available at: <https://books.google.co.za/books?id=07OL251GJPUC&q=Wood+Particleboard+and+Flakeboard+Types,+Grades,+and+Uses&dq=Wood+Particleboard+and+Flakeboard+Types,+Grades,+and+Uses&hl=en&sa=X&ved=0ahUKEwix4rDVmLHhAhXiVhUIHap4A3IQ6AEIKjAA> (accessed 2 April 2019).
- Cetin, N.S. and Özmen, N. (2002), “Use of organosolv lignin in phenol-formaldehyde resins for particleboard production II. Particleboard production and properties”, *International Journal of Adhesion and Adhesives*, Vol. 22, pp. 481–486.
- Chandra, S. (1997), *Waste Materials Used in Concrete Manufacturing*, Noyes Publications, available at: <https://books.google.co.za/books?hl=en&lr=&id=tVjIWdUUF1QC&oi=fnd&pg=PR2&dq=lignin+concrete+admixture&ots=w-4YV5SyZ3&sig=T5kPO-OpicdAyB2uc7V6RIeLoeQ#v=onepage&q=lignin+concrete+admixture&f=false> (accessed 5 April 2019).
- Chimphango, A. (2020), *The Valorisation of Paper Sludge for Green Composite Material*, Stellenbosch University.
- Constant, S., Wienk, H.L.J., Frissen, A.E., Peinder, P. de, Boelens, R., van Es, D.S., Grisel, R.J.H., et al. (2016), “New insights into the structure and composition of technical lignins: a comparative characterisation study”, *Green Chemistry*, Vol. 18 No. 9, pp. 2651–2665.
- Coyne, D. (2018), *World Coal 2018-2050: World Energy Annual Report (Part 4)*, Utah.
- Culbertson Jr., G.C. (2017), *Commercialization of Sustainable Bio-Refinery Projects for the Pulp and Paper Industry*, North Carolina State University.
- Davis, E., Shaler, S.M. and Goodell, B. (2003), “The incorporation of paper deinking sludge into fiberboard”, *Forest Products Journal*, Vol. 53 No. 11, pp. 46–54.
- Dhakal, H.N., Zhang, Z.Y. and Richardson, M.O.W. (2007), “Effect of water absorption on the mechanical properties of hemp fibre reinforced unsaturated polyester composites”, *Composites Science and Technology*, Vol. 67 No. 7–8, pp. 1674–1683.
- Ding, Z., Dong, B., Xing, F., Han, N. and Li, Z. (2014), “Cementing mechanism of potassium phosphate based magnesium phosphate cement”, *Ceramics International*, Vol. 38 No. 8,

pp. 6281–6288.

- Dolan, E. (2013), “Doomsday: Will peak phosphate get us before global warming?”
- Domínguez, J.C., Santos, T.M., Rigual, V., Oliet, M., Alonso, M. V. and Rodriguez, F. (2018), “Thermal stability, degradation kinetics, and molecular weight of organosolv lignins from *Pinus radiata*”, *Industrial Crops and Products*, Vol. 111, pp. 889–898.
- Donahue, P.K. and Aro, M.D. (2010), “Durable phosphate-bonded natural fiber composite products”, *Construction and Building Materials*, Vol. 24 No. 2, pp. 215–219.
- Donkor, K.O. (2019), *Paper Industry Process Wastewater Reclamation and Potential Clarification from Paper Sludge through Integrated Bio-Energy Production*.
- Dowell, F., Wang, D., Xu, F., Yu, J., Tesso, T., Dowell, F. and Wang, D. (2013), “Qualitative and quantitative analysis of lignocellulosic biomass using infrared techniques: A mini-review Qualitative and quantitative analysis of lignocellulosic biomass using infrared techniques: A mini-review”, *Applied Energy*, Vol. 104, pp. 801–809.
- Emblem, A. and Hardwidge, M. (2012), “Adhesives for packaging”, *Packaging Technology*, Woodhead Publishing, pp. 381–394.
- EN 634-2. (2007), *Cement-Bonded Particleboards - Specifications - Part 2: Requirements for OPC Bonded Particleboards for Use in Dry, Humid and External Conditions*, No. 634, London.
- English, B.W. and Falk, R.H. (1995), “Factors that Affect the Application of Wood Fiber-Plastic Composites”.
- Evans, P.D. (2013), “Weathering of Wood and Wood Composites”, in Rowell, R.M. (Ed.), *Handbook of Wood Chemistry and Wood Composites*, Second., London, pp. 151–216.
- Frigerio, P., Zoia, L., Orlandi, M., Hanel, T. and Castellani, L. (2014), “Application of sulphur-free lignins as a filler for elastomers: Effect of hexamethylenetetramine treatment”, *BioResources*, Vol. 9 No. 1, pp. 1387–1400.
- Froass, P.M., Ragauskas, A.J. and Jiang, J. (1996), “Chemical structure of lignin from kraft pulp”, *Journal of Wood Chemistry and Technology*, Vol. 16 No. 4, pp. 347–365.
- Frybort, S., Mauritz, R., Teischinger, A. and Müller, U. (2008), “Cement bonded composites - A mechanical review”, *BioResources*, Vol. 3 No. 2, pp. 602–626.

- Fuentes, C., Le Quan, T.N., Brughmans, G., van Vuure, A.W., Verpoest, I. and Dupont, C. (2014), “Effect of Roughness on the Interface in Natural Fibre Composites: Physical Adhesion and Mechanical Interlocking”, *16th European Conference on Composite Materials*, Vol. 2014.
- Gao, W., Inwood, J.P.W. and Fatehi, P. (2019), “Sulfonation of Phenolated Kraft Lignin to Produce Water Soluble Products”, *Journal of Wood Chemistry and Technology*, Vol. 39 No. 4, pp. 225–241.
- Giles, H.F., Wagner, J.R. and Mount, E.M. (2005), “47 - Extrusion Coating and Lamination”, in Giles, H.F., Wagner, J.R. and Mount, E.M. (Eds.), *Extrusion - The Definitive Processing Guide and Handbook*, Norwich, pp. 465–468.
- Grāvītis, J., Āboliņš, J., Tupčiauskas, R. and Vēveris, A. (2010), “LIGNIN FROM STEAM-EXPLODED WOOD AS BINDER IN WOOD COMPOSITES”, *Journal of Environmental Engineering and Landscape Management*, Vol. 18 No. 2, pp. 75–84.
- Hajiha, H., Sain, M. and Mei, L.H. (2014), “Modification and Characterization of Hemp and Sisal Fibers”, *Journal of Natural Fibers*, Vol. 11 No. 2, pp. 144–168.
- Han, T., Sophonrat, N., Evangelopoulos, P., Persson, H., Yang, W. and Jönsson, P. (2018), “Evolution of sulfur during fast pyrolysis of sulfonated Kraft lignin”, *Journal of Analytical and Applied Pyrolysis*, Vol. 133, pp. 162–168.
- Ház, A., Jablonský, M., Šurina, I., Kačík, F., Bubeníková, T. and Ďurkovič, J. (2019), “Chemical Composition and Thermal Behavior of Kraft Lignins”, *Forests*, Vol. 10 No. 6, pp. 1–12.
- Hollaway, L., Green, G. and Feely, C. (1994), *Handbook of Polymer Composites for Engineers*, Woodhead Publishing, Cambridge.
- Hong, M.-K., Lubis, M.A.R., Park, B.-D., Sohn, C.H. and Roh, J. (2018), “Effects of surface laminate type and recycled fiber content on properties of three-layer medium density fiberboard”, *Wood Material Science & Engineering*, pp. 1–9.
- Humbird, S., Davis, R., Tao, L., Kinchin, C., Hsu, D., Aden, A., Schoen, P., et al. (2011), *Process Design and Economics for Biochemical Conversion of Lignocellulosic Biomass to Ethanol*, Colorado.
- Inwood, J.P.W., Pakzad, L. and Fatehi, P. (2018), “Production of Sulfur Containing Kraft

- Lignin Products”, *BioResources*, Vol. 13 No. 1, pp. 53–70.
- Irle, M., Barbu, M.C., Reh, R., Bergland, L. and Rowell, R.M. (2013), “Wood Composites”, in Rowel, R.M. (Ed.), , Second Ed., London, pp. 321–411.
- ISO 16893:2016. (2016), “International Standard for wood-based panels - Particleboard - ISO 16893:2016”.
- ISO 16893. (2006), “Wood-based panels - Particleboard”, *International Organization for Standardization*, p. 18.
- ISO 9427. (2003), “Specifies a method for determining the density of wood-based panels”, International Organization for Standardization.
- Jakab, G.J., Hemenway, D.R. and Risby, T.H. (2005), *Final Report: Effects of Formaldehyde and Particle-Bound Formaldehyde on Lung Macrophage Functions*, MassaChusetts, available at: https://cfpub.epa.gov/ncer_abstracts/index.cfm/fuseaction/display.highlight/abstract/2316/report/F (accessed 7 April 2019).
- Jeong, H., Park, J., Kim, S., Lee, J. and Cho, J.W. (2012), “Use of acetylated softwood kraft lignin as filler in synthetic polymers”, *Fibers and Polymers*, Vol. 13 No. 10, pp. 1310–1318.
- Jeong, S.Y. and Wagh, A.S. (2002), *Chemically Bonded Phosphate Ceramics: Cementing the Gap between Ceramics and Cements*.
- Jeong, S.Y. and Wagh, A.S. (2003), “Cementing the gap between ceramics, cements, and polymers.”, *Materials Technology*, Vol. 18 No. 3, pp. 162–168.
- Jiang, Z., Qian, C. and Chen, Q. (2017), “Experimental investigation on the volume stability of magnesium phosphate cement with different types of mineral admixtures”, *Construction and Building Materials*, Vol. 157, pp. 10–17.
- Kabir, M.M., Wang, H., Aravinthan, T., Cardona, F. and Lau, K.-T. (2011), “Effects of Natural Fibre Surface on Composite Properties: A Review”, *Energy, Environment and Sustainability*, pp. 94–99.
- Kadla, J.F., Kubo, S., Venditti, R.A., Gilbert, R.D., Compere, A.L. and Griffith, W. (2002), “Lignin-based carbon fibers for composite fiber applications”, *Carbon*, Vol. 40 No. 15,

pp. 2913–2920.

- Kaewtatip, K., Menut, P., Auvergne, R., Tanrattanakul, V., Morel, M.-H. and Guilbert, S. (2010), “Interactions of Kraft Lignin and Wheat Gluten during Biomaterial Processing: Evidence for the Role of Phenolic Groups”, *Journal of Agricultural and Food Chemistry*, Vol. 58, pp. 4185–4192.
- Kamoun, A., Jelidi, A. and Chaabouni, M. (2003), “Evaluation of the performance of sulfonated esparto grass lignin as a plasticizer–water reducer for cement”, *Cement and Concrete Research*, Vol. 33 No. 7, pp. 995–1003.
- Kazzaz, A.E., Feizi, Z.H. and Fatehi, P. (2019), “Grafting Strategies for hydroxy groups of lignin for producing materials”, *Green Chemistry*, Vol. 21 No. 21, pp. 5714–5752.
- Koenigshof, G.A. (1978), *Economic Feasibility of Sanufacturing Com-Ply Studs in the South*, Athens, Georgia.
- Konduo, T. (1997), “The assignment of IR absorption bands due to free hydroxyl groups in cellulose”, *Cellulose*, Vol. 4 No. 281.
- Kowalczyk, P.B. and Drzymala, J. (2016), “Physical Meaning of the Sauter Mean Diameter of Spherical Particulate Matter”, *Particulate Science and Technology*, Vol. 34 No. 6, pp. 645–647.
- Kuokkanen, T., Nurmesniemi, H., Pöykiö, R., Kujala, K., Kaakinen, J. and Kuokkanen, M. (2008), “Chemical and leaching properties of paper mill sludge”, *Chemical Speciation and Bioavailability*, Vol. 20 No. 2, pp. 111–122.
- Lange, H., Decina, S. and Crestini, C. (2013), “Oxidative upgrade of lignin – Recent routes reviewed”, *European Polymer Journal*, Vol. 49 No. 6, pp. 1151–1173.
- Laufenberg, T.L. and Aro, M. (2004), “Phosphate-Bonded Ceramic – Wood Composites: R&D Project Overview and Invitation to Participate”, *Proc. of 9th Intern. Conf. on Inorganic-Bonded Composite Materials*, pp. 84–91.
- Leite, F.L., Bueno, C.C., Da Roz, A.L., Ziemath, E.C. and Oliveira, O.N. (2012), “Theoretical Models for surface forces and adhesion and their measurement using atomic force microscopy”, *International Journal of Molecular Sciences*, Vol. 13 No. 10, pp. 12 773-12 856.

- de Lemos, A.L., Pires, P.G.P., de Albuquerque, M.L., Botaro, V.R., de Paiva, J.M.F. and Domingues, N.S. (2017), “Biocomposites reinforced with natural fibers_ thermal morphological and mechanical characterization”, *Revista Materia*, Vol. 22 No. 2.
- Liao, W., Ma, H., Sun, H., Huang, Y. and Wang, Y. (2017), “Potential large-volume beneficial use of low-grade fly ash in magnesia- phosphate cement based materials”, *Fuel*, Vol. 209, pp. 490–497.
- Liu, W., Mohanty, A.K., Askeland, P., Drzal, L.T. and Misra, M. (2004), “Influence of fiber surface treatment on properties of Indian grass fiber reinforced soy protein based biocomposites”, *Polymer*, Vol. 45 No. 22, pp. 7589–7596.
- Lora, J. (2008), “Industrial commercial lignins: sources, properties and applications”, *Monomers, Polymers and Composites from Renewable Resources*, pp. 225–241.
- Ma, H., Xu, B. and Li, Z. (2014), “Magnesium potassium phosphate cement paste: Degree of reaction, porosity and pore structure”, *Cement and Concrete Research*, Vol. 65, pp. 96–104.
- El Mansouri, N.-E. and Salvadó, J. (2007), “Analytical methods for determining functional groups in various technical lignins”, *Industrial Crops and Products*, Vol. 26 No. 2, pp. 116–124.
- Mansur, H.S., Mansur, A.A. and Bicallho, S.M. (2005), “Lignin-hydroxyapatite/tricalcium phosphate biocomposites: SEM/EDX and FTIR characterization”, *Key Engineering Materials*, Vol. 284, pp. 745–748.
- Marsh, G.M. (1982), “Proportional mortality patterns among chemical plant workers exposed to formaldehyde.”, *British Journal of Industrial Medicine*, Vol. 39 No. 4, pp. 313–22.
- Matthews, F.L. and Rawlings, R.D. (1999), *Composite Materials: Science and Engineering, Engineering*, Vol. 2nd Ed., available at:[https://doi.org/10.1016/S0140-6736\(00\)67208-2](https://doi.org/10.1016/S0140-6736(00)67208-2).
- McDougall, F.R. and Hruska, J.P. (2000), “Report: the use of Life Cycle Inventory tools to support an integrated approach to solid waste management”, *Waste Management & Research*, Vol. 18 No. 6, pp. 590–594.
- Migneault, S., Koubaa, A., Riedl, B., Nadji, H., Deng, J. and Zhang, T. (2011), “BINDERLESS FIBERBOARD MADE FROM PRIMARY AND SECONDARY PULP AND PAPER SLUDGE”, *Wood and Fiber Science*, Vol. 43 No. 2, pp. 180–193.

- Mngomezulu, L.B. (2019), *Phosphate-Bonded Composite Products: The Influence of Filler Materials, Biomass Type, and Processing Method on Panel Properties*, Stellenbosch University.
- Mohr, B.J., El-Ashkar, N.H. and Kurtis, K.E. (2004), “Fiber-Cement Composites for Housing Construction: State-of-the-Art Review”, *Proceedings of the NSF Housing Research Agenda Workshop*, p. 17.
- Monte, M.C., Fuente, E., Blanco, A. and Negro, C. (2009), “Waste management from pulp and paper production in the European Union”, *Waste Management*, pp. 293–308.
- Mosselmans, G., Biesemans, M., Willem, R., Wastiels, J., Leermakers, M., Rahier, H., Brughmans, S., et al. (2007), “Thermal hardening and structure of a phosphorus containing cementitious model material: Phosphoric acid-wollastonite”, *Journal of Thermal Analysis and Calorimetry*, Vol. 88 No. 3, pp. 723–729.
- Motlang, M. and Nembahe, R. (2018), *Energy Price Report*, Pretoria.
- Naron, D.R., Collard, F., Tyhoda, L. and Görgens, J.F. (2017), “Characterisation of lignins from different sources by appropriate analytical methods: Introducing thermogravimetric analysis-thermal desorption-gas chromatography – mass spectroscopy”, *Industrial Crops & Products*, Vol. 101, pp. 61–74.
- Norström, E., Demircan, D., Fogelström, L., Khabbaz, F. and Malmström, E. (2018), “Green Binders for Wood Adhesives”, *Applied Adhesive Bonding in Science and Technology*, pp. 49–71.
- Osman, M.A., Atallah, A. and Suter, U.W. (2004), “Influence of excessive filler coating on the tensile properties of LDPE-calcium carbonate composites”, *Polymer*, Vol. 45 No. 4, pp. 1177–1183.
- Paauw, M. and Pizzi, A. (1993), “Some filler effects on cross-linking of unsaturated polyesters”, *Journal of Applied Polymer Science*, Vol. 50 No. 7, pp. 1287–1293.
- PAMSA. (2019), *Summary Findings on 2019 Production, Import and Export Statistics*, available at: www.recyclepaper.co.za (accessed 8 July 2020).
- PerkinElmer Inc. (2010), “Thermogravimetric Analysis (TGA): A Beginner’s Guide”, available at: https://www.perkinelmer.com/lab-solutions/resources/docs/faq_beginners-guide-to-thermogravimetric-analysis_009380c_01.pdf (accessed 3 August 2020).

- Podschun, J., Stu, A., Buchholz, R.I., Heitmann, M., Schreiber, A., Saake, B. and Lehnen, R. (2016), “Phenolated Lignins as Reactive Precursors in Wood Veneer and Particleboard Adhesion”, *Industrial & Engineering Chemistry Research*, Vol. 55, pp. 5231–5237.
- Qian, S., Zhou, J., de Rooij, M.R., Schlangen, E., Ye, G. and van Breugel, K. (2009), “Self-healing behavior of strain hardening cementitious composites incorporating local waste materials”, *Cement and Concrete Composites*, Vol. 31 No. 9, pp. 613–621.
- Raftery, G.M., Harte, A.M. and Rodd, P.D. (2009), “Bond quality at the FRP-wood interface using wood-laminating adhesives”, *International Journal of Adhesion and Adhesives*, Vol. 29 No. 2, pp. 101–110.
- Robus, C.L.L., Gottumukkala, L.D., van Rensburg, E. and Görgens, J.F. (2016), “Feasible process development and techno-economic evaluation of paper sludge to bioethanol conversion: South African paper mills scenario”, *Renewable Energy*, Vol. 92, pp. 333–345.
- Rowell, R.M. and Rowell, J. (1996), *Paper and Composites from Agro-Based Resources*, CRC press, Florida, available at: [https://books.google.co.za/books?hl=en&lr=&id=V79kbwVW1wQC&oi=fnd&pg=PA3&dq=paper+and+composites+from+agro-based+resources&ots=T8RVeZHayP&sig=6HdB355JKYm7j43cTSH7rh8YNRU#v=onepage&q=paper and composites from agro-based resources&f=false](https://books.google.co.za/books?hl=en&lr=&id=V79kbwVW1wQC&oi=fnd&pg=PA3&dq=paper+and+composites+from+agro-based+resources&ots=T8RVeZHayP&sig=6HdB355JKYm7j43cTSH7rh8YNRU#v=onepage&q=paper+and+composites+from+agro-based+resources&f=false) (accessed 2 April 2019).
- Saheb, D.N. and Jog, J.P. (1999), “Natural Fiber Polymer Composites : A Review”, Vol. 18 No. 4, pp. 351–363.
- Sahoo, S., Seydibeyoğlu, M.Ö., Mohanty, A.K. and Misra, M. (2011), “Characterization of industrial lignins for their utilization in future value added applications”, *Biomass and Bioenergy*, Vol. 35 No. 10, pp. 4230–4237.
- Salanti, A., Zoia, L., Simonutti, R. and Orlandi, M. (2018), “Epoxidized Lignin Derivatives as Bio-based Cross-linkers Used in the Preparation of Epoxy Resins”, *BioResources*, Vol. 13 No. 2, pp. 2374–2396.
- Sawpan, M.A., Pickering, K.L. and Fernyhough, A. (2011), “Effect of various chemical treatments on the fibre structure and tensile properties of industrial hemp fibres”,

- Composites Part A: Applied Science and Manufacturing*, Vol. 42 No. 8, pp. 888–895.
- Schorr, D., Diouf, P.N. and Stevanovic, T. (2014), “Evaluation of industrial lignins for biocomposites production”, *Industrial Crops and Products*, Elsevier, Vol. 52, pp. 65–73.
- Sgriccia, N., Hawley, M.C. and Misra, M. (2008), “Characterization of natural fiber surfaces and natural fiber composites”, *Composites Part A: Applied Science and Manufacturing*, Vol. 39 No. 10, pp. 1632–1637.
- Shen, Q., Zhang, T. and Zhu, M. (2008), “A comparison of the surface properties of lignin and sulfonated lignins by FTIR spectroscopy and wicking technique”, *Colloids and Surfaces A: Physicochemical Engineering Aspects*, Vol. 320, pp. 57–60.
- Singh, D. and Wagh, A.S. (1998), “PHOSPHATE BONDED STRUCTURAL PRODUCTS FROM HIGH VOLUME WASTES”, United States Patent, United States of America.
- Singh, D., Wagh, A.S., Jeong, S.Y. and Dorf, M. (1996), “Leaching behavior of phosphate-bonded ceramic waste forms.”, *Ceramic Transactions*, Vol. 72 No. Environmental Issues and Waste Management Technologies in the Ceramic and Nuclear Industries II, pp. 279–289.
- Sinnott, R.K. (2005), *Coulson & Richardson’s Chemical Engineering*, Fourth Ed., Elsevier Butterworth-Heinemann, Amsterdam.
- Sipponen, M. (2016), *Lignin : Structure and Characterization*, Espoo, Finland.
- Skoog, D.A., West, D.M., Holler, J.F. and Crouch, S.R. (2014), *Fundamentals of Analytical Chemistry*, 9th Ed., Cengage Learning Inc.
- Sluiter, A., Hames, B., Ruiz, R., Scarlata, C., Sluiter, J., Templeton, D. and Crocker, D. (2012), “NREL/TP-510-42618 analytical procedure - Determination of structural carbohydrates and lignin in Biomass”, *Laboratory Analytical Procedure (LAP)*, p. 17.
- Sluiter, A., Ruiz, R., Scarlata, C., Sluiter, J. and Templeton, D. (2005), “Determination of Extractives in Biomass: Laboratory Analytical Procedure (LAP); Issue Date 7/17/2005 - 42619.pdf”, *Technical Report NREL/TP-510-42619*, pp. 1–9.
- Sorrentino, L., de Vasconcellos, D.S., D’Auria, M., Sarasini, F. and Iannace, S. (2015), “Thermoplastic Composites Based on Poly(ethylene 2,6-naphthalate) and Basalt Woven Fabrics: Static and Dynamic Mechanical Properties”, *Polymers and Polymer Composites*,

Vol. 16 No. 2, pp. 101–113.

Soucy, J., Koubaa, A., Migneault, S. and Riedl, B. (2014), “The potential of paper mill sludge for wood-plastic composites”, *Industrial Crops and Products*, Vol. 54, pp. 248–256.

Spelter, H. (1994), *Capacity, Production, and Manufacture of Wood-Based Panels in North America*, Madison, Wisconsin.

Stark, N.M., Cai, Z. and Carll, C. (2010), “Chapter 11 - Wood-Based Composite Materials Panel Products, Glued-Laminated Timber, Structural Materials”, *Wood Handbook - Wood as an Engineering Material*, pp. 1–28.

Sun, J., Wang, C., Yeo, J.C.C., Yuan, D., Li, H., Stubbs, L.P. and He, C. (2016), “Lignin Epoxy Composites: Preparation, Morphology, and Mechanical Properties”, *Macromolecular Materials and Engineering*, Vol. 301 No. 3, pp. 328–336.

Tajvidi, M. and Ebrahimi, G. (2002), “Water Uptake and Mechanical Characteristics of Natural Filler – Polypropylene Composites”.

Thielemans, W., Can, E., Morye, S.S. and Wool, R.P. (2002), “Novel applications of lignin in composite materials”, *Journal of Applied Polymer Science*, Vol. 83 No. 2, pp. 323–331.

Thompson, G., Swain, J., Kay, M. and Forster, C.F. (2001), “The treatment of pulp and paper mill effluent: A review”, *Bioresource Technology*, Vol. 77 No. 3, pp. 275–286.

Toriz, G., Denes, F. and Young, R.A. (2002), “Lignin-Polypropylene Composites. Part 1: Composites From Unmodified Lignin and Polypropylene”, *Polymer Composites*, Vol. 23 No. 5, pp. 806–813.

Tserki, V., Matzinos, P., Kokkou, S. and Panayiotou, C. (2005), “Novel biodegradable composites based on treated lignocellulosic waste flour as filler. Part I. Surface chemical modification and characterization of waste flour”, *Composites Part A: Applied Science and Manufacturing*, Vol. 36 No. 7, pp. 965–974.

Velásquez, J., Ferrando, F. and Salvadó, J. (2003), “Effects of kraft lignin addition in the production of binderless fiberboard from steam exploded *Miscanthus sinensis*”, *Industrial Crops and Products*, Vol. 18 No. 1, pp. 17–23.

Viani, A., Sotiriadis, K., Lanzafame, G. and Mancini, L. (2019), “3D microstructure of magnesium potassium phosphate ceramics from X-ray tomography : new insights into the

- reaction mechanisms”, *Journal of Materials Science*, Vol. 54 No. 5, pp. 3748–3760.
- Vinokurov, S.E., Kulikova, S.A. and Myasoedov, B.F. (2019), “Solidification of high level waste using magnesium potassium phosphate compound”, *Nuclear Engineering and Technology*, Vol. 51 No. 3, pp. 755–760.
- Wagh, A.S. (2004), *Chemically Bonded Phosphate Ceramics*, first edit., Elsevier, United Kingdom.
- Wagh, A.S. (2004), *Chemically Bonded Phosphate Ceramics*, First edit., Elsevier.
- Wagh, A.S. (2013), “Recent Progress in Chemically Bonded Phosphate Ceramics”, *ISRN Ceramics*, Vol. 2013, p. 20.
- Wagh, A.S. (2016), *Chemically Bonded Phosphate Ceramics: Twenty-First Century Materials with Diverse Applications*, 2nd Ed.
- Wagh, A.S. and Jeong, S.-Y. (2003), “Chemically Bonded Phosphate Ceramics: I, A Dissolution Model of Formation”, *Journal of the American Ceramic Society*, Vol. 86 No. 11, pp. 1838–1844.
- Wagh, A.S., Jeong, S.-Y., Lohan, D. and Elizabeth, A. (2003), “Chemically bonded phospho-silicate ceramics”, USA.
- Wang, F., Lu, M., Zhou, S., Lu, Z. and Ran, S. (2019), “Effect of Fiber Surface Modification on the Interfacial Adhesion and Thermo-Mechanical Performance of Unidirectional Epoxy-Based Composites Reinforced with Bamboo Fibers”, *Molecules*, Vol. 24 No. 15.
- Westney, R.E. (1997), *The Engineer’s Cost Handbook*, Marcel Dekker Inc, New York.
- Wool, R. and Sun, X.S. (2011), *Bio-Based Polymers and Composites*.
- Wypych, G. (2016), *Handbook of Fillers*, 4th Ed., ChemTec Publishing, Toronto, available at: https://books.google.co.za/books?hl=en&lr=&id=FJQcCgAAQBAJ&oi=fnd&pg=PP1&dq=additives+vs+fillers&ots=sR_MnE1EPm&sig=5wEat9DNnR4gz_v5IqUltUIsODE#v=onepage&q=additives+vs+fillers&f=false (accessed 29 March 2019).
- Xiao, J., Zuo, Y., Li, P., Wang, J. and Wu, Y. (2018), “Preparation and characterization of straw / magnesium cement composites with high-strength and fire-retardant”, *Journal of Adhesion Science and Technology*, Vol. 4243, pp. 1–15.
- Yang, X., Wang, W. and Huang, H. (2015), “Resistance of paper mill sludge/wood fiber/high-

- density polyethylene composites to water emersion and thermotreatment”, *Applied Polymer Science*, Vol. 132 No. 11.
- Younesi-Kordkheili, H., Pizzi, A. and Niyatzade, G. (2016), “Reduction of Formaldehyde Emission from Particleboard by Phenolated Kraft Lignin”, *The Journal of Adhesion*, Vol. 92 No. 6, pp. 485–497.
- Youngquist, J.A. (1999), “Wood-based Composites and Panel Products”, *Wood Handbook - Wood as an Engineering Material*, pp. 1–31.
- Yu, W., Liu, X., Su, H. and Zhang, Y. (2017), “Drying Kinetics of Paper Mill Sludge”, *Energy and Power Engineering*, Vol. 9 No. 4B, pp. 141–148.
- Zeng, Y., Himmel, M.E. and Ding, S.Y. (2017), “Visualizing chemical functionality in plant cell walls”, *Biotechnol Biofuels*, Vol. 10 No. 263.
- Zhang, W., Wu, J., Weng, L., Zhang, H., Zhang, J. and Wu, A. (2020), “Understanding the role of cellulose fiber on the dewaterability of simulated pulp and paper mill sludge”, *Science of the Total Environment*, Vol. 702.
- Zhang, Y., Tian, Y. and Meng, Y. (2016), “Mechanical interlocking of cotton fibers on slightly textured surfaces of metallic cylinders”, *Scientific Reports*, Nature Publishing Group, Vol. 6 No. 25403, available at: <https://doi.org/10.1038/srep25403>.
- Zhou, Y., Fan, M. and Chen, L. (2016), “Interface and bonding mechanisms of plant fibre composites: An overview”, *Composites Part B: Engineering*, Vol. 101, pp. 31–45.

APPENDIX A: Statistical model verification and process optimisation

A.1. Mechanical performance results for FFD, steepest ascent, and CCD experimental designs

Table A.1: Verification of optimum phosphate to paper sludge ratio as determined by Chimpango (2020).

	Lignin content (%)	Temp (°C)		Phosphate:paper sludge		
				1:3.0	1:1.94	1:1.0
MK	20.0	100.0	MOR (MPa)	1.9	5.5	6.2
			MOE (MPa)	909	669	616
SK	20.0	100.0	MOR (MPa)	2.1	6.8	8.1
			MOE (MPa)	867	927	837

Table A.2: Full factorial design of experiments for MK, SK, and MS composite formulations, where lignin content, processing temperature, and composite density were varied.

Lignin content (%)	Temp (°C)	Density (kg.m ⁻³)	MK		SK		MS	
			MOR (MPa)	MOE (MPa)	MOR (MPa)	MOE (MPa)	MOR (MPa)	MOE (MPa)
5.0	25.0	900	1.0	794	1.1	634	-	-
5.0	100.0	900	1.7	656	1.6	695	0.5	415
5.0	25.0	1 200	1.9	805	1.9	905	-	-
5.0	100.0	1 200	2.0	681	1.8	705	0.9	307
20.0	25.0	900	0.3	264	0.6	277	-	-
20.0	100.0	900	3.3	947	3.6	973	0.6	355
20.0	25.0	1 200	1.4	656	1.5	599	-	-
20.0	100.0	1 200	5.5	1 523	6.8	1 609	1.3	772



Table A.3: Stepwise experimental design following the statistically determined path of steepest ascent of the dependent variables.

Lignin content (%)	Temp (°C)	Density (kg.m ⁻³)	MK		SK		MS	
			MOR (MPa)	MOE (MPa)	MOR (MPa)	MOE (MPa)	MOR (MPa)	MOE (MPa)
40.0	130.0	1 200	3.3	1 220	4.5	1 319		
50.0	170.0	1 200	3.0	778	4.3	978		
60.0	200.0	1 200	2.8	652	3.3	705		
30.0	150.0	1 200					2.9	874
40.0	200.0	1 200					0.9	314

Table A.4: Central composite design of experiments with process variables statistically around the actual conditions for optimum MK and SK composite performance.

Lignin content (%)	Temp (°C)	Density (kg.m ⁻³)	MK		SK	
			MOR (MPa)	MOE (MPa)	MOR (MPa)	MOE (MPa)
17.0	105.0	1 200	1.9	648	5.1	1 703
25.0	90.0	1 200	0.7	283	3.5	982
25.0	120.0	1 200	2.4	909	4.4	1 534
31.0	70.0	1 200	0.6	247	1.3	516
31.0	105.0	1 200	2.8	425	5.4	1 646
31.0	140.0	1 200	2.9	913	4.7	1 407
37.0	90.0	1 200	1.1	496	3.2	1 293
37.0	120.0	1 200	5.8	2 119	5.5	2 131
45.0	105.0	1 200	4.0	1 424	5.1	2 063



Table A.5: Central composite design of experiments with process variables statistically around the actual conditions for optimum MS composite performance.

Lignosulfonate content (%)	Temp (°C)	Density (kg.m ⁻³)	MS	
			MOR (MPa)	MOE (MPa)
0.0	125.0	1 200	1.1	519
12.0	90.0	1 200	0.6	332
12.0	160.0	1 200	2.5	1 505
24.0	42.0	1 200	Fail	Fail
24.0	125.0	1 200	1.7	1 177
24.0	200.0	1 200	Fail	Fail
37.0	90.0	1 200	0.9	664
37.0	160.0	1 200	1.0	667
54.0	125.0	1 200	0.3	263

A.2. Response surface model parameters

The parameters in Table A.1 is used in Equation A.1 to predict the response variable for a set of process conditions – press temperature (x) and lignin content (y).

$$z = ax + a(Q)x^2 + by + b(Q)y^2 + abxy + Int \quad A.1$$

Table A.6: Statistical model parameters for response variable variation due to changes in process conditions.

Mill	Response variable	<i>Int</i>	<i>a</i>	<i>a(Q)</i>	<i>b</i>	<i>b(Q)</i>	<i>ab</i>
Mondi	MOR (MPa)	-81.84	1.096	-0.004	1.041	-0.007	-0.004
	MOE (MPa)	1 775	251.7	-2 114	35.24	-1 916	1 346
Sappi	MOR (MPa)	5.037	1.884	-8.641	0.037	-7.631	9.820
	MOE (MPa)	1 620	-152.7	-2 560	612.9	-1 261	2 076
Mpact	MOR (MPa)	2.038	0.647	-1.480	-1.307	-2.213	-0.711
	MOE (MPa)	1 132	-71.94	-851.6	-612.0	-1 355	-751.6

a = T: temperature (°C) parameters

b = %L: lignin content (wt%) parameters



A.3. Analysis of variance (ANOVA) of process variables

Table A.7: ANOVA results of the statistical significance of process conditions on response variables, where $p < 0.05$ signifies significant effect.

	Mondi		Sappi		Mpact	
	MOR (MPa)	MOE (MPa)	MOR (MPa)	MOE (MPa)	MOR (MPa)	MOE (MPa)
p: L%	0.059	0.932	0.986	0.453	0.071	0.066
p: L% (Q)	0.135	0.025	0.030	0.302	0.043	0.012
p: T	0.034	0.548	0.416	0.858	0.309	0.799
p: T (Q)	0.033	0.012	0.026	0.067	0.172	0.094
P: L%/T interaction	0.376	0.173	0.060	0.264	0.477	0.120

%L: lignin content (wt%)

T: temperature (°C)

A.4. Confirmation of statistical models via experimental results

Table A.8: Comparison between predicted and experimental responses for optimal process conditions.

Mill	Process parameter	Predicted	Experimental results	% error	R ² -value
Mondi	MOR (MPa)	4.9 ± 0.7	5.3 ± 0.3	7.55	0.8101
	MOE (MPa)	1 778 ± 337	2 435 ± 38	26.9	0.9003
Sappi	MOR (MPa)	5.2 ± 2.4	7.2 ± 0.7	27.8	0.7316
	MOE (MPa)	1 667 ± 529	2 793 ± 293	40.3	0.5292*
Mpact	MOR (MPa)	2.4 ± 1.0	3.3 ± 0.3	33.3	0.7599
	MOE (MPa)	1 168 ± 587	1 302 ± 31	10.3	0.5874*



APPENDIX B: Economic analysis

B.1. Mass balance equations

Variable calculated	Unit	Symbol	Calculation	
Dry sludge flow rate	<i>ton/year</i>	PS_{dry}	Known	Boshoff, 2015
Sludge moisture content into plant	$\frac{g \text{ water}}{g \text{ total}}$	MC_{PS}	Known	Boshoff, 2015
Equilibrium sludge moisture content after drying	$\frac{g \text{ water}}{g \text{ total}}$	$MC_{PS,eq}$	Known	Experimental work
Total sludge flow rate into the system	<i>ton/year</i>	PS_{tot}	$\frac{(1 - MC_{PS,eq}) \times PS_{dry}}{1 - MC_{PS}}$	
Required CBPC	<i>ton/year</i>	$CBPC$	$CBPC:PS_{dry}$ is known as 1:1.94	Chimphango, 2020
MgO and KH_2PO_4	<i>ton/year</i>		Ratio of 5.07:1 to achieve $CBPC$ mass	Chimphango, 2020
Total feedstock flowrate	<i>ton/year</i>	T_{feed}	$PS_{tot} + CBPC + Lig + Filler + W_{req}$	
Required lignin	<i>ton/year</i>	Lig	$0.43T_{feed}$ (MK); $0.36T_{feed}$ (SK); $0.18T_{feed}$ (MS)	Experimental work
Required $CaCO_3$ filler	<i>ton/year</i>	$FILLER$	0.1T	Chimphango, 2020
Water required to produce composites	<i>ton/year</i>	W_{req}	$CBPC + Lig + FILLER + (WHC - MC_{PS,eq}) \times PS_{dry}$	Equation 14
Sulfuric acid required	<i>ton/year</i>	SA	$0.465Lig$	Experimental work
Solids content of spent liquor from mill	$\frac{g \text{ lignin}}{g \text{ liquor}}$	SC_{SL}	$0.4 - 0.8$	Discussion with mills
Spent liquor required	<i>ton/year</i>	SL	$SC_{SL} = \frac{Lig}{SL}$	

B.2. Equipment sizing

Table B.1: Equipment sizing and specifications for Mondi (Richards Bay), Sappi (Ngodwana), and Mpact (Piet Retief).

Equipment	Code	Mondi	Sappi	Mpact
Flow operators				
Lignin conveyor	C-108/9	Mass flow: 3 928.2 kg/h Quantity: 2	Mass flow: 3 867.6 kg/h Quantity: 2	NA
Spent (black/sulfite) liquor pump	P-101	Capacity: 4.58 m ³ /h Inlet flow: 6 874.3 kg/h Quantity: 1	Capacity: 4.51 m ³ /h Inlet flow: 6 768.4 kg/h Quantity: 1	Capacity: 0.11 m ³ /h Inlet flow: 162.2 kg/h Quantity: 1
Sulfuric acid pump	P-102	Capacity: 0.70 m ³ /h Inlet flow: 985.2 kg/h Quantity: 1	Capacity: 0.69 m ³ /h Inlet flow: 970 kg/h Quantity: 1	NA
Spent sulfite liquor (SSL) pump	P-103/4	NA	NA	Capacity: 0.1 m ³ /h Inlet flow: 102.3 kg/h Quantity: 2
Acid water pump	P-105	Capacity: 5.58 m ³ /h Inlet flow: 7 249.9 kg/h Quantity: 1	Capacity: 5.49 m ³ /h Inlet flow: 7 138.2 kg/h Quantity: 1	NA
Lignin, H ₂ SO ₄ screw conveyor	SC-103/4	Capacity: 7.45 m ³ /h Inlet flow: 11 178.0 kg/h Power: 5.5 kW Quantity: 1	Capacity: 7.34 m ³ /h Inlet flow: 11 005.9 kg/h Power: 5.5 kW Quantity: 1	NA
Paper sludge conveyor	C-201	Mass flow: 1 893.9 kg/h Quantity: 1	Mass flow: 10 064.9 kg/h Quantity: 1	Mass flow: 75.8 kg/h Quantity: 1



KH ₂ PO ₄ conveyor	C-203	Mass flow: 162.9 kg/h Quantity: 1	Mass flow: 195.8 kg/h Quantity: 1	Mass flow: 6.5 kg/h Quantity: 1
MgO conveyor	C-204	Mass flow: 814.6 kg/h Quantity: 1	Mass flow: 978.9 kg/h Quantity: 1	Mass flow: 32.6 kg/h Quantity: 1
CaCO ₃ conveyor	C-205	Mass flow: 610.9kg/h Quantity: 1	Mass flow: 638.4 kg/h Quantity: 1	Mass flow: 15.9 kg/h Quantity: 1
Water feed pump	P-202	Capacity: 2.85 m ³ /h Inlet flow: 2 840.9 kg/h Quantity: 1	Capacity: 3.42 m ³ /h Inlet flow: 3409.1 kg/h Quantity: 1	NA
Composite mix screw conveyor	SC-208	Capacity: 11.67 m ³ /h Inlet flow: 9 217.7 kg/h Power: 5.5 kW Quantity: 1	Capacity: 13.1 m ³ /h Inlet flow: 10 344.7 kg/h Power: 5.5 kW Quantity: 1	Capacity: 0.3 m ³ /h Inlet flow: 233.1 kg/h Power: 5.5 kW Quantity: 1
Resin feed pump	P-302	Capacity: 0.22 m ³ /h Inlet flow: 348.4 kg/h Quantity: 1	Capacity: 0.24 m ³ /h Inlet flow: 378.9 kg/h Quantity: 1	Capacity: 0.01 m ³ /h Inlet flow: 9.02 kg/h Quantity: 1
Lignin preparation				
Lignin dryer	D-101	Mass flow: 2 749.7 kg/h MC out: 5.0 % Area: 5.8 m ² CM: stainless steel	Mass flow: 2 707.4 kg/h MC out: 5.0 % Area: 5.71 m ² CM: stainless steel	Mass flow: 32.4 kg/h MC out: 68.3 % Area: 0.34 m ² CM: stainless steel



Lignin/water separation filter	F-101	Type: Rotary drum Flow rate: 11 178.0 kg/h MC: 30 % Area: 16.77 m ² CM: Stainless steel	Type: Rotary drum Flow rate: 11 005.9 kg/h MC: 30 % Area: 16.51 m ² CM: Stainless steel	NA
Black liquor/ H ₂ SO ₄ or water agitated mixer	M-101	Type: Vertical Retention time: 24 h Capacity: 100 m ³ Temp: 100 °C Press: 1 bar Quantity: 4 CM: stainless steel	Type: Vertical Retention time: 24 h Capacity: 100 m ³ Temp: 100 °C Press: 1 bar Quantity: 4 CM: stainless steel	Type: Vertical Retention time: 24 h Capacity: 100 m ³ Temp: 100 °C Press: 1 bar Quantity: 1 CM: stainless steel
Lignin/ H ₂ SO ₄ cooled reactor	R-101	Type: Vertical Retention time: 24 h Capacity: 30 m ³ Temp: 100 °C Press: 1 bar Quantity: 9 CM: stainless steel Agitated cooled	Type: Vertical Retention time: 24 h Capacity: 30 m ³ Temp: 100 °C Press: 1 bar Quantity: 9 CM: stainless steel Agitated, cooled	NA
Composite production				
Paper sludge dryer	D-201	Mass flow: 1 761.4 kg/h MC out: 7 % Area: 15.45 m ² CM: carbon steel	Mass flow: 2 113.6 kg/h MC out: 7 % Area: 23.73 m ² CM: carbon steel	Mass flow: 70.5 kg/h MC out: 7 % Area: 0.79 m ² CM: carbon steel



Composite constituent mixing tank; agitated and cooled	M-201	Type: Vertical Retention time: 0.5 h Capacity: 5 m ³ Temp: 80 °C Press: 1 bar Quantity: 1 CM: carbon steel	Type: Vertical Retention time: 0.5 h Capacity: 5 m ³ Temp: 80 °C Press: 1 bar Quantity: 2 CM: carbon steel	Type: Vertical Retention time: 0.5 h Capacity: 5 m ³ Temp: 80 °C Press: 1 bar Quantity: 1 CM: carbon steel
Matt formation and pre-press	PP-201	Type: Multi-layered Dimensions: 1.2x2.4x0.01 m ³ Mass flow: 9 217.7 kg/h Temp: 100 °C Press: 0.5 MPa	Type: Multi-layered Dimensions: 1.2x2.4x0.01 m ³ Mass flow: 10 344.7 kg/h Temp: 100 °C Press: 0.5 MPa	Type: Multi-layered Dimensions: 1.2x2.4x0.01 m ³ Mass flow: 233.1 kg/h Temp: 100 °C Press: 0.5 MPa
Composite heated press	PRESS-201	Type: Multi-layered No. of plates: 30 Dimensions: 1.2x2.4x0.01 m ³ Mass flow: 7 446.2 kg/h Panels: 120 panel/h Temp: 118 °C Press: 2 MPa	Type: Multi-layered No. of plates: 30 Dimensions: 1.2x2.4x0.01 m ³ Mass flow: 8 098.7 kg/h Panels: 130 panel/h Temp: 133 °C Press: 2 MPa	Type: Multi-layered No. of plates: 15 Dimensions: 1.2x2.4x0.01 m ³ Mass flow: 192.8 kg/h Panels: 30 panel/h Temp: 155 °C Press: 2 MPa
Veneer and finishing				
Veneer press	PRESS-301	Type: Multi-layered Dimensions: 1.2x2.4x0.01 m ³ Mass flow: 6 340.6 kg/h Panels: 120 panel/h Temp: 25 °C Press: 0.2 MPa	Type: Multi-layered Dimensions: 1.2x2.4x0.01 m ³ Mass flow: 6 896.3 kg/h Panels: 130 panel/h Temp: 25 °C Press: 0.2 MPa	Type: Multi-layered Dimensions: 1.2x2.4x0.01 m ³ Mass flow: 164.2 kg/h Panels: 30 panel/h Temp: 25 °C Press: 0.2 MPa

CM: Construction material

MC: Moisture content



B.3. Total capital investment

Table B.2: Total capital investment projected for Mondi (Richards Bay), Sappi (Ngodwana), and Mpact (Piet Retief).

	Mondi (R)	Sappi (R)	Mpact (R)
Equipment cost	159 754 000	167 838 000	20 510 000
Additional material	40 500 000	42 547 000	5 244 000
Pipe work	1 800 000	1 891 000	233 000
Concrete	12 000 000	12 607 000	1 554 000
Steel	750 000	788 000	97 000
Instrumentation installation	1 950 000	2 048 000	252 000
Electricity for installation	22 500 000	23 637 000	2 913 000
Paint and Insulation	1 500 000	1 576 000	194 000
Total material costs	190 503 000	200 130 000	24 665 000
Installation labour	51 435 000	54 035 000	6 659 000
	241 939 000	254 165 000	31 324 000
Indirect costs	70 162 000	73 708 000	9 084 000
Sub total	312 101 000	327 873 000	40 408 000
Contractors fee and contingency	56 178 000	59 017 000	7 273 000
Total fixed investment	378 030 000	397 145 000	48 770 000



B.4. Total annual operating expense

Table B.3: Total annual operating expenses projected for Mondi (Richards Bay), Sappi (Ngodwana), and Mpact (Piet Retief).

		Mondi	Sappi	Mpact
Direct production costs (DPC)				
Var	Feedstock material	126 744 000	140 149 000	3 461 000
Fix	Salaries	656 000	656 000	656 000
Var	Utilities	6 071 000	6 274 000	2 894 000
Fix	Maintenance	22 681 000	23 829 000	2 926 000
Fix	Consumables	3 402 000	3 574 000	439 000
Fix	Lab fees	656 000	656 000	656 000
Var	Additional	12 996 000	14 070 000	1 390 000
	Total	179 113 000	195 112 000	18 327 000
Fixed production costs (FPC)				
Fix	Depreciation	25 202 000	26 476 000	3 251 000
Fix	Local tax	7 560 000	7 943 000	975 000
Fix	Insurance	4 725 000	4 964 000	610 000
	Total	37 488 000	39 384 000	4 836 000
Plant overhead cost (POC)				
Fix	Overhead costs	14 621 000	15 195 000	4 743 000
	Production cost (PC)	231 222 000	249 690 000	27 907 000
General costs (GC)				
Fix	Administration costs	2 624 000	2 624 000	2 624 000
Var	Distribution and marketing	9 249 000	9 988 000	1 116 000
Fix	Research and development	9 249 000	9 988 000	1 116 000
	Total	21 122 000	22 599 000	4 857 000
	Subtotal	252 344 000	272 290 000	32 763 000
	Allowance for contingency	12 617 000	13 614 000	1 638 000
	Total cost excluding tax	264 961 000	285 904 000	34 401 000



B.5. Discounted cash flow

Table B.5: Discounted cash flow table for Mondri (Richards Bay).

Year	Production	price/board	a	b	c	Depreciation	e=a-b-c-d	f=%e	G=a-b-c-f	Working capital	Fixed capital investment	Annual cash flow	Cum cash flow
	units/year		Income	Fix cost	Var cost	Depreciation	Profit before tax	Tax	Profit after tax	R/year	R/year	R/year	R/year
1	R -	R 636.00	R -	R -	R -	R -	R -	R -	R -	R -	R 226,818,264.00	-R 226,818,264.00	-R 226,818,264.00
2	R -	R 663.00	R -	R -	R -	R -	R -	R -	R -	R 19,978,908.00	R 159,831,270.00	-R 179,810,178.00	-R 406,628,442.00
3	R 540,697.00	R 692.00	R 393,023,462.00	R 94,629,191.00	R 140,075,020.00	R 25,202,029.00	R 133,117,219.00	R 37,272,821.32	R 121,046,429.68	R -	R -	R 121,046,429.68	-R 285,582,012.32
4	R 617,940.00	R 721.00	R 467,438,054.00	R 100,023,055.00	R 169,210,625.00	R 25,202,029.00	R 173,002,345.00	R 48,440,656.60	R 149,763,717.40	R -	R -	R 149,763,717.40	-R 135,818,294.92
5	R 695,182.00	R 752.00	R 547,298,338.00	R 105,724,369.00	R 201,212,584.00	R 25,202,029.00	R 215,159,354.00	R 60,244,619.12	R 180,116,765.88	R -	R -	R 180,116,765.88	R 44,298,470.96
6	R 772,425.00	R 784.00	R 632,938,911.00	R 111,750,658.00	R 236,313,002.00	R 25,202,029.00	R 259,673,221.00	R 72,708,501.88	R 212,166,749.12	R -	R -	R 212,166,749.12	R 256,465,220.08
7	R 772,425.00	R 818.00	R 658,830,025.00	R 118,120,446.00	R 249,782,843.00	R 25,202,029.00	R 265,724,707.00	R 74,402,917.96	R 216,523,818.04	R -	R -	R 216,523,818.04	R 472,989,038.12
8	R 772,425.00	R 853.00	R 685,827,985.00	R 124,853,311.00	R 264,020,465.00	R 25,202,029.00	R 271,752,179.00	R 76,090,610.12	R 220,863,598.88	R -	R -	R 220,863,598.88	R 693,852,637.00
9	R 772,425.00	R 889.00	R 713,980,107.00	R 131,969,950.00	R 279,069,631.00	R 25,202,029.00	R 277,738,495.00	R 77,766,778.60	R 225,173,747.40	R -	R -	R 225,173,747.40	R 919,026,384.40
10	R 772,425.00	R 927.00	R 743,335,732.00	R 139,492,237.00	R 294,976,600.00	R 25,202,029.00	R 283,664,865.00	R 79,426,162.20	R 229,440,732.80	R -	R -	R 229,440,732.80	R 1,148,467,117.20
11	R 772,425.00	R 967.00	R 773,946,311.00	R 147,443,295.00	R 311,790,267.00	R 25,202,029.00	R 289,510,719.00	R 81,063,001.32	R 233,649,747.68	R -	R -	R 233,649,747.68	R 1,382,116,864.88
12	R 772,425.00	R 1,008.00	R 805,865,492.00	R 155,847,563.00	R 329,562,312.00	R 25,202,029.00	R 295,253,587.00	R 82,671,004.36	R 237,784,612.64	R -	R -	R 237,784,612.64	R 1,619,901,477.52
13	R 772,425.00	R 1,051.00	R 839,149,217.00	R 164,730,874.00	R 348,347,364.00	R 25,202,029.00	R 300,868,949.00	R 84,243,305.72	R 241,827,673.28	R -	R -	R 241,827,673.28	R 1,861,729,150.80
14	R 772,425.00	R 1,096.00	R 873,855,821.00	R 174,120,533.00	R 368,203,163.00	R 25,202,029.00	R 306,330,094.00	R 85,772,426.32	R 245,759,698.68	R -	R -	R 245,759,698.68	R 2,107,488,849.48
15	R 772,425.00	R 1,143.00	R 910,046,134.00	R 184,045,404.00	R 389,190,744.00	R 25,202,029.00	R 311,607,956.00	R 87,250,227.68	R 249,559,758.32	R -	R -	R 249,559,758.32	R 2,357,048,607.80
16	R 772,425.00	R 1,192.00	R 947,783,582.00	R 194,535,992.00	R 411,374,616.00	R 25,202,029.00	R 316,670,943.00	R 88,667,864.04	R 253,205,109.96	R -	R -	R 253,205,109.96	R 2,610,253,717.76
17	R 772,425.00	R 1,243.00	R 987,134,305.00	R 205,624,544.00	R 434,822,969.00	R 25,202,029.00	R 321,484,763.00	R 90,015,733.64	R 256,671,058.36	R -	R -	R 256,671,058.36	R 2,866,924,776.12

Table B.6: Discounted cash flow table for Sappi (Ngodwana).

Year	Production	price/board	a	b	c	Depreciation	e=a-b-c-d	f=%e	G=a-b-c-f	Working capital	Fixed capital investment	Annual cash flow	Cum cash flow
	units/year		Income	Fix cost	Var cost	Depreciation	Profit before tax	Tax	Profit after tax	R/year	R/year	R/year	R/year
1	R -	R 636.00	R -	R -	R -	R -	R -	R -	R -	R -	R 238,286,900.00	-R 238,286,900.00	-R 238,286,900.00
2	R -	R 663.00	R -	R -	R -	R -	R -	R -	R -	R 20,989,104.00	R 167,912,836.00	-R 188,901,940.00	-R 427,188,840.00
3	R 588,081.00	R 692.00	R 448,067,019.00	R 99,376,984.00	R 151,844,102.00	R 26,476,322.00	R 170,369,611.00	R 47,703,491.08	R 149,142,441.92	R -	R -	R 149,142,441.92	-R 278,046,398.08
4	R 672,093.00	R 721.00	R 531,945,915.00	R 105,041,472.00	R 183,427,675.00	R 26,476,322.00	R 217,000,446.00	R 60,760,124.88	R 182,716,643.12	R -	R -	R 182,716,643.12	-R 95,329,754.96
5	R 756,104.00	R 752.00	R 621,747,731.00	R 111,028,836.00	R 218,118,434.00	R 26,476,322.00	R 266,124,139.00	R 74,514,758.92	R 218,085,702.08	R -	R -	R 218,085,702.08	R 122,755,947.12
6	R 840,116.00	R 784.00	R 717,836,389.00	R 117,357,479.00	R 256,167,983.00	R 26,476,322.00	R 317,834,605.00	R 88,993,689.40	R 255,317,237.60	R -	R -	R 255,317,237.60	R 378,073,184.72
7	R 840,116.00	R 818.00	R 745,996,453.00	R 124,046,856.00	R 270,769,558.00	R 26,476,322.00	R 324,703,717.00	R 90,917,040.76	R 260,262,998.24	R -	R -	R 260,262,998.24	R 638,336,182.96
8	R 840,116.00	R 853.00	R 775,360,360.00	R 131,117,526.00	R 286,203,423.00	R 26,476,322.00	R 331,563,089.00	R 92,837,664.92	R 265,201,746.08	R -	R -	R 265,201,746.08	R 903,537,929.04
9	R 840,116.00	R 889.00	R 805,979,575.00	R 138,591,225.00	R 302,517,018.00	R 26,476,322.00	R 338,395,010.00	R 94,750,602.80	R 270,120,729.20	R -	R -	R 270,120,729.20	R 1,173,658,658.24
10	R 840,116.00	R 927.00	R 837,907,761.00	R 146,490,925.00	R 319,760,489.00	R 26,476,322.00	R 345,180,025.00	R 96,650,407.00	R 275,005,940.00	R -	R -	R 275,005,940.00	R 1,448,664,598.24
11	R 840,116.00	R 967.00	R 871,200,876.00	R 154,840,908.00	R 337,986,836.00	R 26,476,322.00	R 351,896,810.00	R 98,531,106.80	R 279,842,025.20	R -	R -	R 279,842,025.20	R 1,728,506,623.44
12	R 840,116.00	R 1,008.00	R 905,917,273.00	R 163,666,840.00	R 357,252,086.00	R 26,476,322.00	R 358,522,025.00	R 100,386,167.00	R 284,612,180.00	R -	R -	R 284,612,180.00	R 2,013,118,803.44
13	R 840,116.00	R 1,051.00	R 942,117,795.00	R 172,995,850.00	R 377,615,455.00	R 26,476,322.00	R 365,030,168.00	R 102,208,447.04	R 289,298,042.96	R -	R -	R 289,298,042.96	R 2,302,416,846.40
14	R 840,116.00	R 1,096.00	R 979,865,890.00	R 182,856,613.00	R 399,139,536.00	R 26,476,322.00	R 371,393,419.00	R 103,990,157.32	R 293,879,583.68	R -	R -	R 293,879,583.68	R 2,596,296,430.08
15	R 840,116.00	R 1,143.00	R 1,019,227,716.00	R 193,279,440.00	R 421,890,490.00	R 26,476,322.00	R 377,581,464.00	R 105,722,809.92	R 298,334,976.08	R -	R -	R 298,334,976.08	R 2,894,631,406.16
16	R 840,116.00	R 1,192.00	R 1,060,272,260.00	R 204,296,368.00	R 445,938,248.00	R 26,476,322.00	R 383,561,322.00	R 107,397,170.16	R 302,640,473.84	R -	R -	R 302,640,473.84	R 3,197,271,880.00
17	R 840,116.00	R 1,243.00	R 1,103,071,458.00	R 215,941,261.00	R 471,356,728.00	R 26,476,322.00	R 389,297,147.00	R 109,003,201.16	R 306,770,267.84	R -	R -	R 306,770,267.84	R 3,504,042,147.84

Table B.7: Discounted cash flow table for Mpack (Piet Retief).

Year	Production units/year	price/board	a Income R/year	b Fix cost R/year	c Var cost R/year	Depreciation R/year	e=a-b-c-d R/year	f=%e R/year	G=a-b-c-f R/year	Working capital R/year	Fixed capital investment R/year	Annual cash flow R/year	Cum cash flow R/year
1	R -	R 636.00	R -	R -	R -	R -	R -	R -	R -	R -	R 29,262,139.00	-R 29,262,139.00	-R 29,262,139.00
2	R -	R 663.00	R -	R -	R -	R -	R -	R -	R -	R 2,577,506.00	R 20,620,054.00	-R 23,197,560.00	-R 52,459,699.00
3	R 13,999.00	R 692.00	R 10,572,653.00	R 24,902,379.00	R 7,373,907.00	R 3,251,348.00	-R 24,954,981.00	-R 6,987,394.68	-R 14,716,238.32	R -	R -	-R 14,716,238.32	-R 67,175,937.32
4	R 15,999.00	R 721.00	R 12,556,032.00	R 26,321,814.00	R 8,907,679.00	R 3,251,348.00	-R 25,924,809.00	-R 7,258,946.52	-R 15,414,514.48	R -	R -	-R 15,414,514.48	-R 82,590,451.80
5	R 17,999.00	R 752.00	R 14,680,409.00	R 27,822,158.00	R 10,592,344.00	R 3,251,348.00	-R 26,985,441.00	-R 7,555,923.48	-R 16,178,169.52	R -	R -	-R 16,178,169.52	-R 98,768,621.32
6	R 19,999.00	R 784.00	R 16,954,448.00	R 29,408,021.00	R 12,440,120.00	R 3,251,348.00	-R 28,145,041.00	-R 7,880,611.48	-R 17,013,081.52	R -	R -	-R 17,013,081.52	-R 115,781,702.84
7	R 19,999.00	R 818.00	R 17,624,813.00	R 31,084,278.00	R 13,149,207.00	R 3,251,348.00	-R 29,860,020.00	-R 8,360,805.60	-R 18,247,866.40	R -	R -	-R 18,247,866.40	-R 134,029,569.24
8	R 19,999.00	R 853.00	R 18,323,837.00	R 32,856,082.00	R 13,898,711.00	R 3,251,348.00	-R 31,682,304.00	-R 8,871,045.12	-R 19,559,910.88	R -	R -	-R 19,559,910.88	-R 153,589,480.12
9	R 19,999.00	R 889.00	R 19,052,744.00	R 34,728,878.00	R 14,690,938.00	R 3,251,348.00	-R 33,618,420.00	-R 9,413,157.60	-R 20,953,914.40	R -	R -	-R 20,953,914.40	-R 174,543,394.52
10	R 19,999.00	R 927.00	R 19,812,812.00	R 36,708,425.00	R 15,528,321.00	R 3,251,348.00	-R 35,675,282.00	-R 9,989,078.96	-R 22,434,855.04	R -	R -	-R 22,434,855.04	-R 196,978,249.56
11	R 19,999.00	R 967.00	R 20,605,372.00	R 38,800,805.00	R 16,413,436.00	R 3,251,348.00	-R 37,860,217.00	-R 10,600,860.76	-R 24,008,008.24	R -	R -	-R 24,008,008.24	-R 220,986,257.80
12	R 19,999.00	R 1,008.00	R 21,431,815.00	R 41,012,451.00	R 17,349,002.00	R 3,251,348.00	-R 40,180,986.00	-R 11,250,676.08	-R 25,678,961.92	R -	R -	-R 25,678,961.92	-R 246,665,219.72
13	R 19,999.00	R 1,051.00	R 22,293,587.00	R 43,350,160.00	R 18,337,895.00	R 3,251,348.00	-R 42,645,816.00	-R 11,940,828.48	-R 27,453,639.52	R -	R -	-R 27,453,639.52	-R 274,118,859.24
14	R 19,999.00	R 1,096.00	R 23,192,201.00	R 45,821,120.00	R 19,383,155.00	R 3,251,348.00	-R 45,263,422.00	-R 12,673,758.16	-R 29,338,315.84	R -	R -	-R 29,338,315.84	-R 303,457,175.08
15	R 19,999.00	R 1,143.00	R 24,129,231.00	R 48,432,923.00	R 20,487,995.00	R 3,251,348.00	-R 48,043,035.00	-R 13,452,049.80	-R 31,339,637.20	R -	R -	-R 31,339,637.20	-R 334,796,812.28
16	R 19,999.00	R 1,192.00	R 25,106,318.00	R 51,193,600.00	R 21,655,810.00	R 3,251,348.00	-R 50,994,440.00	-R 14,278,443.20	-R 33,464,648.80	R -	R -	-R 33,464,648.80	-R 368,261,461.08
17	R 19,999.00	R 1,243.00	R 26,125,176.00	R 54,111,635.00	R 22,890,192.00	R 3,251,348.00	-R 54,127,999.00	-R 15,155,839.72	-R 35,720,811.28	R -	R -	-R 35,720,811.28	-R 403,982,272.36